

CHARACTERIZATION OF RENAL CATIONIC DRUG TRANSPORT
WITH AMANTADINE

BY

LEO T. Y. WONG

A THESIS SUBMITTED TO THE FACULTY OF GRADUATE STUDIES
IN PARTIAL FULFILLMENT OF THE REQUIREMENTS
FOR THE DEGREE OF

DOCTOR OF PHILOSOPHY

DEPARTMENT OF PHARMACOLOGY & THERAPEUTICS
FACULTY OF MEDICINE
UNIVERSITY OF MANITOBA
WINNIPEG, MANITOBA R3E 0W3
CANADA

DECEMBER 1991



National Library
of Canada

Acquisitions and
Bibliographic Services Branch

395 Wellington Street
Ottawa, Ontario
K1A 0N4

Bibliothèque nationale
du Canada

Direction des acquisitions et
des services bibliographiques

395, rue Wellington
Ottawa (Ontario)
K1A 0N4

Your file *Votre référence*

Our file *Notre référence*

The author has granted an irrevocable non-exclusive licence allowing the National Library of Canada to reproduce, loan, distribute or sell copies of his/her thesis by any means and in any form or format, making this thesis available to interested persons.

L'auteur a accordé une licence irrévocable et non exclusive permettant à la Bibliothèque nationale du Canada de reproduire, prêter, distribuer ou vendre des copies de sa thèse de quelque manière et sous quelque forme que ce soit pour mettre des exemplaires de cette thèse à la disposition des personnes intéressées.

The author retains ownership of the copyright in his/her thesis. Neither the thesis nor substantial extracts from it may be printed or otherwise reproduced without his/her permission.

L'auteur conserve la propriété du droit d'auteur qui protège sa thèse. Ni la thèse ni des extraits substantiels de celle-ci ne doivent être imprimés ou autrement reproduits sans son autorisation.

ISBN 0-315-77795-8

Canada

**CHARACTERIZATION OF RENAL CATIONIC
DRUG TRANSPORT WITH AMANTADINE**

BY

LEO T.Y. WONG

A thesis submitted to the Faculty of Graduate Studies of the University of Manitoba in partial fulfillment of the requirements for the degree of

DOCTOR OF PHILOSOPHY

© 1992

Permission has been granted to the LIBRARY OF THE UNIVERSITY OF MANITOBA to lend or sell copies of this thesis to the NATIONAL LIBRARY OF CANADA to microfilm this thesis and to lend or sell copies of the film, and UNIVERSITY MICROFILMS to publish an abstract of this thesis.

The author reserves other publication rights, and neither the thesis nor extensive extracts from it may be printed or otherwise reproduced without the author's written permission.

TABLE OF CONTENTS

ABSTRACT	v
ACKNOWLEDGEMENTS	vii
LIST OF FIGURES	viii
LIST OF TABLES	xiii
INTRODUCTION	1
Forward	1
Passive Diffusion	1
Carrier-Facilitated Diffusion	5
Active Transport	11
Transport Inhibition	14
Compendium I	20
Renal Epithelial Transport	21
Organic Anion Transport	23
Organic Cation Transport	28
Amantadine	35
Current Objectives	36
I. Stringency in Molecular & Spatial Requirements of Renal Tubular Organic Cation Transport	38
II. Renal Drug Interactions with Two Pharmacological Congeners	39
III. Potential Alteration of Renal Organic Cation Transport in Tobacco users	40
Compendium II	41
MATERIALS AND METHODS	43
Preamble	43
Renal Tubules	44
Renal Cortical Slices	49
Expression of Transport	53
Chemicals	55

RESULTS	56
I. Diastereoisomers & Renal Organic Cation Transport	
Purity of Tubule Suspensions	56
Control Amantadine Uptake	56
Control Amantadine Efflux	70
Uptake Inhibition by Quinine & Quinidine	70
Human Renal Cortical Slices	82
II. Pharmacological Congeners & Organic Cation Transport	
Control Uptake of Amantadine	90
Mixed Effects of Cimetidine	90
Inhibition by Ranitidine	94
Effects of Imidazole & Guanidine	94
III. Nicotine & Cotinine & Renal Organic Cation Transport	
Control Uptake in Tubules	94
(-) & (+) Nicotine on Amantadine Uptake	94
Nicotine on Amantadine Efflux	99
(-) Cotinine on Amantadine Uptake	99
Renal Cortical Slices	102
DISCUSSION	105
Amantadine as a Marker Organic Cation	105
Diastereoisomers & Organic Cation Transport	109
Congeners & Organic Cation Transport	114
Nicotine & Organic Cation Transport	118
Synopsis	122
Further Investigations	124
REFERENCES	130

ABSTRACT

The present experimentation addressed three aspects of renal tubular organic cation transport and interactions in rat and human preparations *in vitro*. Amantadine was employed as the marker organic cation with principal advantages being its therapeutic relevance, homogeneous and achiral chemical properties, and limited metabolism in mammalian tissue. Under control conditions, amantadine was concentrated actively by renal cortical slices, isolated proximal tubule and distal tubule. Apparent affinity (K_m) for uptake was observed to be comparable in all three preparations, while apparent maximal capacity (V_{max}) varied considerably in the order of proximal tubule > distal tubule > cortical slice. The first experimental series investigated chiral preferences in renal organic cation transport. Addition of 8S, 9R-(-)-quinine or 8R, 9S-(+)-quinidine stereoselectively inhibited amantadine accumulation in rat and human cortical slices (quinine > quinidine). Stereoselectivity was subsequently confirmed in proximal tubule, but not distal tubule. Functional mechanisms underlying such a phenomenon, and its clinical significance are discussed herein. The second aspect of investigation examined the effects of two pharmacological congeners, cimetidine and ranitidine. The predecessor drug, cimetidine, interfered with amantadine transport in isolated tubules in a biphasic fashion. High-affinity enhancement of amantadine accumulation by cimetidine was observed in the proximal tubule, whereas competitive inhibition of lower-affinity was evident in both tubule fractions. Conversely, ranitidine only produced competitive uptake inhibition at highly toxic concentrations. This relatively inert nature of low therapeutic plasma concentrations of ranitidine is supportive of its lower incidence of renal interaction with cationic drugs than its predecessor. The final series of experimentation studied two clinically and environmentally relevant organic cations, nicotine and cotinine.

The addition of nicotine or cotinine invoked similar biphasic interference of amantadine transport in proximal tubules, and maximal enhancement of uptake was elicited by concentrations documented in plasma of habitual tobacco smokers. In distal tubules, low-affinity inhibition of amantadine uptake was observed with highly toxic nicotine concentrations, and cotinine was without effect. Adjunct efflux experimentation with nicotine provided further insight into the current dichotomy of amantadine uptake, and putative mechanisms underlying such an interaction are postulated. Furthermore, the current data suggest potential alterations in renal cationic drug elimination in habitual tobacco users.

ACKNOWLEDGEMENTS

My utmost sincere gratitude to my two tolerant supervisors, Drs. Daniel S. Sitar and Donald D. Smyth, for their continual guidance and expertise, humour and friendship. I would also like to express my earnest appreciation to other "mentorious" figures (in alphabetical order): Dr. Gary B. Glavin, Dr. Patrick Montgomery, Dr. S. Brian Penner for their invaluable contributions towards my project and my well-being throughout the duration. Thank-you to Dr. Patrick Vinay for assuming the rôle as my external examiner, et merci d'être venu.

My laboratorial colleagues are definitely of worthy mention (again in alphabetical order): Mr. Thomas Davie, Dr. Francis Darkwa, Ms Dianne Kropp, Dr. Ping Li and Mr. James Sherwin for their continuous support. In specific, my heartiest thanks to Mr. Larry Bluhm, Mr. Donald Jones, Mrs. Catherine Lydon-Hassen, Ms Alison Taylor, Ms Sharon Thom and Ms Marilyn I. M. Vandel for the alacrity and excellence of their technical assistance, altruistic support and friendship. I am also grateful to the Manitoba Health Research Council for their financial support, and to all members of the Department of Pharmacology and Therapeutics.

Lastly, this thesis is dedicated to my family and to Ms Shirley Fitzpatrick for their continual encouragement. Do you feel like nineteen sixty-six? Do you feel the same?

© TO ALL LOST AND FOUND ©

LIST OF FIGURES

Figure I-1.	Graphical representation of Fick's Law on transmembrane diffusion of substrate (S).	3
Figure I-2.	The <i>Shuttle-Carrier</i> hypothesis in carrier-mediated substrate diffusion.	6
Figure I-3.	Carrier-mediated facilitated diffusion of a solute <i>via</i> a conformational change of the transport protein.	8
Figure I-4.	Graphical representation of the Michaelis-Menten equation on substrate transport kinetics.	10
Figure I-5.	Schematic diagram illustrating the sodium-dependent co-transport of sugar and proton in the small intestines.	13
Figure I-6a.	Representative Dixon plots showing competitive inhibition.	17
Figure I-6b.	Representative Dixon plots showing non-competitive inhibition.	18
Figure I-7.	A simplified diagram of the nephron with schematic representations showing the morphology of epithelial cells within individual tubule segments.	22
Figure I-8.	Schematic model for proximal tubular secretion of organic anions across basolateral and brush border cell membranes.	27
Figure I-9.	Chemical structure of N ¹ -methylnicotinamide (NMN).	32
Figure I-10.	Schematic model for proximal tubular secretion of organic cations across basolateral and brush border cell membranes.	34

Figure I-11.	Chemical structures of the organic cations employed in the present experimentation.	37
Figure M-1.	A schematic diagram illustrating the separation of rat renal cortical tissue on 50% Percoll gradient.	46
Figure M-2.	Schematic illustration of the preparation of rat renal cortical slices.	50
Figure M-3.	Effects of three concentrations of sodium hydroxide on the scintillation counting efficiency for tritiated amantadine.	54
Figure R-1.	Specific activities of enzyme markers in fractions of rat renal cortical nephron segments.	57
Figure R-2.	Active accumulation of [³H]amantadine by rat renal cortical slices as a function of time.	58
Figure R-3.	Active accumulation of [³H]amantadine by rat renal proximal tubules as a function of time .	59
Figure R-4.	A representative experiment demonstrating the effects of tetraethylammonium (TEA) and guanidine on amantadine accumulation into rat renal proximal tubules .	61
Figure R-5.	Representative saturation isotherm for active amantadine accumulation by rat cortical slices.	62
Figure R-6.	Representative saturation isotherm for active amantadine accumulation by isolated proximal tubules.	63
Figure R-7.	Representative saturation isotherm for active amantadine accumulation by isolated rat distal tubules.	64

Figure R-8.	Representative Lineweaver-Burk transformation of control amantadine uptake values in rat renal cortical slices.	65
Figure R-9.	Representative Lineweaver-Burk transformation of control amantadine uptake values in isolated rat proximal tubules.	66
Figure R-10.	Representative Lineweaver-Burk transformation of control amantadine uptake values in isolated rat distal tubules.	67
Figure R-11.	Conversion of rat renal cortical slice wet weight to cortical slice protein.	68
Figure R-12.	Michaelis-Menten kinetic parameters for rat renal cortical slices, isolated proximal tubules and distal tubules.	69
Figure R-13.	Effects of unlabelled amantadine on [^3H]amantadine efflux from rat renal proximal tubules.	71
Figure R-14.	Representative experiment showing [^3H]amantadine efflux from rat renal cortical slices.	72
Figure R-15.	A representative experiment showing the effects of quinine and quinidine on amantadine accumulation into rat renal cortical slices .	73
Figure R-16.	Effects of quinine and quinidine on amantadine accumulation into rat renal proximal tubules.	74
Figure R-17.	Effects of quinine and quinidine on amantadine accumulation into rat renal distal tubules.	75
Figure R-18.	Dixon analysis for [^3H]amantadine uptake by rat renal cortical slices in the presence of quinine .	76

Figure R-19. Dixon analysis for [^3H]amantadine uptake by rat renal cortical slices in the presence of quinidine.	77
Figure R-20. Dixon analysis for [^3H]amantadine uptake by rat renal proximal tubules in the presence of quinine.	78
Figure R-21. Dixon analysis for [^3H]amantadine uptake by rat renal proximal tubules in the presence of quinidine.	79
Figure R-22. Accumulation of [^3H]amantadine by human renal cortical slices as a function of time.	83
Figure R-23. Representative saturation isotherm for active amantadine accumulation by human cortical slices.	84
Figure R-24. Lineweaver-Burk transformation of control amantadine uptake values in human renal cortical slices.	85
Figure R-25. Conversion of human renal cortical slice wet weight to cortical slice protein.	86
Figure R-26. Dixon analysis for inhibition of [^3H]amantadine uptake by human renal proximal tubules by quinine.	87
Figure R-27. Dixon analysis for inhibition of [^3H]amantadine uptake by human renal proximal tubules by quinidine.	88
Figure R-28. Effects of cimetidine on amantadine accumulation into rat renal cortical slices.	91
Figure R-29. Effects of cimetidine on amantadine accumulation into rat renal proximal and distal tubules.	92

Figure R-30. Effects of ranitidine on amantadine accumulation into rat renal cortical slices.	95
Figure R-31. Effects of ranitidine on amantadine accumulation into rat renal proximal and distal tubules.	96
Figure R-32. A representative experiment demonstrating the effects of imidazole and guanidine on amantadine accumulation into rat renal proximal tubules.	97
Figure R-33. Effects of (-) and (+) nicotine on amantadine accumulation into rat renal proximal tubules.	98
Figure R-34. Effects of (-) and (+) nicotine on amantadine accumulation into rat renal distal tubules .	100
Figures R-35. Effects of (-) & (+) nicotine and cimetidine on amantadine efflux from rat renal proximal tubules and distal tubules.	101
Figure R-36. Effects of (-) cotinine on amantadine accumulation into rat renal proximal and distal tubules.	103
Figure R-37. Inhibition of (-) nicotine on amantadine accumulation in rat renal cortical slices.	104
Figure D-1. Putative sites of interaction between the diastereoisomers and amantadine in isolated rat renal proximal tubule.	112
Figure D-2. Putative sites of interaction between histamine H ₂ -receptor antagonists and amantadine in isolated rat renal tubules.	117
Figure D-3. Putative sites of interaction between nicotine and amantadine in isolated rat renal proximal tubule.	120

LIST OF TABLES

Table I-A.	Endogenous and synthetic organic anions transported actively by the renal tubules.	25
Table I-B.	Endogenous and synthetic organic cations transported actively by the renal tubules.	30
Table M-A.	Demography for patients who underwent unilateral nephrectomy and donated renal cortical tissue.	52
Table R-A.	[³ H]Amantadine accumulation by rat renal proximal tubules using 30 second and 4 minute incubation times.	80
Table R-B.	Inhibition of [³ H]amantadine accumulation into rat renal proximal tubules and cortical slices by quinine and quinidine.	81
Table R-C.	Michaelis-Menten and Dixon kinetic parameters for control [³ H]amantadine accumulation by human renal cortical slices using 30 second incubation.	89
Table R-D.	Effects of cimetidine and ranitidine on amantadine accumulation into rat renal proximal and distal tubules.	93
Table D-A.	Pharmacokinetic data for cationic drugs employed.	106

INTRODUCTION

Foreword. The fundamental focus of the present dissertation centers upon mechanisms and characteristics of organic solute handling by the mammalian kidney. Hitherto the introduction of the relatively more detailed aspects in renal tubular solute transport, it is imperative to first consider and comprehend the basic issues in regard to the transmembrane passage of chemical substances.

All biological membranes have common overall structures, which are assemblies of lipid and protein molecules held together by non-covalent interactions (Singer & Nicolson, 1972). The amphipathic lipid molecules (phospholipids, cholesterol and glycolipids) are arranged as a continuous double layer in which the hydrophobic interior of this bilayer serves as an efficient mean to restrict "undesired" traffic of water-soluble contents within and between cells. However, in view of the essentiality that living cells must regulate intracellular ion concentrations, ingest nutrients and eliminate endogenous and exogenous toxins; effective specific transmembrane transfer of inorganic and organic solutes represents a process of utter importance for the survival of any given organism. For this very reason, the teleological development of carrier-mediated intra- and inter-cellular transport processes was necessitated to facilitate the shuttle of such molecules.

Passive Diffusion. In thermodynamic terms, the tendency of a solute to move spontaneously in the direction of equilibrium can be viewed as a reflection of the general tendency of natural systems to strive to attain a condition of minimum free energy, or maximum entropy. Essentially if time is permitted, any chemical molecule is able to diffuse across a protein-free lipid bilayer down its concentration gradient by means of passive diffusion. However, the rate at which transfer occurs

varies enormously, and movement or flux of the substance can be described by *Fick's Law*:

$$V = \frac{dS}{dt} = \frac{P_k \cdot A}{x} ([S_1] - [S_2]) \quad (1)$$

"([S₁] - [S₂])" denotes the gradient between two regions of high and low solute concentrations respectively, and represents the primary driving force for diffusion ("V" or "dS / dt"). "A" represents the area of interface, "x" is the thickness of the membrane, and "P_k" denotes the permeability coefficient or diffusivity of the solute. The above equation states that the overall rate of penetration for a solute (S) is a linear function of the concentration gradient. This relationship is illustrated graphically in Figure I-1. It is evident that the gradient or slope generated in this plot is equal to (P_k.A / x), and that the permeability coefficient (P_k) can be calculated readily, if "A" and "x" are identified parameters. Previous studies have established the dependency of "P_k" upon temperature with direct proportionality, and the molecular size and shape of the solute. Such inter-relationships were first proposed in detail by the German physiologist, E. Overton, towards the end of the last century (Overton, 1899 & 1902). The "Overton's rules" state that permeability of uncharged small non-polar molecules is directly proportional to lipid solubility or lipophilicity, whereas permeability of uncharged polar or hydrophilic molecules is inversely proportional to the molecular size. Moreover, lipid bilayers are highly impermeable to all charged ions irrespective of their sizes (Michaelis, 1926).

In view of the fact that numerous endogenous and xenobiotic agents are weak organic acids or bases, the ability of such compounds to penetrate the cell membrane relies principally upon their state of ionization. These compounds are considerably more lipid-soluble in their nonionized form, and more water-soluble in their ionized form. The proportion of ionization depends upon the negative log

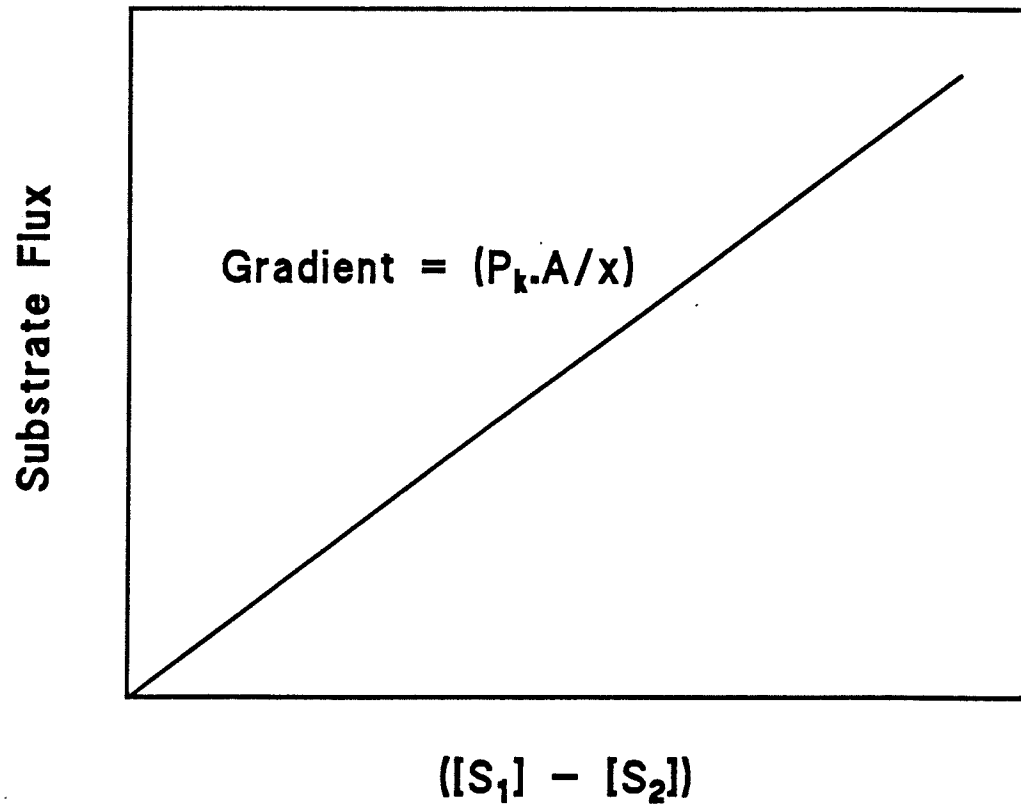
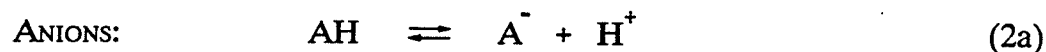


Figure I-1. Graphical representation of Fick's Law on transmembrane diffusion of substrate (S). $[S_1] - [S_2]$ denotes the concentration gradient across the membrane.

value of the ionization constant (pK_a) for the compound and the pH of the medium.

This can be evinced by the Henderson-Hasselbalch equations:



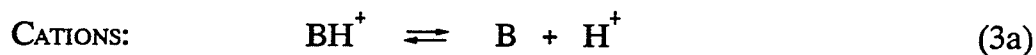
In solution, an uncharged anion is able to dissociate into its ionized form with the concurrent liberation of a proton. Hence with reference to **Le Chatelier's principle**, which states that *"if any constraint is applied to a system in equilibrium, the system will change in such a manner as to counteract this constraint as far as is possible"*, the extent of dissociation is variable as a function of the intrinsic proton concentration of the surrounding medium (pH).

$$K_a = \frac{[\text{A}^-][\text{H}^+]}{[\text{AH}]} \quad (2b)$$

$$\frac{K_a}{[\text{H}^+]} = \frac{[\text{A}^-]}{[\text{AH}]} \quad (2c)$$

$$pK_a - pH = \text{Log} \frac{[\text{AH}]}{[\text{A}^-]} \quad (2d)$$

Similarly, a cation may associate with a proton to become its ionized form in a pH -dependent manner.



$$K_a = \frac{[\text{B}][\text{H}^+]}{[\text{BH}^+]} \quad (3b)$$

$$\frac{K_a}{[H^+]} = \frac{[B]}{[BH^+]} \quad (3c)$$

$$pK_a - pH = \text{Log} \frac{[BH^+]}{[B]} \quad (3d)$$

Carrier-Facilitated Diffusion. The permeabilities mentioned insofar are related to the physical properties of the membrane bilayer, with the movement of substances according to their lipid solubility, molecular size and charge. However certain substances, including some highly charged polar molecules, traverse the membrane at faster rates than those accounted for by passive diffusion. These compounds utilize specific membrane transport mechanisms whereby their passage is facilitated by a carrier macromolecule with which they reversibly combine. Each receptive site is only able to "recognize" a single molecule or a limited range of chemically related molecules (e.g., sugars, amino acids and ions), and such specificity of the transport process was first inferred by previous investigations in which single gene mutations were observed to abolish the transport of certain sugars in procaryotes. Similar mutations are now recognized in humans who suffer from a variety of inherited diseases affecting the transport of specific solutes in the kidney or intestine (Oxender & Quay, 1975; Wilson, 1978).

Following binding, the conventional idea states that the substrate-carrier complex is considered to be lipid soluble, and translocation occurs whereby the entire complex traverses down its concentration gradient across to the opposite side of the membrane. The substrate is subsequently released and the carrier is recycled (Figure I-2). More recent concepts have challenged the probability of the above-mentioned mechanism, and the *shuttle proteins* have been superseded by carrier proteins which span the entire cross-section of the membrane *via* amphipathic

Concentration Gradient

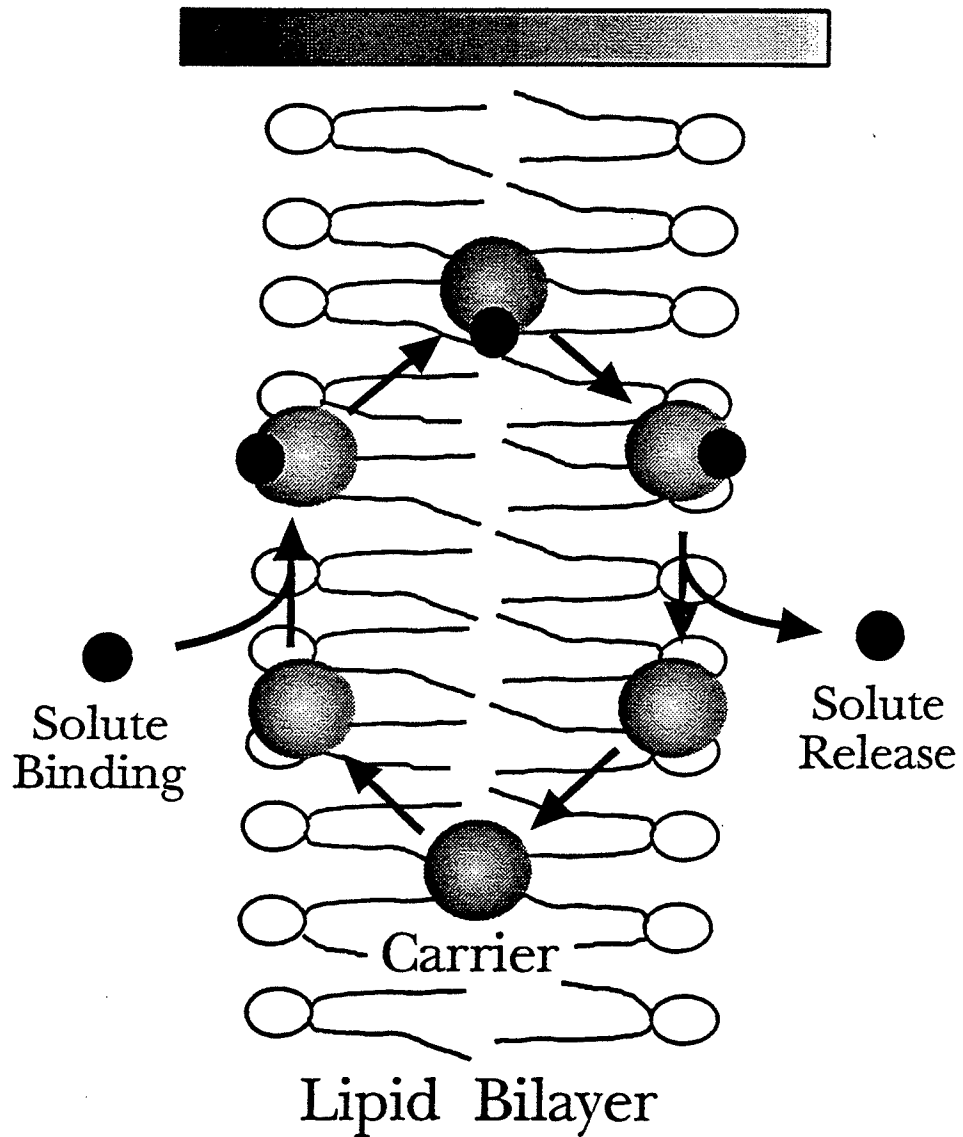
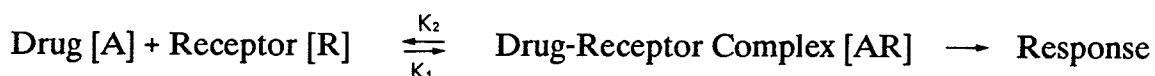
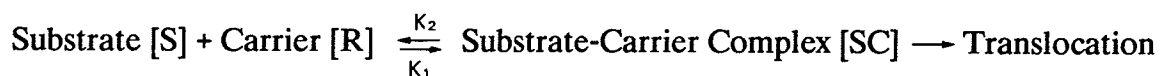


Figure I-2. The *Shuttle-Carrier* hypothesis in carrier-mediated substrate diffusion. The transported substrate is represented by filled circles, and the shuttling carrier molecule by shaded circle.

interactions. Subsequent to substrate recognition, such transmembrane proteins undergo conformational changes and mediate the translocation of the substrate across the membrane (Figure I-3). It is of importance that these transmembrane carriers are not to be confused with channel proteins (transmembrane pores which simply enable the tunneling of molecules of limited size and charge), although their kinetic characteristics have been documented previously to exhibit parallelism to each other (Patlak, 1957).

The association between the carrier receptor and its substrate can be viewed to be analogous to that between an enzyme and its substrate or between a drug and its receptor. In consideration of the *Occupation Theory* for drug-receptor interaction in quantitative pharmacology (Clark, 1937), the fundamental analogy can be summarized as follows:



"K₁" and "K₂" represent rate constants for association and dissociation of the complex, respectively. According to the law of mass action, the rate of the forward reaction is given by (K₁·[A]·[R]), whereas that for the reverse is (K₂·[AR]). At equilibrium, the rates of association and dissociation are equal. Therefore:

$$\frac{K_2}{K_1} = K_D = \frac{[A] \times [R]}{[AR]} \quad (4)$$

where "K_D" is the dissociation constant. The total number of receptors "[R_{tot}]" is the sum of receptors engaged in the formation of the complex "[AR]" and free receptors "[R]":

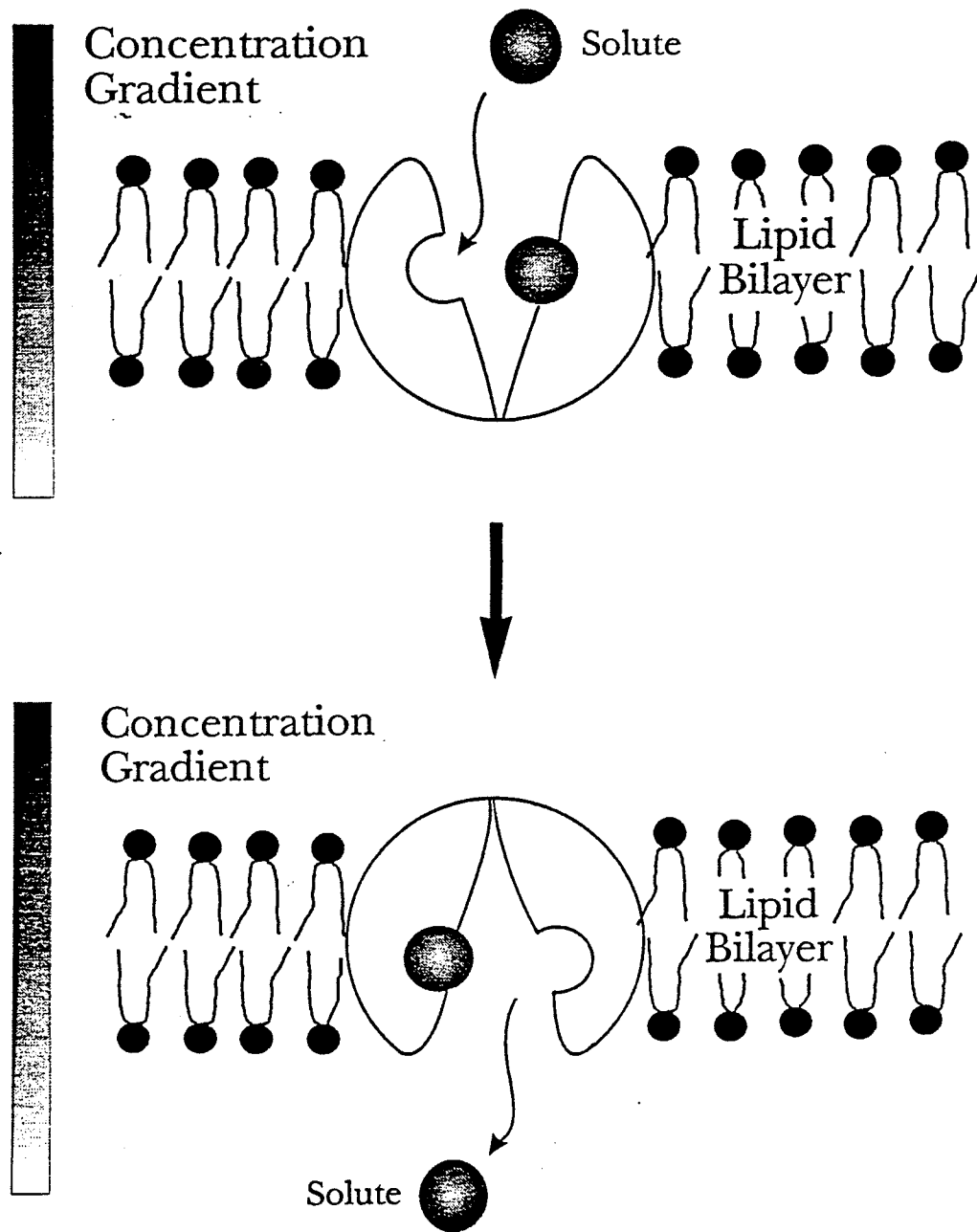


Figure I-3. Carrier-mediated facilitated diffusion of a solute *via* a conformational change of the transport protein. The carrier protein is able to assume two different conformational states, in which the substrate binding site becomes exposed and available at either surface of the membrane bilayer. Such a process is reversible, and the direction of substrate movement depends primarily upon its concentration gradient across the cell membrane.

$$[R] = [R_{tot}] - [AR] \quad (5)$$

By exchanging for R in equation 4, it can be rearranged to become a function of *fractional receptor occupation* in relation to its maximum ($[AR]/[R_{tot}]$) or *fractional response* (E/E_M) (Clark, 1937):

$$\frac{[AR]}{[R_{tot}]} = \frac{E}{E_M} = \frac{1}{1 + K_D/[A]} \quad (6)$$

In carrier-mediated transport, fractional binding or response is substituted by fractional velocity of transport (V) in relation to saturation (V_{max}):

$$\frac{V}{V_{max}} = \frac{1}{1 + K_m/[S]} \quad (7)$$

$$V = \frac{V_{max}}{1 + K_m/[S]} = \frac{V_{max}}{([S] + K_m)/[S]} \quad (8)$$

$$V = \frac{V_{max} \cdot [S]}{[S] + K_m} \quad (9)$$

The above transformation of the Clark equation has evidently revealed its equivalence to the classical Michaelis-Menten equation (Michaelis & Menten, 1903), and "K_D" is accordingly simulated by the Michaelis Constant (K_m). Transport exhibits saturation kinetics and flux velocity as a function of substrate concentration accommodates to the classical Langmuir isotherm (Figure I-4). Reiteration to

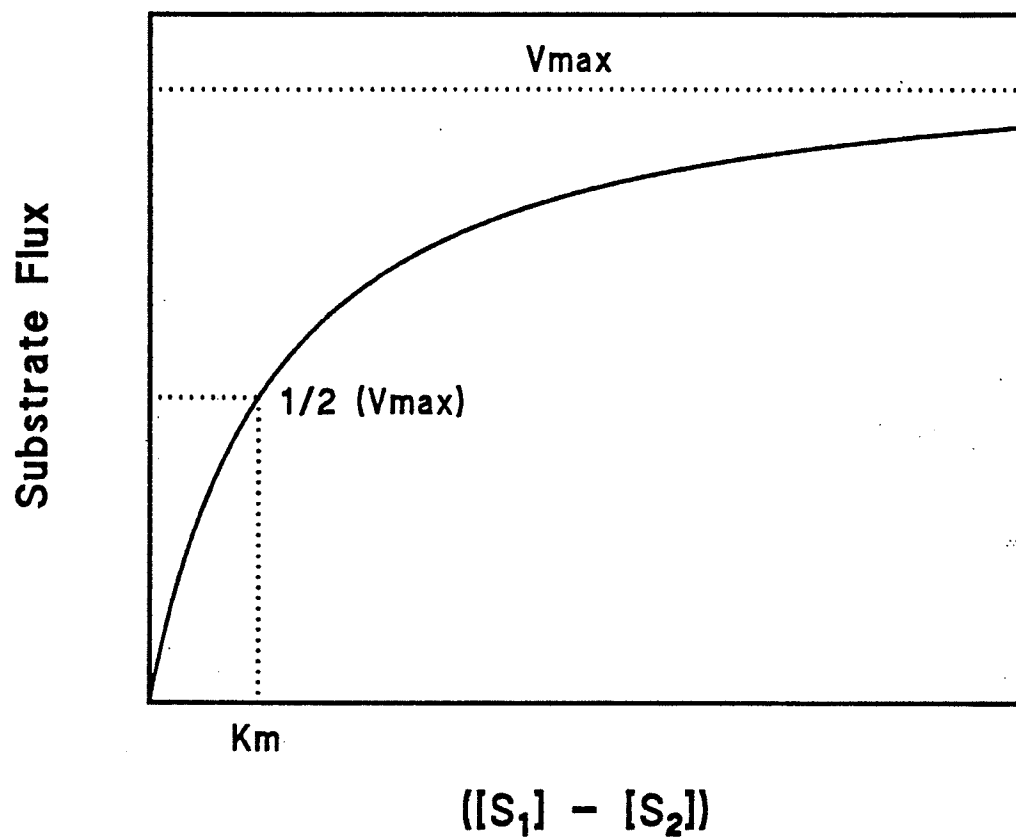


Figure I-4. Graphical representation of the Michaelis-Menten equation on substrate transport kinetics. $([S_1] - [S_2])$ denotes the substrate concentration gradient across the biological membrane. V_{max} is a measure of the apparent maximal capacity of the transport carrier, whereas K_m ($([S_1] - [S_2])$ at half V_{max}) is indicative of the apparent substrate affinity by the carrier.

Fick's law on simple diffusion reinstates the emphasis upon the concentration gradient being the primary driving force, and such an equation is adapted accordingly to incorporate the high and low substrate concentrations ($[S_1]$ and $[S_2]$ in equation 1):

$$V = V_{\max} \left[\frac{[S_1]}{[S_1] + K_m} - \frac{[S_2]}{[S_2] + K_m} \right] \quad (10)$$

With exhaustion of the concentration gradient at equilibrium (when $[S_1] = [S_2]$), net diffusion rate via the carriers (V) eventually becomes zero.

Active Transport. The transport processes mentioned above can only lead to equilibrium, and not accumulation. However in systems capable of "uphill" transport, net substrate transfer (V) should not equate to zero when $[S_1]$ and $[S_2]$ equilibrate. Kinetically, this is achieved by the introduction of different values of K_m on either side of the membrane through linkage with metabolism. Transport must be compensated energetically by a spontaneous process, and molecular flow of the substrate through the membrane is frequently mediated by an alternate flow produced primarily by the metabolic reaction (Rosenberg, 1948; Rosenberg & Wilbrandt, 1955).

To date, there exist few *primary active* transport processes in which transport is coupled directly to the energy source (Carafoli & Scarpa, 1982; Hoffman & Forbush, 1983; Ullrich, 1990). The majority of accumulative transport is *secondarily active via* co-transport systems (West, 1980; Geck & Heinz, 1989). These latter processes transport one solute in adjunct with a simultaneous or sequential transfer of a second solute. Vector of movement may occur either in the same direction *via symports* (Crane, 1960, 1962 & 1977; Mitchell, 1963), or in opposite directions *via*

antiports (Heinz *et al.*, 1972). Examples of such systems include the luminal reabsorption of glucose and secretion of protons in the intestinal tract, in which both processes are coupled to the inward sodium electrochemical gradient generated by the basolateral Na^+/K^+ ATPase (Figure I-5).

Two distinct influences of the driving current on the translocator have been postulated to be instrumental for coupling *via* symports and antiports. The presence of a driving ion may either modify the velocity of the translocator (*velocity effects*), and/or the affinity of the latter for the substrate (*affinity effects*). Under the usual assumption that carrier translocation represents the major rate-limiting step for overall transport rate, the relationship between energetic coupling and the magnitudes of transport parameters can be expressed by the following expression (Heinz *et al.*, 1972):

$$\text{Ratio} = R_{ab} \frac{(P_{ab} \cdot P_o)}{(P_a \cdot P_b)} \quad (11)$$

" R_{ab} " is the cooperativity coefficient with respect to the binding of the substrate (a) and the corresponding driving ion (b) to the carrier. " P_o , P_a , P_b and P_{ab} " are the permeation probabilities or velocity constants for the empty carrier, carrier-substrate complex, carrier-ion complex and the ternary complex respectively.

The occurrence of a velocity effect is identified by a difference between the ratio of velocity constants and unity. Symport coupling requires a ratio value of greater than unity, whereas coupling at the antiport requires a negative ratio. Whenever the ratio equates to unity, no energy transfer is possible. An affinity effect would result from cooperativity between substrate and driver ion for binding to the translocator, and values of " R_{ab} " must be positive and negative in symport and antiport coupling respectively.

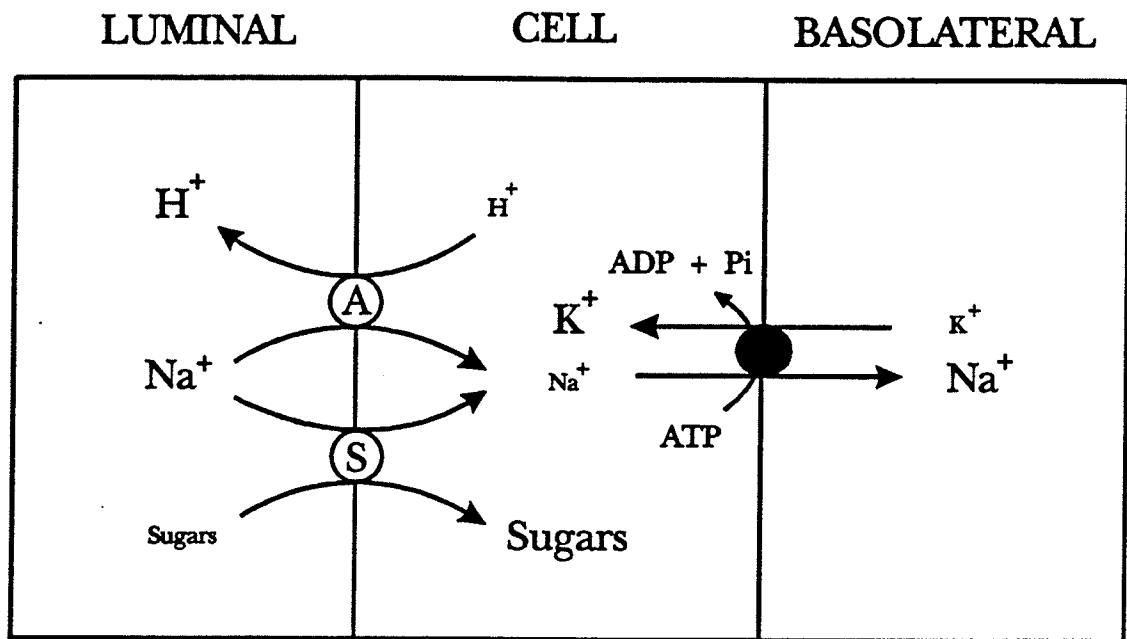


Figure I-5. Schematic diagram illustrating the sodium-dependent co-transport of sugar and proton in the small intestines. The reabsorptive flux of sodium is coupled to concurrent sugar reabsorption and proton secretion *via* a specific symport and antiport respectively. As such a sodium gradient is generated primarily by basolateral Na^+/K^+ -ATPase, the coupled fluxes of sugar and proton are termed secondarily active transport processes.

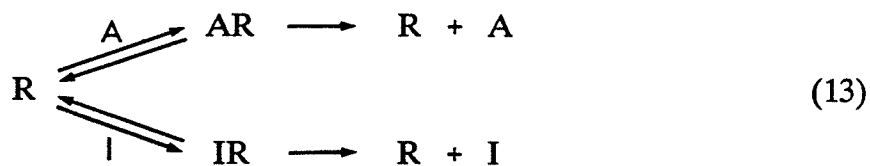
A more valid distinction between cooperativity and affinity effects may be based upon the Michaelis-Menten kinetics of equilibrium exchange, in which the equation is modified by the incorporation of the parameters from the above expression:

$$V = V_{\max} \frac{(1 + (P_{ab}/P_a) \cdot R_{ab} \cdot \beta) \cdot \alpha}{1 + \alpha + \beta + R_{ab} \cdot \alpha \cdot \beta} \quad (12)$$

With $\alpha = a/K_a$ and $\beta = b/K_b$ (Heinz *et al.*, 1972).

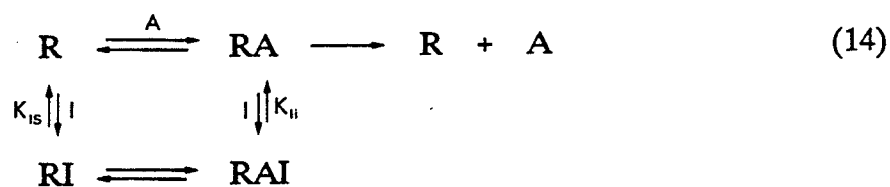
Few attempts have been made insofar to estimate the magnitude of the parameters in the above equation for any transport system, and only the following limited information may be extracted from the scattered data currently available in the literature. Experimentally, velocity effects are revealed by *trans*-effects of the driver current on substrate flux rate with the absence of the substrate on the *trans*-side. Conversely when substrate transfer is *cis*-affected by the driver current without significant alterations in V_{\max} , such a phenomenon is highly indicative of an affinity effect.

Transport Inhibition. In view of the substrate specificity of carrier-mediated transport, compounds with similar chemical configurations are liable to be recognized by common binding site(s). Consequently, the simultaneous exposure of a second substrate to the carriers will compete for translocation and inhibit that of the original one:



Before entering into the discussion of inhibition kinetics, it is useful to consider the different types of inhibition which may be encountered.

In a system involving active accumulation of the substrate, an obvious distinction between inhibitors would be ones which block the energy supply and linkage for transport, and those that interfere with substrate binding. A further division of the former include a blockade of the supply of the driver current for co-transport, and the direct inhibition of the energy yielding process. Examples of such compounds are cyanide, carbon monoxide, 2, 4-dinitrophenol and azides, and they are termed *metabolic* or *secondary* inhibitors. Inhibition of the adsorption and translocation of the substrate is produced by *primary* inhibitors, and it is this group which offers the most interest for the purposes of this present dissertation. Amongst primary inhibition, a number of different types are expected, depending upon the complexity of the system visualized. The two most commonly encountered types are *competitive* inhibition as mentioned above, and *non-competitive* inhibition in which inhibition occurs at a different binding site to the translocator:



The distinction between the two types of inhibition is facilitated by graphical methods such as the Lineweaver-Burk (Lineweaver & Burk, 1934; Cleland, 1963) and Eadie-Hofstee (Eadie, 1942; Scatchard, 1949; Hofstee, 1952) analyses. In competitive inhibition, only the apparent affinity of the receptor for the substrate (K_m) is decreased by the addition of the inhibitor, and the apparent maximal capacity (V_{max}) is relatively unchanged. Conversely in non-competitive inhibition, the situation is reversed in which V_{max} is apparently decreased with K_m unaffected. Such concepts can be viewed to be analogous to the affinity and velocity effects as

mentioned above.

The potency of an inhibitor is dependent upon its affinity at the site of interaction. If one envisages the adsorption of an inhibitor (I) to its site of inhibition (R) with reference to Clark's Occupation Theory (*vide supra*):

$$\frac{[IR]}{[R_{tot}]} = \frac{1}{1 + K_i / [I]} = \frac{[I]}{K_i + [I]} \quad (15)$$

IR represents the inhibitor-receptor complex and K_i is the inhibitory constant. The incorporation of the parameter $(1 + [I]/K_i)$ extends the Michaelis-Menten equation to:

$$V = \frac{V_{max} \cdot [S]}{[S] + K_m \cdot (1 + [I] / K_i)} \quad (16)$$

With rearrangements, the equation is transformed into a linear function of $(y = m \cdot x + c)$ (Dixon, 1953) and is illustrated graphically in Figures I-6a and 6b:

$$\frac{1}{V} = \frac{K_m}{V_{max} \cdot [S]} + \frac{1}{V_{max}} + \frac{K_m}{V_{max} \cdot [S]} \frac{[I]}{K_i} \quad (17)$$

In competitive inhibition, the intersection point for lines S_I and S_{II} ($1/V = [I]$) lies above the abscissa, and its down-extrapolation onto the abscissa provides the negative value of K_i . However in non-competition, S_I and S_{II} do not intersect but meet at a point on the abscissa giving $-K_i$. The actual X-intercepts by S_I and S_{II} represent a function of $(-K_i ([S]/K_m + 1))$, and the relative variability of such a parameter in Figure I-6a in comparison to that in Figure I-6b once again illustrates

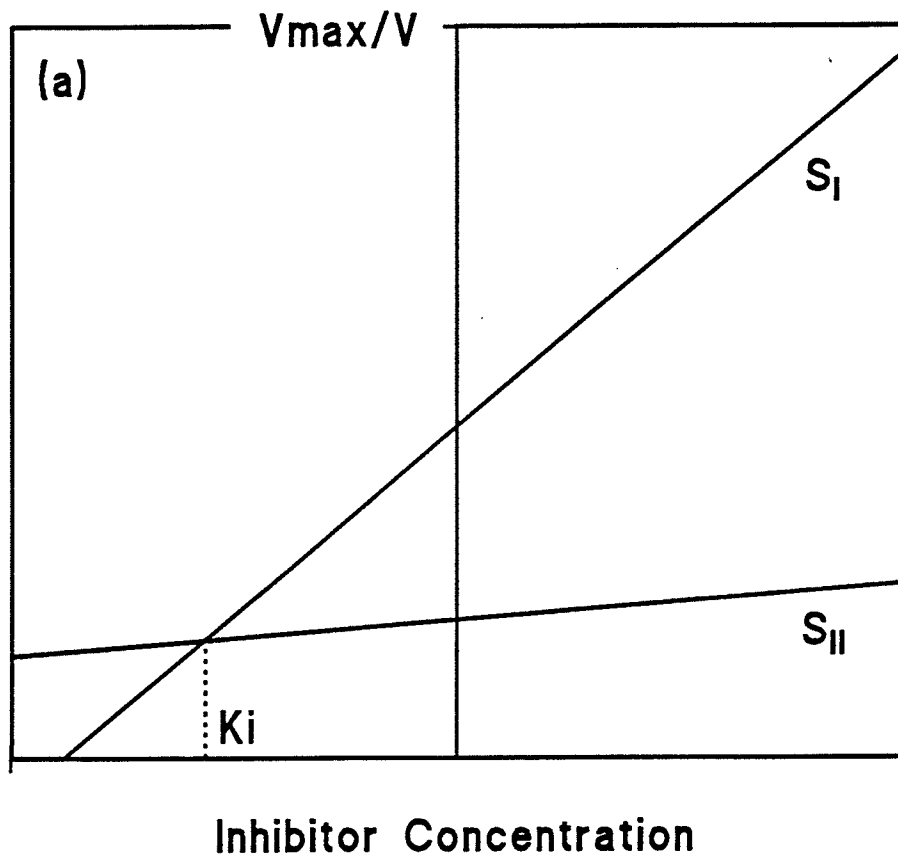


Figure I-6a. Representative Dixon plots showing competitive inhibition. V represents the rate of substrate movement and V_{max} is the apparent maximal capacity of transport. S_I and S_{II} represent the two substrate concentrations, and down-extrapolation of their intercept onto the abscissa presents the inhibitory constant (K_i).

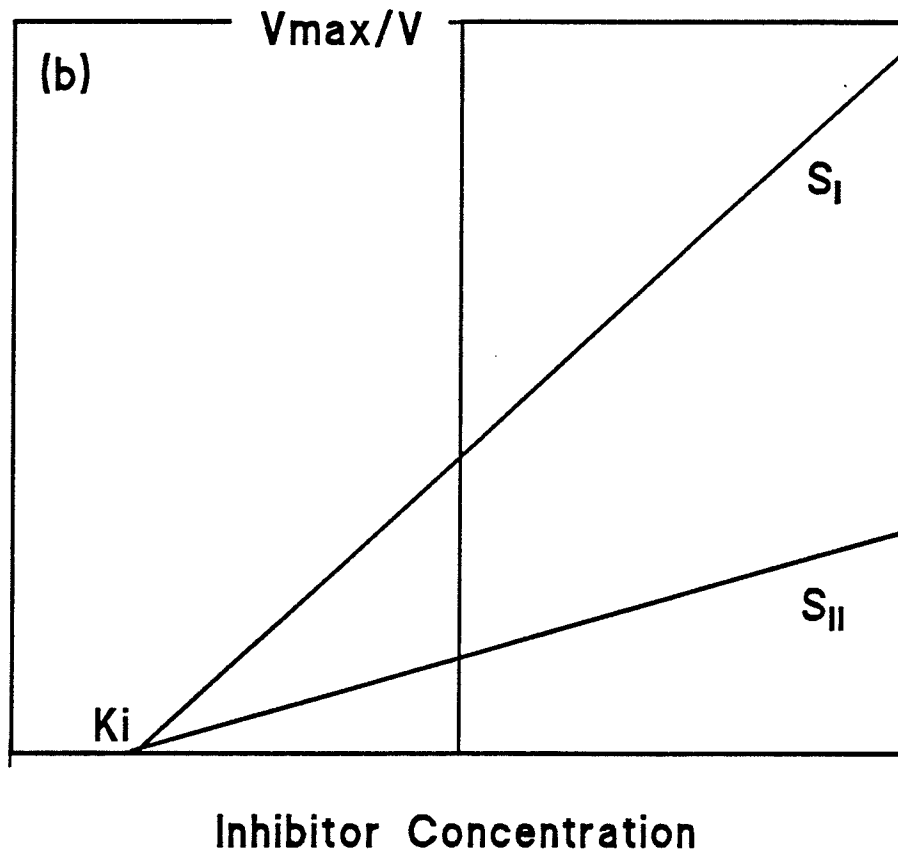


Figure I-6b. Representative Dixon plots showing non-competitive inhibition. V represents the rate of substrate movement and V_{max} is the apparent maximal capacity of transport. S_I and S_{II} represent the two substrate concentrations, and their intercept at the abscissa denotes the inhibitory constant (K_i).

competitive and non-competitive inhibition respectively.

In spite of the simplicity of the Dixon procedure in determining inhibitory constant values, the use of an arithmetic scale for inhibitor concentrations on the abscissa attenuates its ability to detect multiple-site interactions. An alternative method has been documented which involves the use of the IC₅₀ value (Cheng & Prusoff, 1973). IC₅₀ is the concentration of the inhibitor at which 50 % inhibition is produced, and it is readily extracted or calculated from the semi-logarithmic competition or displacement curves. However it is imperative to stress the invalidity of direct comparison of IC₅₀ values between laboratories, as such a parameter is widely variable depending upon the substrate concentrations employed in individual experiments.

The association between IC₅₀ and K_i can be demonstrated with the use of equations 13 and 16 (competitive inhibition). When [I] = IC₅₀, V = 2V_i (velocity of transport in the presence of inhibitor).

$$\frac{V_{\max} \cdot [S]}{[S] + K_m} = \frac{2 V_{\max} \cdot [S]}{[S] + K_m (1 + IC_{50} / K_i)} \quad (18)$$

By rearrangement, K_i can be calculated accordingly:

$$IC_{50} = K_i \left[1 + \frac{[S]}{K_m} \right] \quad (19)$$

In the case of non-competitive inhibition, the inhibitor exerts its action by binding onto disparate site(s) to the translocator site of the free carrier or the substrate-carrier complex (equation 14). Hence the corresponding inhibition component needs to be incorporated into both denominators in the Michaelis-

Menten equation:

$$V_i = \frac{V_{\max} \cdot [S]}{[S] + K_m} = \frac{2 V_{\max} \cdot [S]}{K_m (1 + IC_{50} / K_{Is}) + [S] (1 + IC_{50} / K_{Ii})} \quad (20)$$

When $K_{Is} = K_{Ii}$ (equation 14), the IC_{50} value approximates to K_i .

Compendium I. General criteria and properties for carrier-mediated transport of a substance are as follows (Wilbrandt & Rosenberg, 1961):

1. Transmembrane flux of the substrate is greater than that anticipated with simple diffusion.
2. Rate of transport exhibits saturation kinetics: As the substrate concentration increases, rate of transfer reaches an eventual asymptote.
3. The carrier protein possesses chemical specificity, so that only substrates with the requisite chemical structure are transported. In general, specificity of most transport systems is not absolute, and it is relatively less stringent than that of enzymes.
4. Structurally related molecules may alter the transport of the substrate. These may compete for a common carrier and inhibit transfer (*cis-competition*); or facilitate counter-transport of the substrate in the reverse direction (*trans-stimulation*).
5. The demonstration of uphill concentrative transfer of a substrate is highly suggestive of carrier-mediated transport.

Carrier-mediated transport has been widely examined and documented in

numerous tissues of epithelial origin, viz. kidneys, liver, gastrointestines, thyroid, choroid plexus and anterior uvea. In general, tissues utilize transport mechanisms in relocation of both inorganic and organic anions and cations within body fluids, and only the liver and kidney employ such mechanisms for their elimination from the body.

Renal Epithelial Transport. The kidneys play a critical role in maintaining the consistency of the internal environment by regulating water and electrolyte balance within the body. They also have the responsibility to eliminate both endogenous waste products and exogenous toxins, while simultaneously conserving valuable nutrients to the organism.

The functional unit of the kidney is the nephron, which is enumerated to be approximately one million per human kidney. Depending upon their morphological location within the kidney, they are categorized into *superficial cortical*, *midcortical* or *juxtamedullary* nephrons. These three nephrons are heterogeneous in their morphological structure and overall functions (Beeuwkes, 1980; Bulger & Dobyan, 1982). However, the general sequence and nomenclature for the individual tubular segments are as follows (Kriz & Bankir, 1988). Each nephron consists of a vascular component called the *glomerulus* which links to a tubular component *via* the Bowman's capsule. The entire tubule is composed of a single layer of epithelial cells of heterogeneous morphology and function (Tisher & Madsen, 1991; Vander, 1991) (Figure I-7). For the purpose of reference, the tubular component is traditionally divided into four segments. At the beginning in the renal cortex, the segment that drains the Bowman's capsule is the **proximal tubule**. It consists of numerous coils termed *pars convoluta*, followed by a straight portion descending into the renal medulla (*pars recta*). The medullary segment of the nephron is called the thin **Loop of Henle**, and it is distinguished into descending and ascending limbs.

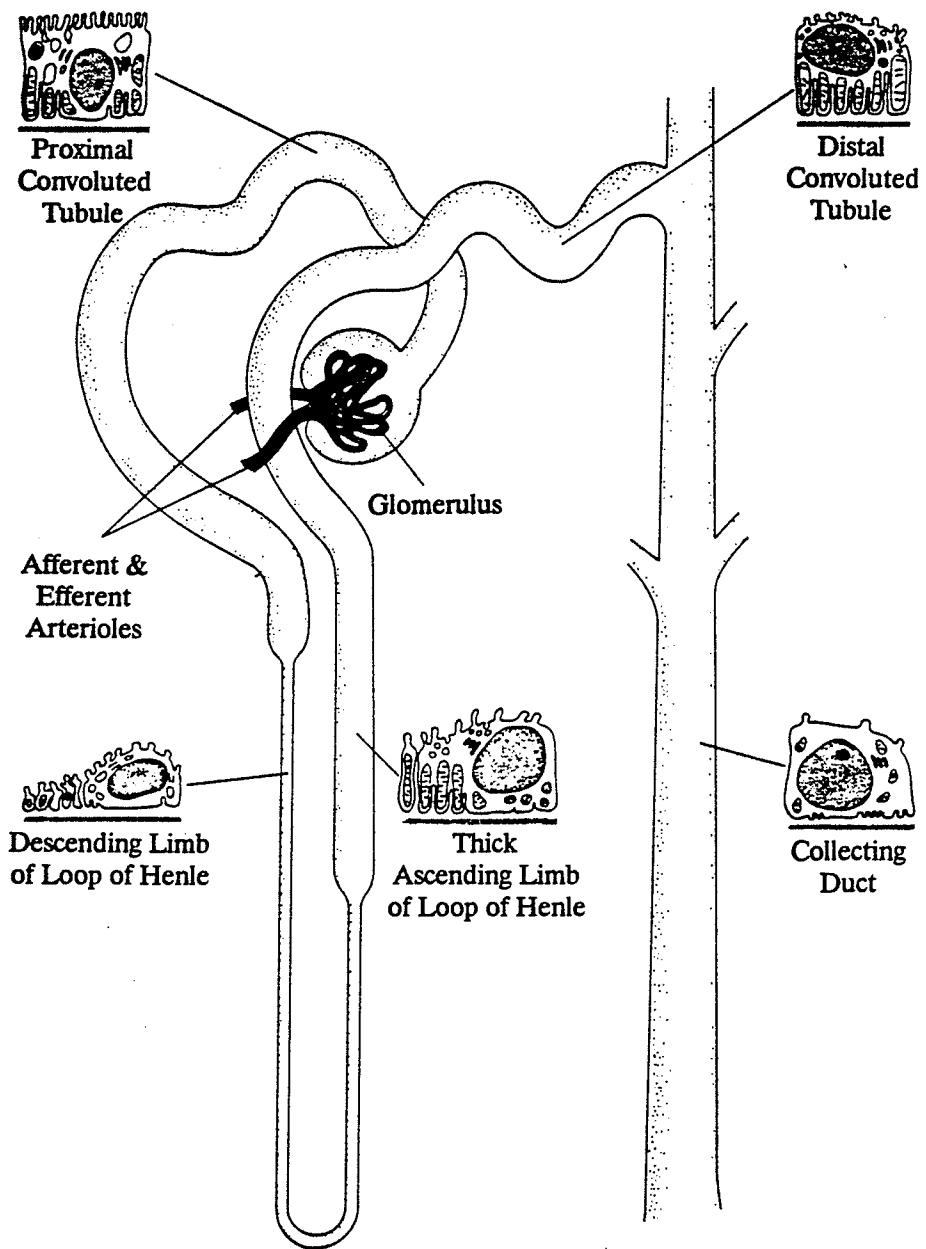


Figure I-7. A simplified diagram of the nephron with schematic representations showing the morphology of epithelial cells within individual tubule segments (adapted from Figure 1-3, pp. 8, Vander, 1991).

Upon re-entry into the cortex, the ascending thin Loop of Henle leads into the thick Loop of Henle and distal convoluted tubule. These are collectively referred to as the **distal tubule**. The distal tubule then coalesces with the **collecting tubule**, which ultimately drains into the cortical and medullary **collecting ducts**.

Historically, the concurrent assessment of the renal *Malpighian bodies* (Malpighi, 1666; Hayman, 1925) by William Bowman (1816-1892) and Carl Ludwig (1816-1895) had revealed the role of the glomerulus to be "*an apparatus designed to separate from the blood the watery portion*" (Bowman, 1842). However with regard to the function of the remainder of the nephron, their ideas were altogether divergent. Ludwig doctrined the formation of the watery portion at the glomeruli by means of a process called *ultrafiltration*, and the renal tubules were agents for reabsorption. The salvage of filtrate constituents was proposed to be a non-specific physicochemical process termed *endosmosis*. Conversely, Bowman conceived of the renal tubules to be secretory agents. Waste products of the body are compacted into *effete particles* and are then discharged into the tubular lumen in an analogous manner to the apocrine glands. These two seemingly competing theories at the time were considered in their entirety: they were either entirely "right" or "wrong" with no giving ground. It was conceivable that the "Ludwig hypothesis" of tubular reabsorption was prevalent up to the early nineteenth century. Subsequently, experimental evidence continued to accumulate in support of both phenomena, and it was decades later when their co-function was mutually recognized.

Organic Anion Transport. The first cogent studies which support renal tubular secretion were performed by Marshall and co-workers using an organic anionic dye (Marshall & Vickers, 1923; Marshall & Crane, 1924; Marshall, 1931; Marshall & Grafflin, 1932). In these studies, cortical tubular accumulation of phenolsulfonephthalein (phenol red) was demonstrated in canine kidney in the

absence of glomerular filtration. Thereafter, such observations had incited the potential physiological and pharmacological significance of tubular secretion in renal handling of endogenous and therapeutic organic solutes. The renal excretion of numerous other organic anions (Table I-A) was examined extensively by other investigators, and functional characteristics of the tubular transport carriers involved were pursued through the use of prototypic organic anion markers such as 3, 5-diiodo-4-pyridone-N-acetic acid (Diodrast[®]), para-di-N-propylsulfamylbenzoic acid (probenecid) and para-aminohippuric acid (PAH) (Smith *et al.*, 1938; Beyer *et al.*, 1950; Forster & Copenhaver, 1956; Sperber, 1959; Tune *et al.*, 1969; Ross & Weiner, 1972; Möller & Sheikh, 1983).

Throughout the development of the underlying mechanism for renal organic anion secretion, acceptance is granted in general for the involvement of a translocating process for the ionized species of organic anions. Paracellular flux of organic anions has been shown to be negligible in relation to total net transfer (Wedeen & Jernow, 1968; Wedeen & Weiner, 1973 a & b). Numerous studies using methodology such as clearance, micropuncture, stop-flow and in vitro microperfusion techniques have confirmed independently that organic anions are actively transported in the proximal tubules of a wide spectrum of animal species. The primary driving current is believed to be the sodium electrochemical gradient generated by ATP hydrolysis through Na^+/K^+ ATPase in the tubular basolateral membrane (Foulkes & Miller, 1959; Burg & Orloff, 1962; Podevin & Boumendil-Podevin, 1977; Möller & Sheikh, 1983; Ross & Holohan, 1983; Grantham & Chonko, 1991). Such an inward current is coupled to dicarboxylate ions (such as glutaric acid) at basolateral symports where they are co-transported into the cell. Subsequently, the deposited dicarboxylate is exchanged for extracellular organic anion *via* a tertiary active antiport, and is then carried into the lumen by simple or facilitated diffusion across the brush-border membrane (Cho & Cafruny, 1970; Tune

Table I-A. Endogenous and synthetic organic anions actively transported by the renal tubules.

Endogenous	Synthetic
Bile acids	Acetazoleamide
Cyclic AMP	<i>p</i> -Aminohippuric acid
Di- and Tri- carboxylic acids	Aminosalicyclic acid
Fatty acids	Cephaloridine
Glucuronic acid conjugates	Chlorpropamide
Glycine conjugates	Chlorthiazide
Hippuric acid	Diodrast
Hydroxybenzoic acids	Ethacrynic acid
5-Hydroxyindolacetic acid	Frusemide
Lactic acid	Indomethacin
Nicotinic acid	Mersalyl
Oxalic acid	Penicillin
Prostaglandins	Phenol red
Uric acid	Phenylbutazone
Sulphate conjugates	Probenecid
	Saccharin
	Salicylic acid
	Thiazides

& Fernholt, 1973; Wedeen & Weiner, 1973 a & b; Foulkes, 1977; Ross & Holohan, 1983). This "state of the art" model for renal tubular organic anion secretion is presented in Figure I-8 (Pritchard, 1988; Shimada *et al.*, 1988).

Pronounced intratubular heterogeneity of organic anion transport has been observed in the proximal tubule (Burg *et al.*, 1966; Tune *et al.*, 1969; Woodhall *et al.*, 1978 and Shimomura *et al.*, 1981). As above-mentioned, each proximal tubule is comprised of initial convoluted (*pars convoluta*) and terminal straight (*pars recta*) segments. But within these two subdivisions, there are further anatomical differences as one proceeds axially from the convoluted to straight portions. In the convoluted tubule (S₁ segment), the epithelial cells have relatively thick brush-borders and the intracellular basolateral membranes are highly folded (Ross & Holohan, 1983). The junction of convoluted and straight tubules is designated the S₂ segment, and the last portion of the *pars recta* is the S₃ region. Rates of PAH secretion and intracellular accumulation have been observed to be heterogeneous between proximal tubule segments in both superficial and juxtamedullary nephrons. This axial heterogeneity has been suggested to be a reflection of an uneven distribution of transporters of common affinity along the tubule, although an absolute rank order of transport capacity between segments is unavailable owing to significant species differences (Haberle, 1975; Schali & Roch-Ramel, 1981; Shimomura *et al.*, 1981). In both superficial and juxtamedullary proximal tubules of the rabbit, PAH is mainly secreted in the S₂ segment; the secretory rate is approximately five-fold lower in S₁ and S₃ portions (Shimomura *et al.*, 1981).

Prominent examples of clinically significant advances that resulted from the above-mentioned experimentation include an improved understanding of alterations in disposition of endogenous and xenobiotic organic anions in drug co-administration and renal insufficiency (White, 1966; Preuss *et al.*, 1966; Hook & Munro, 1968; Bourke *et al.*, 1970; Porter *et al.*, 1975), and the introduction of

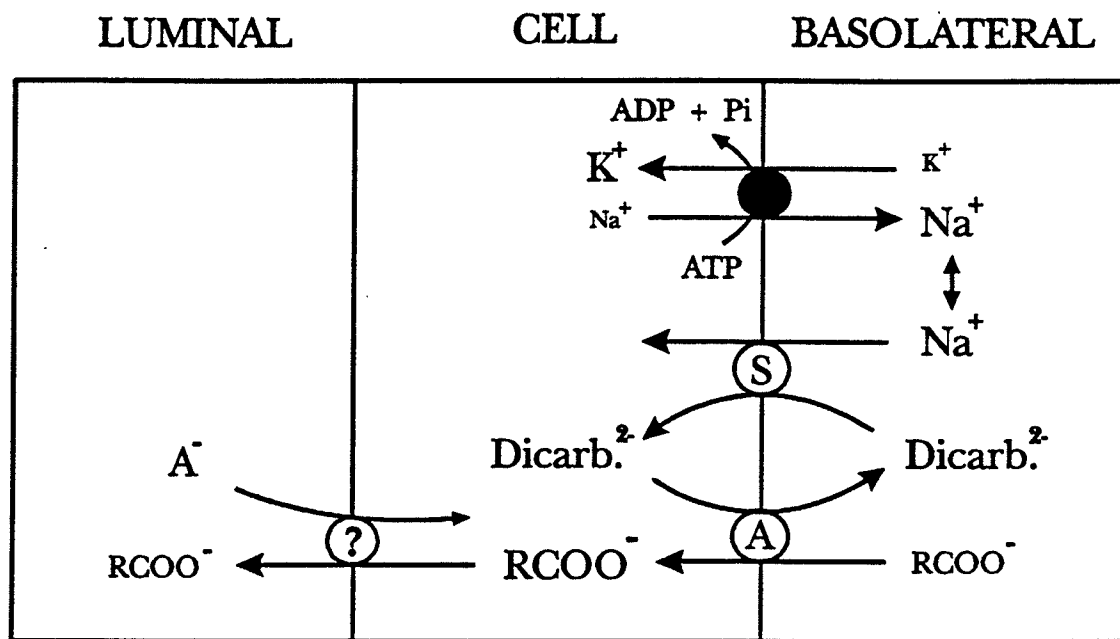


Figure I-8. Schematic model for proximal tubular secretion of organic anions across basolateral and brush border cell membranes. Active and carrier-mediated facilitated transport sites are represented by filled and open circles respectively. (S) and (A) denote symport and antiport respectively, and characteristics of the luminal antiport is not fully elucidated at present.

probenecid and "loop diuretics" in drug therapy: Following the serendipitous discovery of the penicillins, their remarkable antibacterial properties had ensued their widespread use in chemotherapy (Fleming, 1946; Florey, 1946; Chain, 1954). However, the action durations of penicillins and their congeners are inconveniently brief owing to their avid elimination from the body *via* active renal proximal tubular secretion. Co-administration of probenecid competitively inhibits the renal elimination of such antibiotic agents and significantly prolongs their plasma half-life values (Beyer *et al.*, 1944; Beyer, 1950). Secondly, the uricosuric effect of probenecid has been proven invaluable in gout therapy (Gutman, 1966; Boss & Seegmiller, 1979; Rodnan, 1982; Grantham & Chonko, 1991). The latter condition is a chemical disease with precipitation of urate crystals in joint tissues, and treatment with probenecid alleviates the hyperuricemia by inhibition of urate reabsorption in renal proximal tubule. Lastly, the "loop" or "high-ceiling" diuretic agents are secreted by the organic anion transport system (examples are furosemide, ethacrynic acid and bumetanide). As these compounds are extensively bound to serum proteins, carriage of the active drug to its luminal sites of action relies predominantly upon active proximal tubular secretion (Imai, 1977; Flamenbaum & Friedman, 1982; Reineck & Stein, 1982; Stoner & Trimble, 1982; Brater, 1983). Hence it is of prime importance that the dosage regime must be adjusted accordingly when such agents are co-administered with other anionic drugs in combination therapy, as the latter compounds are liable to compete with their renal excretion and displace their plasma protein binding (Hook & Williamson, 1965; Bailie *et al.*, 1975).

Organic Cation Transport. In comparison to the voluminous magnitude of investigation into the physiology and pharmacology of renal tubular organic anion transport, renal transport of organic cations has been relatively neglected (Rennick

& Farah, 1956; Berndt, 1981; van Ginneken & Russel, 1989). Such an appreciable prevalence is analogized befittingly by Grantham and Chonko as: "*If the renal secretion of organic anions has seldom been in the 'center court' of renal physiology, the organic cation transport system has never even received an invitation to the tournament*" (Grantham & Chonko, 1986).

The first demonstration of renal tubular secretion of organic cations was documented over a decade subsequent to Marshall's experimentation on PAH, when Robert Chambers (1881-1957) and Rudolph Kempton (1902-1972) described the excretion of an organic base, neutral red, by doubly-perfused frog kidneys (Chambers & Kempton, 1937; Kempton, 1939). Owing to the fact that phenol red is extensively bound to plasma proteins, excretion of this compound was scarce when it was presented to the renal glomeruli *via* the arterial system. However, excretion was observed to be abundant when neutral red was presented directly to the peritubular circulation *via* the renal portal system. In 1947, Barbara Rennick and her colleagues demonstrated the mammalian tubular secretion of tetraethylammonium (TEA) in canine kidneys (Rennick *et al.*, 1947); whilst Ivar Sperber reported almost simultaneously the renal secretion of another organic cation, N¹-methylnicotinamide (NMN), in chickens (Sperber, 1947 & 1948). Thereafter, a diverse group of organic cations, ranging from primary amines to quaternary ammonium compounds, has been reported to be transported by the kidney *in vitro* (Table I-B). The more commonly employed organic cation probes include TEA and NMN as mentioned above, in addition to choline and procainamide. TEA is principally the substrate of choice, as it is not metabolized appreciably by renal tubule cells (Rennick, 1981; Besseghir *et al.*, 1981).

An obvious issue in regard to the mechanism underlying organic cation secretion is whether organic anions and cations are transported by common processes. Investigation with various prototypic anionic and cationic substrates as

Table I-B. Endogenous and synthetic organic cations actively transported by the renal tubules.

Endogenous	Synthetic
Acetylcholine	Amantadine
Adrenaline	Amiloride
Choline	Amprolium
Creatinine	Atropine
Dopamine	Cimetidine
Guanidine	Decamethonium
Histamine	Hexamethonium
5-Hydroxytryptamine	Mecamylamine
N ¹ -methylnicotinamide	Meperidine
Noradrenaline	Mepiperphenidol
Thiamine	Morphine
	Neostigmine
	Nicotine
	Paraquat
	Procainamide
	Quinine & quinidine
	Tetraethylammonium
	Tolazoline

competitive inhibitors did not demonstrate cross-inhibition between the two classes of compounds (Sperber, 1949 & 1954). However, more recent studies have demonstrated affirmations and exceptions to the rule (Hsyu *et al.*, 1988; Gisclon *et al.*, 1989; Inotsume *et al.*, 1990; Ott *et al.*, 1990; Lam *et al.*, 1991), and this issue of cross-interaction remains controversial. An aspect of interest and importance is the consideration of potentially heterogeneous chemical constituents within the compounds of examination. Although the "cationic" NMN is utilized widely in the examination of organic cation transport, it does however possess an acidic amido moiety within its structure (Figure I-9). Therefore it is prudent to instigate the question of applicability for the proposed role of NMN as a representative marker for organic cations.

With the proliferation of micropuncture techniques, axial heterogeneity in the secretion of organic cations along the proximal tubule has also been documented (McKinney *et al.*, 1981; McKinney, 1982; McKinney & Speeg, 1982). However, in comparison with that observed in the organic anion transport system (*vide supra*), its distribution pattern for the transporters appears to be dissimilar. In the rabbit, secretory rates for procainamide were shown to follow a sequential pattern of $S_1 > S_2 > S_3$ in the superficial proximal tubule, whereas secretion was higher in S_1 and S_2 than S_3 segments in juxtamedullary segments (McKinney, 1982; McKinney & Speeg, 1982). Although renal organic cation transport is reported to exhibit substantial variability among animal species (McIsaac, 1965 & 1969; Besseghir *et al.*, 1981; Rennick, 1981; Grantham & Chonko, 1991), such a discrepancy within the same species represents further evidence for the individuality of the two types of transporters involved.

In general, renal tubular secretion of organic cations into the lumina is believed to be mediated *via* an active process, and the energy is derived primarily from the sodium electrochemical gradient generated by the basolateral Na^+ / K^+

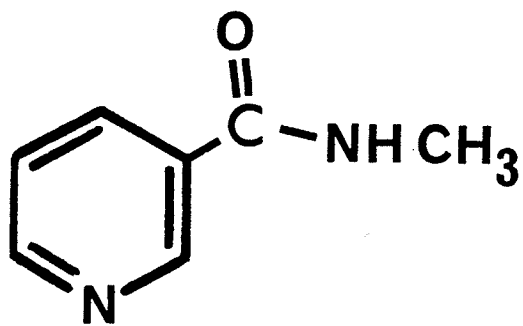


Figure I-9. Chemical structure of N^L-methylnicotinamide (NMN).

ATPase (Peters, 1960; Berndt, 1976 & 1981; Holohan & Ross, 1980; Rennick, 1981). With the development of the methodology for preparation of sealed membrane vesicles of basolateral or antiluminal origin (Fitzpatrick *et al.*, 1969; Heidrich *et al.*, 1972; Kinsella *et al.*, 1979b; Boumendil-Podevin & Podevin, 1983), more intricate investigations into the translocation and coupling mechanisms for the secretory process at the sub-cellular level were enabled.

Traditionally, transfer of the organic cation across the basolateral membrane is thought to involve a potential-sensitive, facilitated diffusion pathway (Kinsella *et al.*, 1979a; Holohan & Ross, 1980 & 1981; Ross & Holohan, 1983; Takano *et al.*, 1984; Somogyi, 1987; Smith *et al.*, 1988; Sokol & McKinney, 1990). However, this postulate is supplemented by more recent evidence which supports the participation of an active basolateral transporter (Schali *et al.*, 1983; Tarloff & Brand, 1986; Wright & Wunz, 1987; Besseghir *et al.*, 1990a; Brändle & Greven, 1991). The luminal transfer of organic cations has been proposed to be a tertiary active process, and the link between the primary sodium electrochemical gradient and the organic cation secretory carrier is the Na⁺/H⁺ antiport in the luminal membrane. The primary sodium current in the reabsorptive direction (lumen to cell) facilitates the secretory flux of hydrogen ions at the Na⁺/H⁺ antiport. The secreted proton in the tubule lumen then exchanges for an intracellular organic cation *via* a disparate luminal organic cation/H⁺ antiport with 1 : 1 stoichiometry (Sokol *et al.*, 1985). An updated version of the working model for renal tubular secretion of organic cations is presented in Figure I-10.

Prior to the development of the newer therapeutic organic cations, the use of the conventional compounds in *in vivo* experimentation has been limited primarily by their intense toxicity and ability to invoke cardiovascular disturbances in the whole animal situation, *viz.* TEA and mecamylamine (Rennick, 1981; Ross & Holohan, 1983; Somogyi, 1987). Although the Sperber approach *in vivo* exploits the

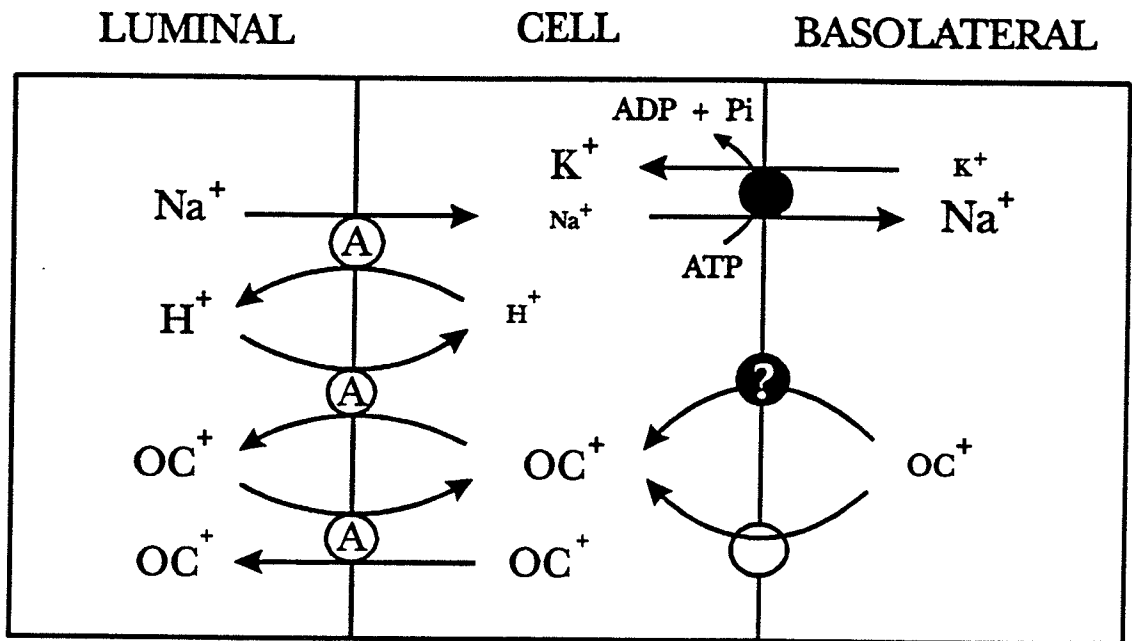


Figure I-10. Schematic model for proximal tubular secretion of organic cations across basolateral and brush border cell membranes. Active and carrier-mediated facilitated transport sites are represented by filled and open circles respectively. (A) Denotes luminal antiports. Characteristics and energy linkage for the tentatively active basolateral organic cation secretory site is presently undefined.

renal portal circulation in chickens and minimizes systemic toxicity problems (Sperber, 1946; Odlind, 1978), species difference and extrapolation of non-mammalian data remain as major concerns. With the introduction of the histamine H₂-receptor antagonist, cimetidine, into clinical practice, its relatively non-toxic property and widespread use have facilitated its use in whole animal and human experimentation (Somogyi *et al.*, 1983; Somogyi & Bochner, 1984; Muirhead *et al.*, 1985; van Crugten *et al.*, 1986; Somogyi *et al.*, 1988; van Ginneken & Russel, 1989). At present, there is ample evidence in support of the direct involvement of renal tubular organic cation secretion in cimetidine elimination, in addition to its ability to elicit competitive inhibition of the transport of other organic cations at common carriers. Consequently, cimetidine has been proposed the role as the prototypic inhibitor for renal organic cation transport, in an analogous manner to probenecid in organic anion transport (Somogyi, 1987). Nevertheless, one disadvantage of such a choice is that cimetidine undergoes significant biotransformation in mammalian species (Schunack, 1989), and that its metabolic pathways may interfere with the renal tubular transport kinetics of concern.

Amantadine. In the present research series, an achiral aliphatic primary amine is recommended and employed as a prototypic organic cation marker. Amantadine is an organic compound with diverse pharmacological actions. Its clinical uses range from the treatment of Parkinsonism to the prophylaxis against influenza A viral infection (Schwab *et al.*, 1969; Parkes, 1974; Oxford *et al.*, 1980; Aoki & Sitar, 1988). The metabolism of amantadine in the mammalian body has been reported to be very limited, and this organic cation is mainly excreted unchanged by means of renal glomerular filtration and active tubular secretion (Koppel & Tenczer, 1985; Cedarbaum, 1987; Aoki & Sitar, 1988).

The major advantages behind the use of amantadine as the marker organic

cation are as follows:

1. Amantadine is an incontrovertible organic cation which consists of a tricyclic aliphatic ring structure with one amino moiety (Figure I-11).
2. It is a compound of clinical significance (Symmetrel[®]). Adverse symptoms associated with acute administration of amantadine in human volunteers have been observed to be minimal at therapeutic doses (Aoki & Sitar, 1988), which support its suitability as an organic cation marker in human experimentation *in vivo*.
3. The minimal intracellular metabolism of amantadine obviates the possibility of its interference with experimental transport kinetics.
4. Stereochemically, the molecule of amantadine does not contain any chiral centers; hence it is not differentiated into enantiomers. Such a unique property renders this compound suitable as a probe in the examination of stereospecificity and stereoselectivity in renal organic cation transport.

Current Objectives. The primary objective of the present studies is to establish optimum experimental conditions and control transport kinetics for the accumulation of amantadine by three previously well-documented renal preparations *in vitro*. These are namely the isolated renal proximal tubules, distal tubules and cortical slices of the rat. In conjunction, three individual aspects of renal tubular organic cation transport are investigated through the use of multiple pharmacological agents. All of these compounds are exemplary organic cations (Figure I-11). The initial two sections involve the investigation into the basic molecular and spatial requirements for recognition by the tubular organic cation carriers, whereas the third experimental series accommodates to an aspect of both environmental and clinical significance.

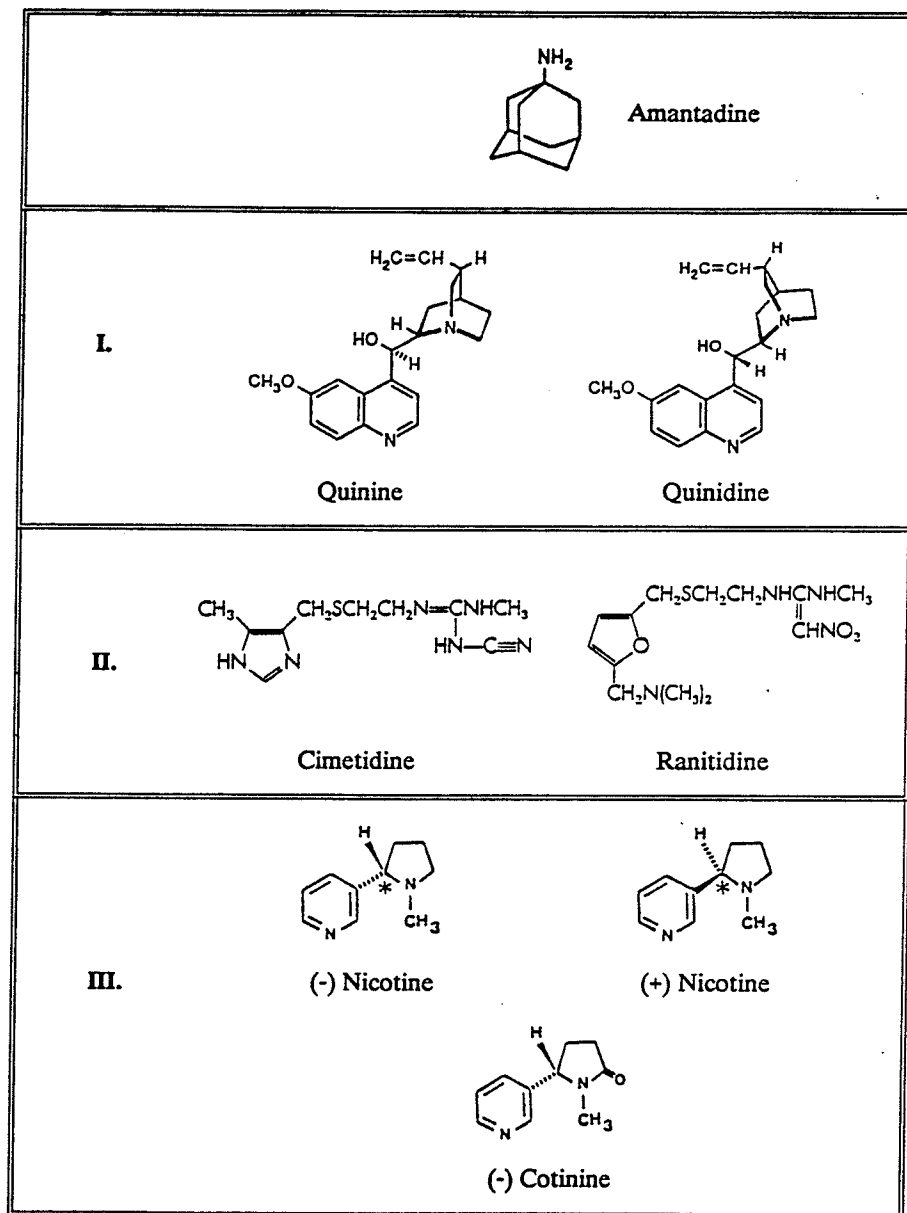


Figure I-11. Chemical structures of the organic cations employed in the present experimentation.

The following represents the three consecutive series of experimentation:

I. Stringency in molecular and spatial requirements of renal tubular transport sites. Enantiomeric preferences are well documented phenomena in biological systems. Although stereoisomers possess very similar chemical and physical properties, the chiral macromolecules in the body, especially proteins, are very specific to the spatial arrangements of drug molecules. Consequently, stereospecific or stereoselective pharmacodynamics and pharmacokinetics are often encountered (Jahnchen & Muller, 1983; Ariëns, 1983; Hsyu & Giacomini, 1985; Ariëns, 1986; Drayer, 1986; Somogyi, 1987).

Quinine and quinidine are clinically important organic cations, and they are diastereoisomers. The 8S, 9R(-)-isomer, quinine, is the conventional antimalarial drug (Howells, 1982; White *et al.*, 1983), whereas the 8R, 9S(+)-isomer, quinidine, is a class I antidysrhythmic agent (Alexander *et al.*, 1947; Vaughan Williams, 1985). Since these two organic cations are extensively plasma protein bound in man, active renal tubular secretion would contribute significantly to the elimination of the unchanged drug by the kidney. In 1986, Notterman *et al.* reported stereoselectivity in human renal tubular secretion of quinidine (8R, 9S(+)-isomer) over quinine (8S, 9R(-)-isomer) in an approximate ratio of four to one. Such a postulate is further supported by our own laboratory (Gaudry *et al.*, 1990; Sitar *et al.*, 1990), and a report on stereospecific inhibition of digoxin renal clearance in humans by quinidine (Hedman, 1990).

Principal intentions of the present experimental series include the characterization of the transport process(es) involved in the stereoselective renal handling of quinine and quinidine, in addition to the ramification for qualitative and quantitative comparisons between observations from the two rat renal preparations *in vitro*. The availability of fresh human kidney tissue throughout the project also commissioned the investigation into potential species difference between human

and rat renal tubular transport of the organic cations employed.

II. Renal drug interactions with two chemically-related pharmacological congeners. The potent histamine H₂-receptor antagonists, cimetidine and ranitidine, are weak bases ($pK_a = 6.8$ and 8.2 respectively; van Crugten *et al.*, 1985; personal communication, Glaxo Laboratories, Toronto, Canada). They are employed widely in the treatment of gastrointestinal ulceration by decreasing basal and stimulated gastric acid secretion (Bradshaw *et al.*, 1979; Daly *et al.*, 1981; Brater *et al.*, 1982; Howard *et al.*, 1985; Grant *et al.*, 1989). At therapeutic plasma concentrations, these agents are predominantly excreted unchanged by the kidney *via* glomerular filtration and active tubular secretion (Schunack, 1989). The renal clearance of either compound is considerably greater than the corresponding glomerular filtration rate, which reflects the significance of the renal tubular secretory process in their elimination (Weiner & Roth, 1981; Somogyi *et al.*, 1983; Roberts, 1984).

Numerous clinical interactions have been documented between cimetidine and other therapeutic agents during concurrent administration, and the underlying mechanisms were attributed to the ability of cimetidine to inhibit their hepatic biotransformation and/or renal excretion (Powell & Donn, 1984; Murray, 1987). Previous *in vivo et vitro* studies had shown that cimetidine is able to compete with other organic cations for the active renal proximal tubular secretory process (Somogyi *et al.*, 1983; Muirhead *et al.*, 1985; Takano *et al.*, 1985; van Crugten *et al.*, 1985; Schunack, 1989), and this agent has recently been proposed to be potentially the prototypic inhibitor for renal organic cation secretion (Somogyi, 1987).

Conversely, ranitidine has been postulated to have few pharmacokinetically or clinically significant effects on the elimination of concurrently administered drugs (Kirch *et al.*, 1984). In comparison to its predecessor cimetidine, the major

molecular modification in ranitidine is the substitution of a furan ring for the original imidazole moiety. Consequently, ranitidine is shown to be a relatively more selective and weaker inhibitor of hepatic mixed-function oxidases. However, in view of the relatively higher pK_a value for ranitidine (pK_a 8.2 versus 6.8 for cimetidine), the degree of ionization for ranitidine at physiological pH is expected to be correspondingly higher and its anticipated ability to interact renally with other therapeutic agents remains controversial and less extensively documented (Somogyi & Bochner, 1984; Rodvold *et al.*, 1987; Bendayan *et al.*, 1990b).

The specific aims of the second experimental series are directed towards the reinforcement of the proposed ability of cimetidine to interfere with renal organic cation transport in the present experimental settings *in vitro*, and subsequently the relative potency and efficacy for ranitidine to interact at these renal tubular transport sites may be evaluated.

III. Potential alteration of renal organic cation transport in tobacco users. Nicotine is a major pharmacologically active component in tobacco smoke. Whilst this *Nicotiana* alkaloid is consumed widely through the recreational use of tobacco (Dawson & Vestal, 1982; Bendayan *et al.*, 1990b), it is also prescribed therapeutically as nicotine-resin chewing gum (Benowitz *et al.*, 1988). The molecular structure of nicotine is that of a combination of a pyridine and a pyrrolidine ring, and it is a weak base ($pK_a = 7.9$). Stereochemically, nicotine possesses one chiral carbon center at position 2 of the pyrrolidine ring and is differentiated into S-(-) nicotine and R-(+) nicotine. (-) Nicotine is the principal isomer present in tobacco smoke with a proportion of the (+) isomer ranging from 3 - 12 % of total content (Klus & Kuhn, 1977; Nwosu *et al.*, 1988). In habitual tobacco smokers, plasma nicotine concentrations are maintained routinely at constant levels between 0.1 - 0.3 μM , of which approximately 5 % is plasma protein bound (Russell,

1978; McMorrow & Foxx, 1983; Benowitz & Jacob, 1985; Benowitz *et al.*, 1988; Bowman & Rand, 1980; Jaffe, 1990). Its major route of elimination is extensive metabolism, and both the parent compound and its metabolites are excreted renally by glomerular filtration and active tubular transport (Nwosu *et al.*, 1988; Bendayan *et al.*, 1990b; Kyerematen *et al.*, 1990; Kyerematen & Vesell, 1991). Cotinine is a major mammalian metabolite of nicotine with a considerably longer elimination half-life than the parent compound. Its level in physiological fluids of tobacco smokers can accumulate to approximately ten-fold of that for nicotine and is considered a sensitive index of nicotine exposure (Pilotti, 1980; Bjercke *et al.*, 1990; Kyerematen *et al.*, 1990).

Previous documentation had reported extensively significant alterations in the metabolism of numerous substances by nicotine, cotinine and other tobacco constituents, *viz.* polycyclic aromatic hydrocarbons (Jusko, 1979; Dawson & Vestal, 1982; Barbieri *et al.*, 1987; Bjercke *et al.*, 1990). Conversely, the determination of possible interference at renal excretory sites has been neglected. In view of the cationic nature of nicotine, this final experimental series investigated the potential effects of both isomers of this compound and (-) cotinine on renal organic cation transport in the rat renal preparations. Furthermore, in the anticipated event of significant interactions between amantadine and nicotine in rat models, such observations shall be extended by the implementation of a clinical trial in which renal clearance of amantadine will be compared and contrasted between control subjects and habitual tobacco smokers.

Compendium II. The present study investigated certain aspects of renal tubular transport of organic cations through the use of distinct pharmacological tools. In spite of the predominance of the current focus upon experimentation and observations *in vitro*, it is of common interest that the overall motive of this study

was to incite partially the extrapolation of basic scientific observations to potentially significant clinical perspectives in biomedical research.

MATERIALS AND METHODS

Preamble. In comparison to other fields of renal investigation, a major part of our current knowledge in regard to tubular transport mechanisms has been achieved through the use of *in vitro* preparations. The particular advantage of such techniques is that substrate uptake can be monitored under well controlled conditions. In addition, secondary effects such as changes in blood flow, plasma protein binding, toxicity of the compound in a whole animal situation, and hormonal interferences are also obviated. Numerous methods are currently available for the examination of segment-specific renal transport and metabolic function. Microdissection techniques enable the isolation of specific nephron segments with certainty, but major disadvantages include a limited tissue yield, together with a relatively time-consuming procedure which compromises tissue viability. Tissue culture of renal tubule cells represents an alternative approach which provides larger amounts of tissue. Nevertheless, the possibility of cell dedifferentiation remains, and qualitative and quantitative changes may occur that may not be representative of events that occur in normal tubule cells.

In the present experimental series, two major preparations were chosen, and these are namely the isolated renal tubules and cortical slices. The effective use of tissue slices in examining physiological and biochemical processes is extensively documented (Murthy & Foulkes, 1967; Berndt, 1976; Möller & Sheikh, 1983). Despite the relative simplicity of the preparation procedure, disadvantages associated with their use include an ambiguity in the direction of transport and the semi-quantitative nature of the measurements. This latter concern is compensated by the concomitant use of isolated renal tubules. Enzymatic-dissection of fragmented tubule segments of proximal and distal origin collaborates the advantages of nephron site specificity with improved tissue yield and cell viability.

In view of the opposite physical states of the tubule lumina within the two preparations during incubation (closed lumina in cortical slices and patent lumina in isolated tubules), the concurrent use of slices and tubules at relatively brief incubation periods facilitates the deduction of individual interaction site(s) in relation to basolateral and luminal membranes of the tubule cell.

Renal Tubules. Rat renal proximal and distal tubules were isolated by a sequential centrifugation technique which involves a Percoll density gradient step (Vinay *et al.*, 1981; Gesek *et al.*, 1987; Sundaresan *et al.*, 1987; Wong *et al.*, 1990, 1991 & 1992). Fresh kidneys from 4 anesthetized (pentobarbital 50 mg/kg i.p. or ether anaesthesia) male Sprague-Dawley rats (250-300 g) were excised from the peritoneal cavity *via* a mid-line incision. The kidneys were decapsulated, and longitudinally bisected in ice-cold Krebs-Henseleit solution (KHS: 118 mM NaCl, 4.7 mM KCl, 1.2 mM MgCl₂, 1.4 mM KH₂PO₄, 25 mM NaHCO₃, 2.5 mM CaCl₂ and 11 mM glucose (pH 7.4 adjusted with NaOH). Renal medulla with cortical tissue approximately 1 mm from the cortico-medullary junction were manually dissected and discarded; the remainder of cortical tissue was finely minced with the use of a McIlwain tissue chopper (Mickle Laboratory Engineering Co. Ltd., Gomshall, Surrey, UK). Renal cortical tissue was placed as a monolayer on the chopping surface and slivered for 2 cycles in perpendicular directions at 1 mm cutting interval. Following washing in 10 ml KHS, the mixture was oxygenated (95% O₂ / 5% CO₂) in KHS-enzyme solution (15 ml KHS, 1 ml 10% bovine serum albumin and 30 mg collagenase per eight kidneys) for 2 minutes, and shaken in a Dubnoff metabolic incubator (100 oscillations per minute) at 37°C for 45 minutes with intermittent agitation at 15-minute intervals using a Pasteur pipette. Digestion was then terminated by the addition of 30 ml ice-cold KHS. The suspension was filtered through a tea-strainer and centrifuged at 60 x g (600 rpm, model CS centrifuge,

International Equipment Company, Boston, MA, USA) at 4°C for approximately 2 minutes. The pellet was washed 4 times by resuspension in 40 ml KHS and centrifugation (60 x g, International model CS centrifuge) at 4°C for approximately 2 minutes. The resulting pellet was resuspended in oxygenated Percoll solution (100 ml equal parts of Percoll and calcium-free 2 times concentrated KHS oxygenated with 95 % O₂ / 5 % CO₂ for 2 hours, pH 7.4 (Gesek *et al.*, 1987)), and centrifuged at 27,000 x g (18,500 rpm, Sorvall RC2-B automatic refrigerated centrifuge with SS34 centrifuge rotor, Du Pont Company, Wilmington, DE, USA) at 4°C for 30 minutes. The distal and proximal tubule fractions (II and IV respectively) were isolated using a Pasteur pipette (Figure M-1), and washed 3 times by resuspension in 40 ml KHS followed by centrifugation (200 x g, 1050 rpm, International model CS centrifuge) at 4°C for approximately 2 minutes. The final tissue pellets were suspended in desired volumes of physiological KHS, and their protein concentrations were determined using the Biuret protein assay (Gornall *et al.*, 1949). Briefly, 100 μ l aliquots of either tubule suspension were incubated with 400 μ l Biuret reagent (0.15 % CuSO₄.5H₂O, 0.6 % NaKC₄H₂O₆.4H₂O, 3 % NaOH (w/v)) at room temperature for 30 minutes. Protein content was then calculated by monitoring spectrophotometric absorbance at 550 nm on a Spectronic 3000 Array spectrophotometer (Milton Roy Company, Rochester, NY, USA) with bovine serum albumin (1 - 10 mg/ml) serving as standards.

In the possible event of a dissatisfactory separation of the distal tubule fraction (II) from fraction I, an additional documented step to the protocol was available (Gesek *et al.*, 1987): The two fractions involved were pooled, and centrifuged in 35% Percoll solution at 17,540 x g for 10 minutes at 4°C (15000 rpm, Sorvall RC2-B automatic refrigerated centrifuge with SS34 centrifuge rotor). The diffuse uppermost band contained individual and broken cells, whereas the distinct bottom band was enriched in distal tubule segments. This additional step was not

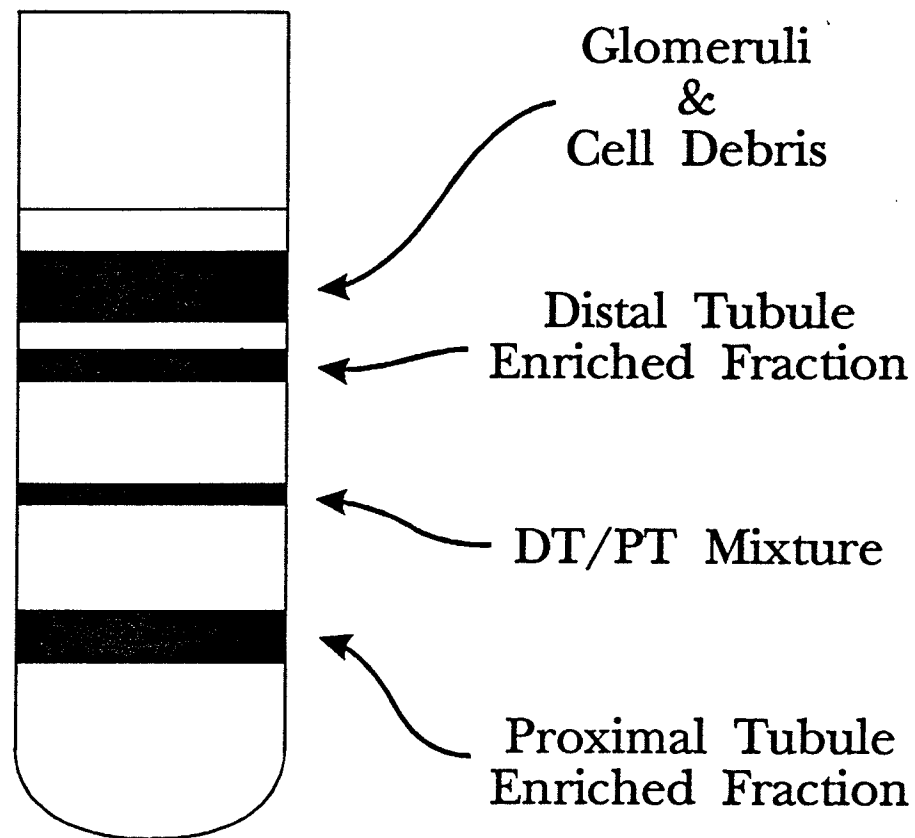


Figure M-1. A schematic diagram illustrating the separation of rat renal cortical tissue on 50% Percoll gradient. Purity of proximal tubule and distal tubule enriched fractions were confirmed by microscopic and enzymatic examination prior to their utilization in the present experimentation.

necessitated in the present experimental series.

The purity of the isolated tubule fractions was confirmed by i) light microscopy of unstained tubules with an Olympus photomicroscope using magnification of 100 and 200 x, and ii) enzymatic examination according to established methodology (Scholer & Edelman, 1979; Vinay *et al.*, 1981; Gesek *et al.*, 1987; Wong *et al.*, 1991 & 1992).

Microscopic inspection at low magnification revealed intact tubule segments with considerable differences in structure between the proximal and distal fractions. Primarily, proximal tubules displayed the characteristic granular yellow cytoplasm in comparison to the clear cytoplasm of the distal tubules. Diameter of the proximal tubules was also relatively larger than that of the distal tubules. Visual enumeration of the tubules of either fraction using haemocytometry indicated purity of $\geq 80\%$.

Alkaline phosphatase and hexokinase are documented to be distributed selectively in renal proximal and distal tubules respectively (Scholer & Edelman, 1979; Guder & Ross, 1984) and were employed as enzyme markers. Experimental procedures are as follows. Isolated tubules (1 ml) were disrupted on ice with a Sonicator W350 by 2 x 6-second bursts at setting 3.5 (Heat Systems - Ultrasonics, Inc., New York), and the enzyme markers were assayed in the 6000 x g x 2-minute supernatant (7700 rpm in a Sorvall RC2-B automatic refrigerated centrifuge with SM24 centrifuge rotor). Alkaline phosphatase content was determined by the addition of supernatant (50 - 100 μ l) to 1.1 ml reaction medium (1.6 mM *p*-nitrophenyl phosphate, 4.4 μ M zinc acetate, 18 μ M magnesium chloride and 88 mM glycine, pH 10.5 adjusted with KOH). The initial constant rate of *p*-nitrophenol formation was estimated by the monitoring of spectrophotometric absorbance change at 410 nm with computation on the basis of *p*-nitrophenol standards (0 - 100 μ M). Hexokinase was determined by the preincubation of supernatant (50 - 100 μ l) in medium (0.75 ml) containing 18 mM D-glucose, 24 mM magnesium chloride, 0.8

as the cocktail and a LS5801 scintillation counter with automated quench correction (Beckman Instruments, Inc., Fullerton, CA). Non-specific binding of amantadine onto the tissue was quantified from incubations with: 1) 2, 4-dinitrophenol (5 μ M) pretreated tissue, and 2) twice-frozen tissue. Both methods indicated a similar extent of non-specific binding (approximately 10 - 15 % of total uptake), and the twice frozen tissue data were used in background subtraction.

The experimental procedures for examination of the potential effects of an additional organic cation on amantadine efflux from renal tubules were derived from previous documentation with minor modifications (Hopfer *et al.*, 1973; Holohan & Ross, 1980; Tamai *et al.*, 1988). Aliquots (50 μ l) of tubules were first subjected to preincubation with [3 H]amantadine (10 μ M) for 30 seconds in a total volume of 200 μ l. Efflux was initiated by the addition of 3,130 μ l KHS containing the organic cation of examination to the preincubated tubule suspension for 30 or 60 seconds, and was terminated subsequently by rapid filtration as described above. Potentially significant uptake of the diluted amantadine during efflux incubation was deemed to be negligible, as incubation of untreated tubules in 3330 μ l KHS with 0.6 μ M [3 H]amantadine did not indicate significant active uptake. Non-specific binding was determined as described above.

Renal cortical slices. The methodology in preparation of kidney slices conformed to previous reports (Cross & Taggart, 1950; Berndt, 1976) (Figure M-2). Fresh kidneys from male adult Sprague-Dawley rats (250-300 g) were decapsulated and bisected longitudinally. Four sagittal slices of the cortex (approximately 0.5 mm in thickness) were cut freehand from each kidney-half (Stadie & Riggs, 1944) using a Stadie-Riggs microtome (Thomas Co., Philadelphia, PA) and each first slice with only one cut surface was discarded. The slices were stored in pH 7.4 phosphate buffered Ringer's solution (Cross-Taggart Medium (CTM): 0.11 M NaCl, 15 mM

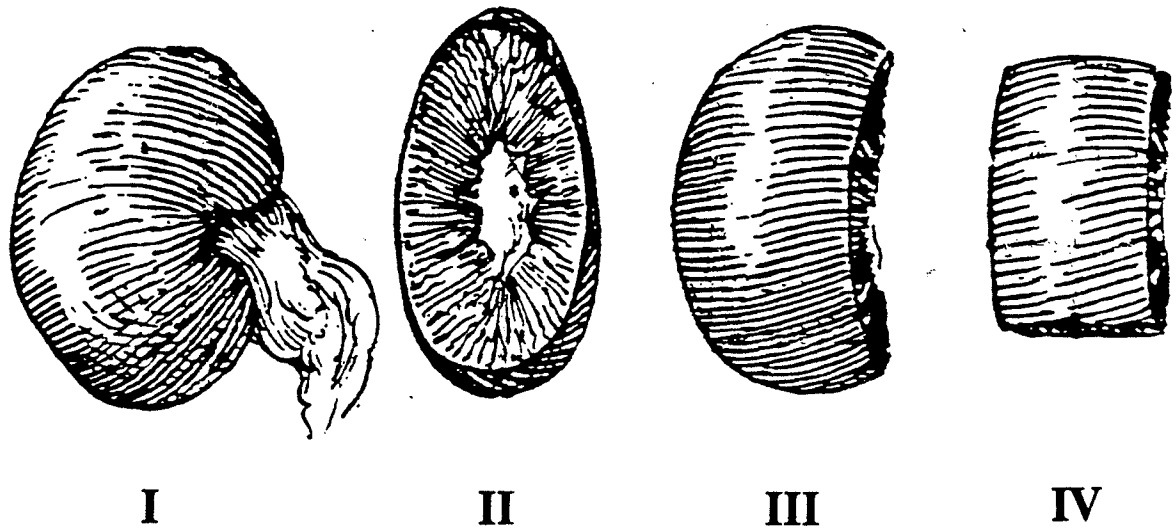


Figure M-2. Schematic illustration of the preparation of rat renal cortical slices. In sequence, rat kidneys were excised and decapsulated. Each kidney was bisected longitudinally into two equivalent halves with edges trimmed and discarded. Sagittal cortical slices of uniform thickness (approximately 0.5 mm) were prepared subsequently using a Stadie-Riggs microtome.

sodium phosphate buffer (pH 7.4), 8 mM KCl, 2 mM MgSO₄ and 1 mM CaCl₂ (pH 7.4 adjusted with NaOH); Foulkes & Miller, 1959; Wong *et al.*, 1990, 1991 & 1992) with constant oxygenation (95 % O₂ / 5 % CO₂) at room temperature until use (\leq 1 hour). Cortical slices were also prepared from human renal cortex obtained from uninvolved portions of kidneys from 8 male or female patients diagnosed with renal cell carcinoma (6 males and 2 females, age 42-76 years (mean \pm S.D. = 61 \pm 12 years)). Patient demography is represented in Table M-A. Following surgical uninephrectomy, the kidneys were bisected immediately. Disease-free samples of the renal cortex were confirmed by the pathologist involved and dissected in ice-cold oxygenated CTM. Sagittal slices were then prepared as described above. The interval between the excision of each kidney and the actual use of the slices did not exceed 1 hour. The use of human kidney tissue for the purposes described herein was approved by the Faculty Committee on the Use of Human Subjects in Research, University of Manitoba.

In transport studies, each slice (20-35 mg) was incubated in a 25 ml Erlenmeyer flask containing 3 ml oxygenated CTM with [³H]amantadine either in the absence or presence of a predetermined concentration of the additional organic cation. The flasks were oxygenated and shaken in a Dubnoff metabolic incubator (100 oscillations per minute) at 25°C for 30 seconds. After incubation, the slices were withdrawn quickly, blotted on filter paper and weighed. They were then digested for 30 minutes in 1 ml of 0.5 M sodium hydroxide in a shaking bath at 50°C (Cacini *et al.*, 1982). Radioactivity in the digested slice or medium was assayed by liquid scintillation with automated quench correction. Potential interference of counting by chemiluminescent product(s) in the samples was examined by comparing the counting efficiency between control samples containing radioactivity in scintillant and samples containing radioactivity in scintillant with incorporated NaOH (1 ml of 0.1, 0.5 or 1 M into 11.5 ml scintillation medium). The presence of

Table M-A

Demography for patients who underwent unilateral nephrectomy and donated renal cortical tissue.

R/L and M/F denote right or left kidney tissue from male or female donor respectively.

Patient No.	Age (Years)	Gender	Kidney
1	42	M	L
2	51	M	R
3	55	M	R
4	56	M	L
5	69	M	R
6	69	F	R
7	70	F	L
8	76	M	R

NaOH at a final concentration of 0.08 M increased significantly the apparent counting efficiency for tritiated amantadine. However, counting of samples incorporated with two lower concentrations of NaOH (0.04 and 0.008 M) was observed to be comparable to control (Figure M-3). Non-specific binding of amantadine onto the tissue was quantified to be approximately 25% of total uptake by using 2, 4-dinitrophenol-pretreated and twice frozen slices as above-mentioned. In determining the protein content of the cortical slices, untreated slices of predetermined weights were used as standards and the Biuret protein analysis was employed (Gornall *et al.*, 1949).

Expression of transport. [³H]Amantadine accumulation in either preparation was expressed primarily as tissue (μ mol amantadine concentrated in 1 g tubule protein or slice wet weight) to medium (μ mol amantadine present in 1 ml medium) ratio, and as the velocity of accumulation (μ mol amantadine accumulated in 1 mg tubule protein (actual or estimated) or slice wet weight in 1 minute).

Conversion of renal cortical slice wet weights to cortical slice protein content was calculated using the gradient generated by weighted linear regression (through origin) of the two variables involved. Conversion coefficients are 0.184 and 0.171 for rat and human cortical slices respectively. Proximal tubule protein in cortical slices was subsequently estimated on the basis that proximal tubules represent approximately 40 % of total renal cortex (Vinay *et al.*, 1981).

Michaelis-Menten kinetic parameters were calculated by monitoring initial uptake of varying concentrations of amantadine and the use of weighted Lineweaver-Burk analysis (Lineweaver & Burk, 1934). Amantadine concentrations employed were determined upon the basis of even distribution of data points within the range of one tenth to five fold of K_m for control uptake. With the use of a longer incubation of 4 minutes, a back-extrapolation process was employed in order

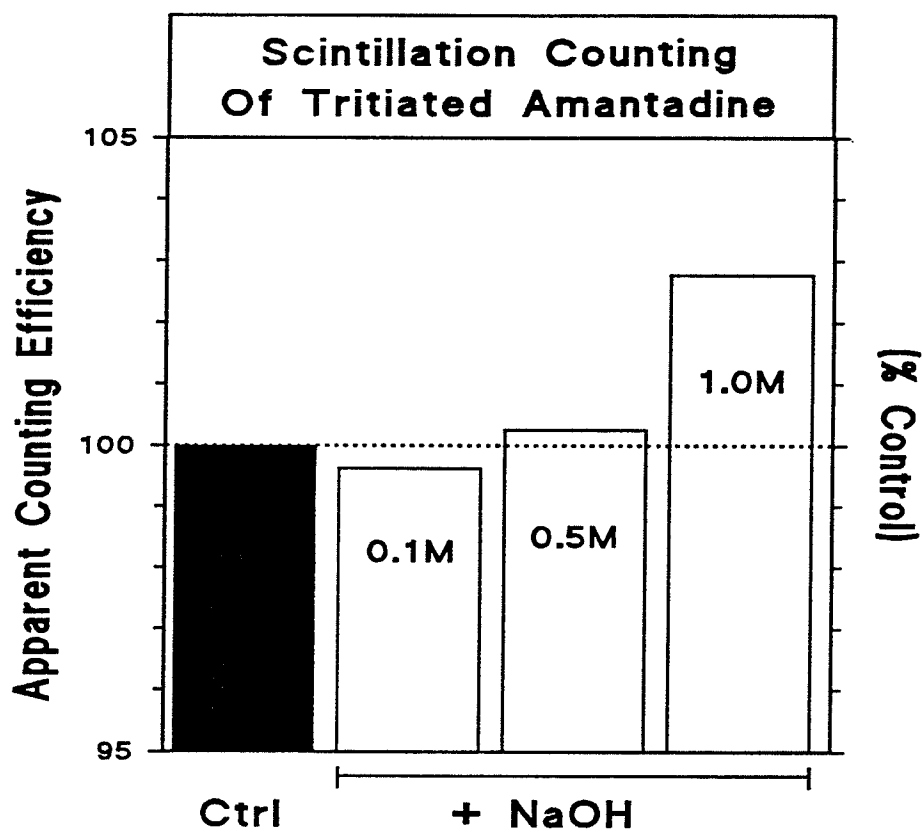


Figure M-3. Effects of three concentrations of sodium hydroxide on the scintillation counting efficiency for tritiated amantadine in a Beckman LS5801 scintillation counter with automated quench correction. All samples contained equivalent amounts of tritiated amantadine (20 μ l), and were performed in triplicates. Control samples each contained 1 ml Cross-Taggart buffer with 11.5 ml scintillation cocktail, and the former was substituted by 1 ml of 0.1, 0.5 or 1.0 M NaOH in test samples.

to compensate for the deviation of uptake as a function of time from linearity (Cornish-Bowden, 1979). Non-linear amantadine uptake observed at 4-minute incubation was time-corrected by horizontal extrapolation onto the hypothetically extended initial linear uptake phase (V_i) to provide a more realistic estimate of initial uptake velocity values for the calculation of V_{max} . Uptake value at 30-second incubation period was observed to lie within the initial linear uptake phase, and compensation was not implemented for such data.

Efflux of amantadine from preloaded tubules was expressed as the initial egress rate in pmol amantadine from 1 mg tubule protein after a 30-second efflux period.

All values are reported as mean \pm SEM from 4 separate experiments unless otherwise stated. Statistical significance was determined using the appropriate analysis of variance (ANOVA) model, followed by Tukey's HSD test and Newman-Keuls tests, with Type I error probability controlled experimentwise. The two-tailed independent or paired Student's *t*-tests were also used whenever appropriate. The level of probability for significance was established at $p < 0.05$.

Chemicals. [^3H]Amantadine (350 mCi/mmol) was obtained from Amersham International Limited (Buckinghamshire, UK); unlabelled amantadine was obtained from Du Pont Canada, Inc. (Mississauga, Ontario); quinine, quinidine, (+) & (-) nicotine and (-) cotinine were obtained from Sigma Co. (St Louis, MO, USA); cimetidine was obtained from Smith Kline & French Canada, Ltd. (Mississauga, Ontario); ranitidine was obtained from Glaxo Laboratories (Toronto, Ontario); collagenase A (0.228 U/mg lyophilisate) was obtained from Boehringer Mannheim (Laval, Quebec) and Percoll was obtained from Pharmacia Biotechnology (Baie D'urfe, Quebec). All other chemicals were of the highest grade available from commercial suppliers.

RESULTS

For the purpose of cross-reference, the sequence of experimentation reported herein conforms to that presented in the *Introduction* section. The majority of the data has been presented at scientific meetings and published (Wong *et al.*, 1990, 1991 & 1992). The three consecutive aspects of examination are as follows:

I. Diastereoisomers & Renal Organic Cation Transport:

Purity of Rat Renal Tubule Suspensions. Subsequent to isolation of renal proximal and distal tubules, inspection at low magnification revealed intact tubule segments with considerable differences in structure between the two fractions. Proximal tubules displayed the characteristic granular opaque cytoplasm with large diameter, whereas distal segments were distinguished by their clear cytoplasm and thinner appearance. Visual enumeration of the tubules in both preparations by hemocytometry indicated a purity of $\geq 80\%$. Enzymatic analyses of the tubule fractions revealed heterogeneous distribution of alkaline phosphatase and hexokinase activity between the two rat nephron segments. Alkaline phosphatase activity was predominant in the proximal tubule fraction, and hexokinase activity was predominant in the distal tubule fraction (Figure R-1).

Control Amantadine Uptake. [^3H]Amantadine (10 μM) was concentrated by renal cortical slices, isolated proximal tubules and distal tubules. The uptake process as a function of incubation time is presented in Figures R-2 and R-3. Initial rate or velocity of uptake (V_i) remained constant for approximately 3 minutes in cortical slices, and for approximately 1 minute in isolated proximal tubules. In cortical slices, slice/medium ratios for 30-second and 4-minute incubations were 0.4

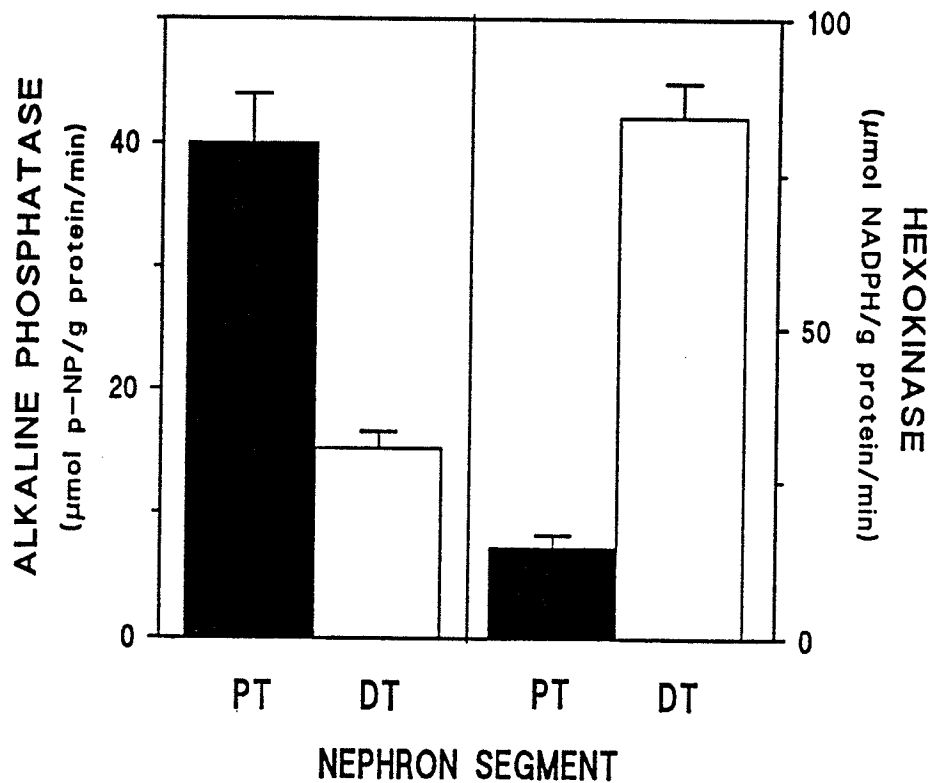


Figure R-1. Specific activities of enzyme markers in fractions of rat renal cortical nephron segments (mean \pm SEM, n=4). PT represents fractions enriched in proximal tubules; DT represents fractions enriched in distal tubules and *p*-NP represents *p*-nitrophenol.

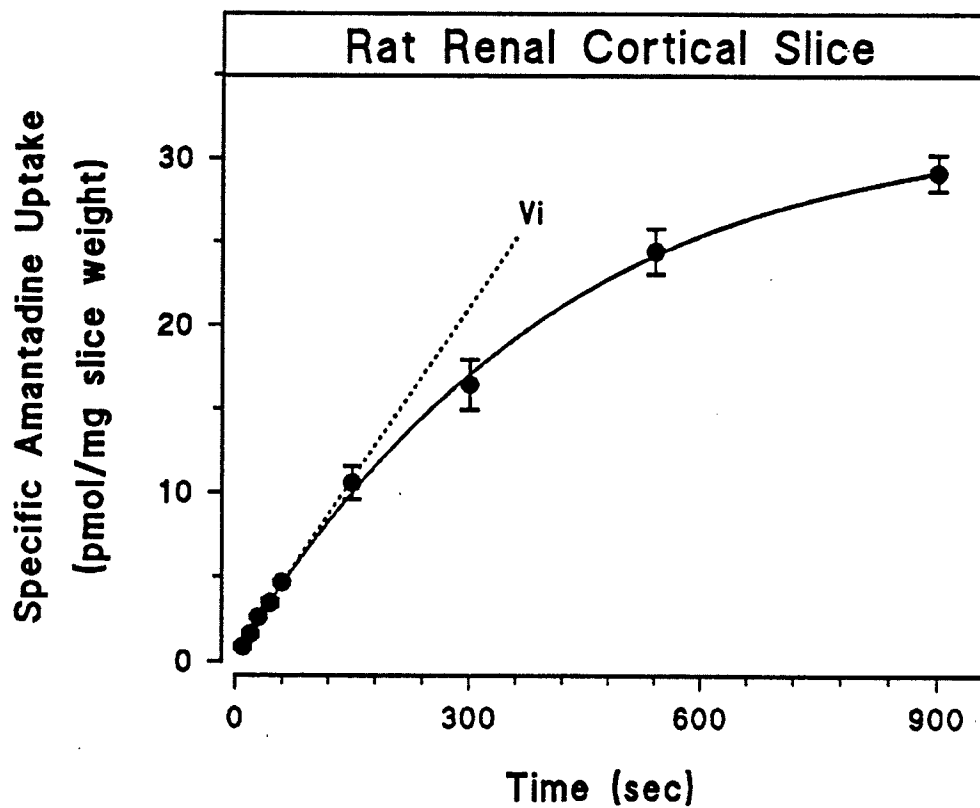


Figure R-2. Active accumulation of [^3H]amantadine by rat renal cortical slices as a function of time from 0-900 seconds. Incubation medium (3 ml) contained 5 μM amantadine and 30-50 mg of a cortical slice. Data points represent mean \pm SEM from 4 separate determinations. The dotted line represents the extrapolated linear phase of initial uptake (V_i).

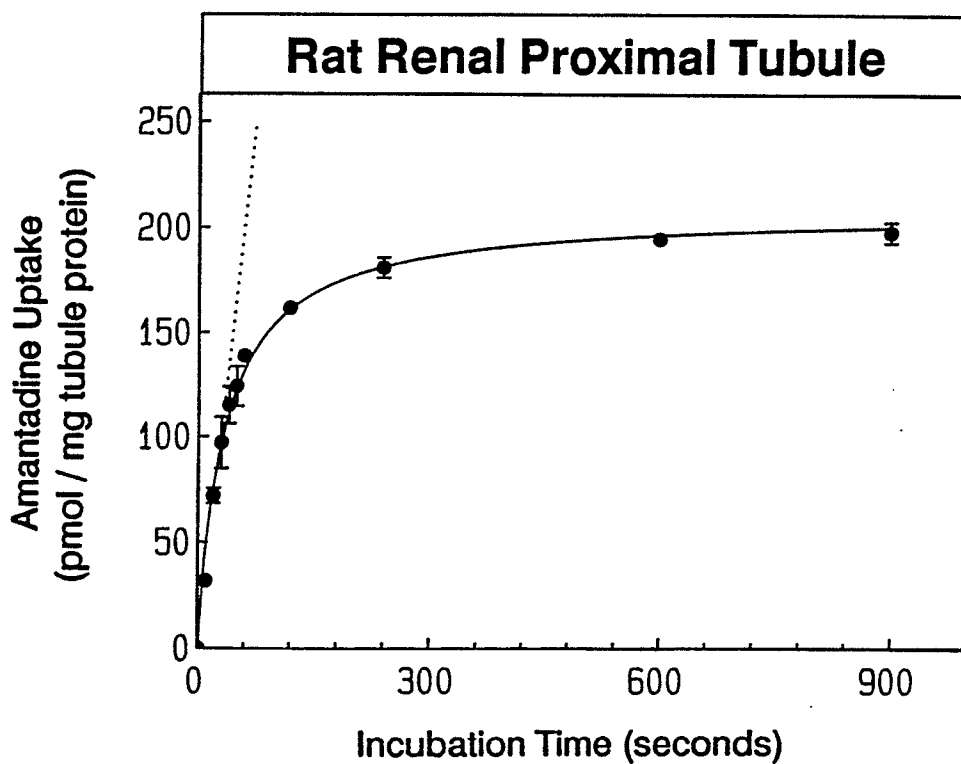


Figure R-3. Active accumulation of [³H]amantadine by rat renal proximal tubules as a function of time from 0-900 seconds. Incubation medium (200 μ l) contained 2.3 μ M amantadine and approximately 0.4 mg tubular protein. Data points represent mean \pm SEM from 3 separate determinations. The dotted line represents the extrapolated linear phase of initial uptake (V_i).

± 0.03 and 3.3 ± 0.3 respectively (mean \pm SEM; 10 μ M amantadine; n=4).

Tissue/medium ratios for 30-second incubations in proximal and distal tubules were 38 ± 3 and 20 ± 2 respectively (10 μ M amantadine; n=4). The use of twice-frozen tissue or preincubation of tissue with the metabolic inhibitor, 2,4-dinitrophenol, abolished a majority of such accumulation in all three preparations. Moreover, the incorporation of conventional organic cation probes into the incubation medium significantly interfered with amantadine accumulation in isolated proximal tubules (Figure R-4).

With the use of 30-second initial linear uptake values, Figures R-5, R-6 and R-7 illustrate representative saturation curves for the three preparations in which the rate of amantadine uptake was plotted against varying initial concentrations. Lineweaver-Burk transformation of the data yielded individual Michaelis-Menten kinetic parameters (Figures R-8, R-9 and R-10).

In cortical slices, apparent K_m and V_{max} values were $99 \pm 8 \mu$ M and 86 ± 11 pmol amantadine/mg slice wet weight/minute (n=5). In order to facilitate a direct comparison between cortical slice and isolated tubule data, the denominator, cortical slice wet weight, was adapted to slice protein content (Figure R-11). The latter was approximated subsequently to proximal tubule protein, and apparent V_{max} for uptake in cortical slices was modified correspondingly to 1.16 ± 0.14 nmol amantadine/mg estimated proximal tubule protein/minute (Figure R-12).

Apparent K_m values in proximal and distal tubules were observed to be comparable to that in the cortical slices (81 ± 6 and $76 \pm 3 \mu$ M respectively (n=4)), whereas apparent maximal capacity values for uptake (V_{max}) were higher than that observed in the cortical slice preparation (7.6 ± 0.3 and 4.0 ± 0.4 nmol/mg tubule protein/minute ($p < 0.05$)).

In proximal tubules, uptake of amantadine with a longer incubation was also examined. Tissue/medium ratio for a 4-minute incubation was 96 ± 2 (n=18), and

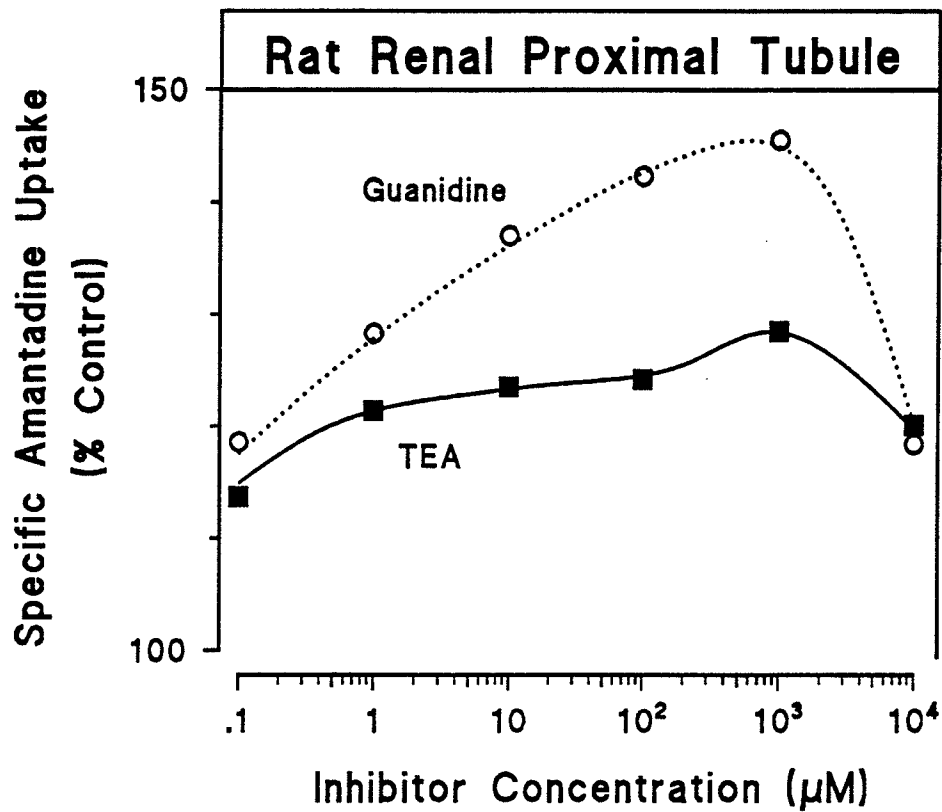


Figure R-4. A representative experiment demonstrating the effects of tetraethylammonium (TEA) and guanidine on amantadine accumulation into rat renal proximal tubules. Incubation medium (200 μl) contained 10 μM amantadine \pm TEA or guanidine (0.1 μM - 10 mM) with approximately 0.4 mg tubular protein. After 30-second incubation, tubule/medium ratio was 3.4.

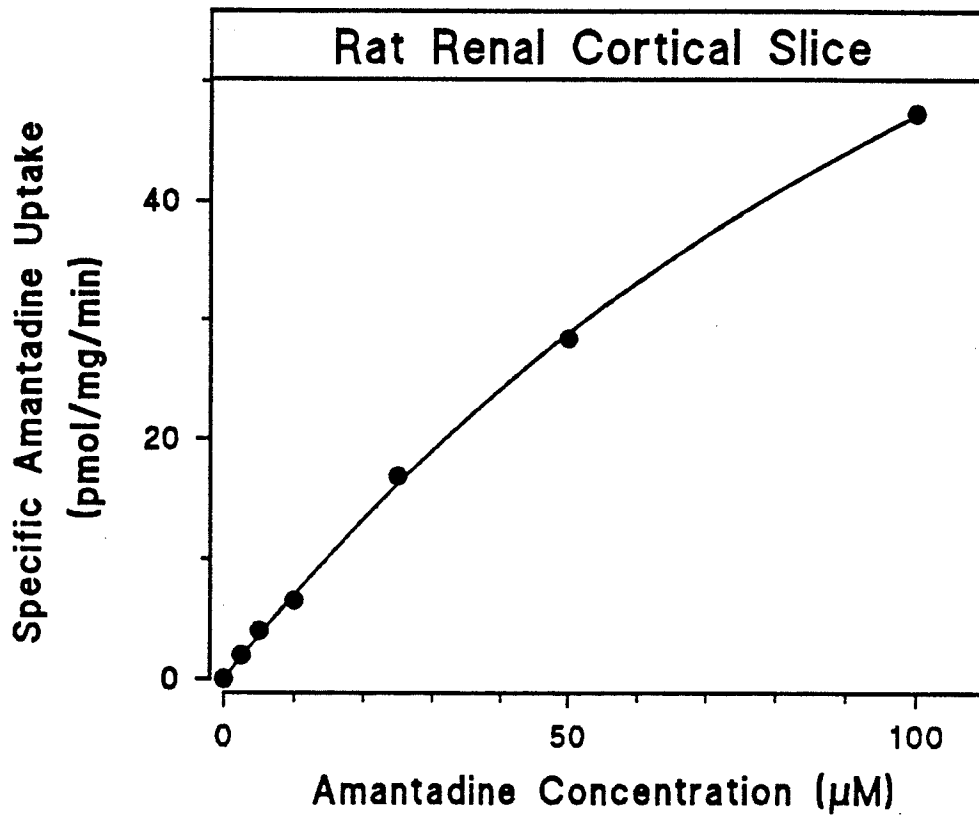


Figure R-5. Representative saturation isotherm for active amantadine accumulation by rat cortical slices (30-second incubation). Incubation medium (3 ml) contained 2.5 - 100 μM amantadine and 20-40 mg of a cortical slice.

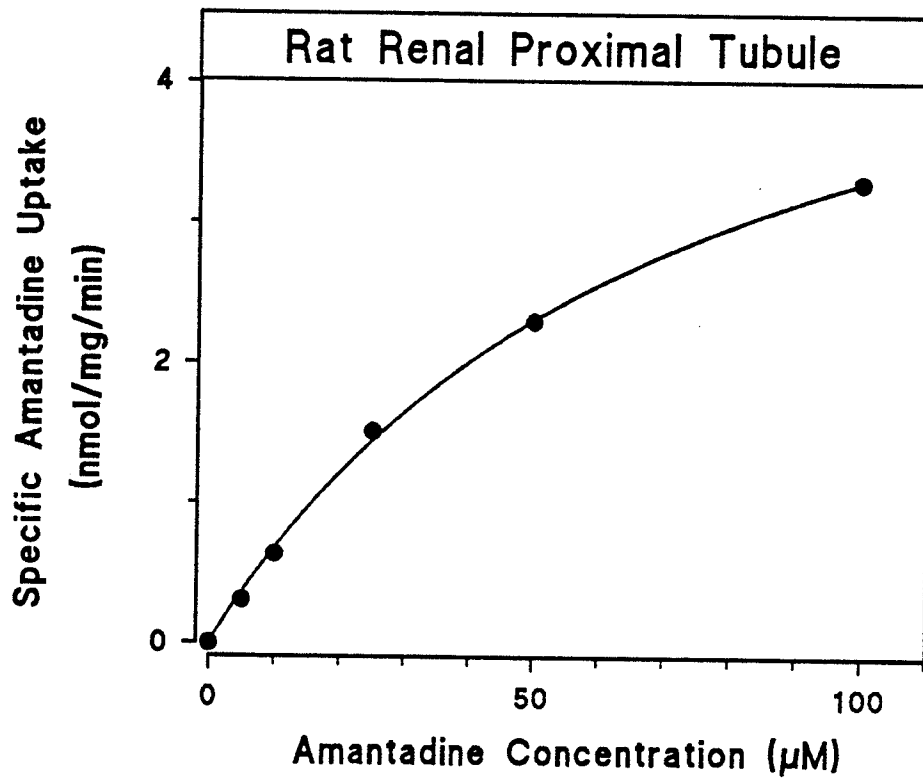


Figure R-6. Representative saturation isotherm for active amantadine accumulation by isolated proximal tubules. Incubation medium (200 μl) contained 2.5 - 100 μM amantadine and incubation period was 30 seconds.

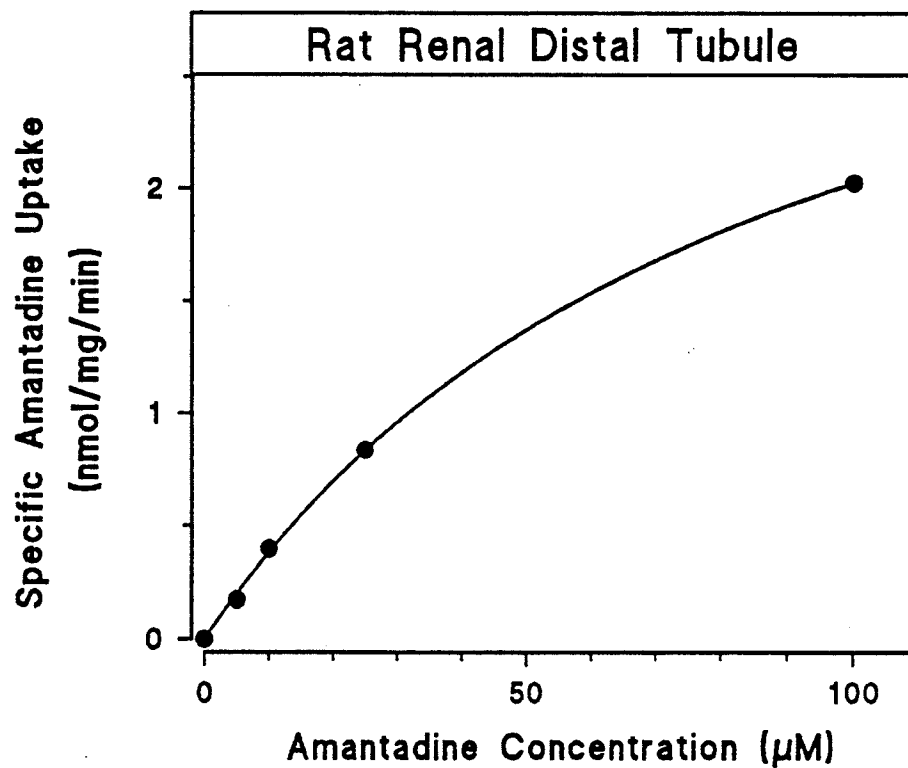


Figure R-7. Representative saturation isotherm for active amantadine accumulation by isolated rat distal tubules. Incubation medium (200 μl) contained 5 - 100 μM amantadine and incubation period was 30 seconds.

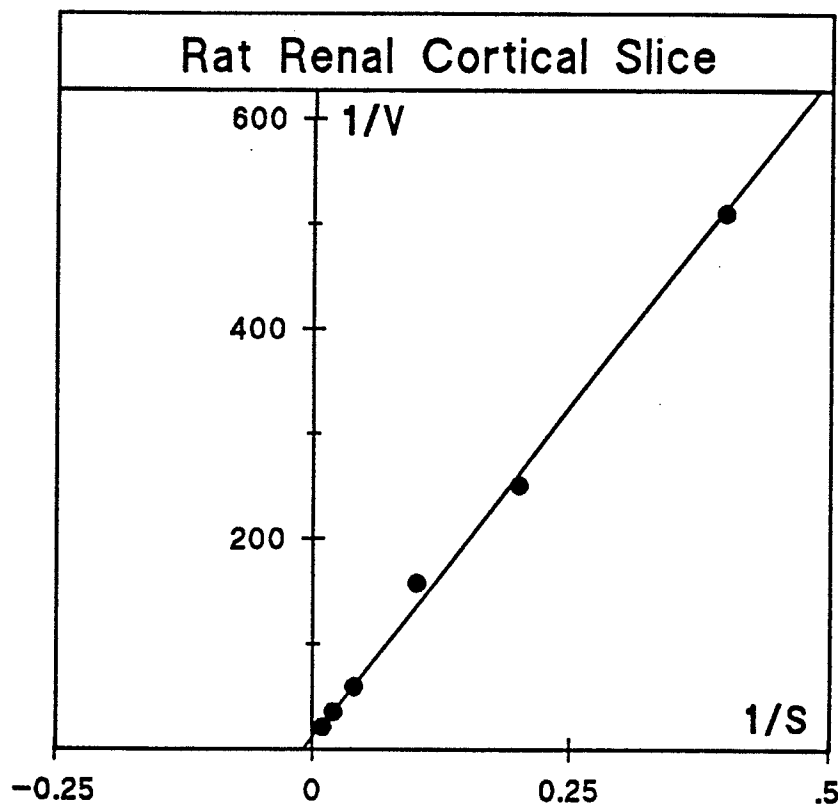


Figure R-8. Representative Lineweaver-Burk transformation of control amantadine uptake values in rat renal cortical slices. Velocity of accumulation (V) is expressed in $\text{nmol amantadine/mg slice wet weight/minute}$, and amantadine concentration (S) is in micromolar. Apparent K_m is calculated from the negative reciprocal of the abscissa intercept ($94 \mu\text{M}$), whereas apparent V_{max} is the reciprocal of the ordinate intercept ($76 \text{ pmol/mg slice wet weight/minute}$).

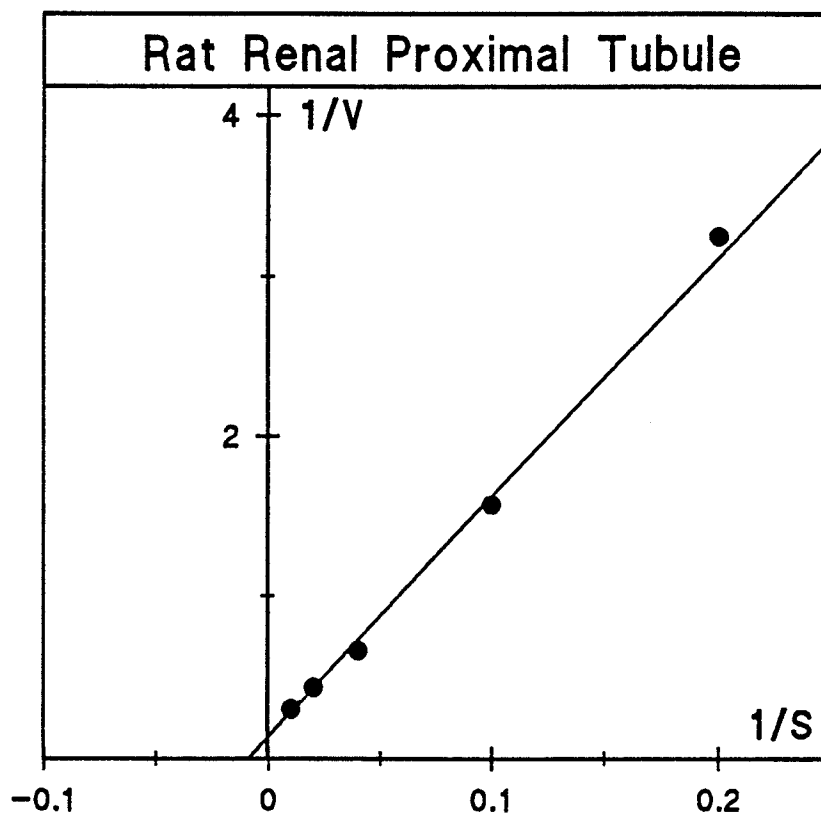


Figure R-9. Representative Lineweaver-Burk transformation of control amantadine uptake values in isolated rat proximal tubules. Velocity of accumulation (V) is expressed in μmol amantadine/mg slice wet weight/minute, and amantadine concentration (S) is in micromolar amounts. Apparent K_m is calculated from the negative reciprocal of the abscissa intercept ($100 \mu\text{M}$), whereas apparent V_{max} is the reciprocal of the ordinate intercept ($7.1 \text{ nmol/mg tubule protein/minute}$).

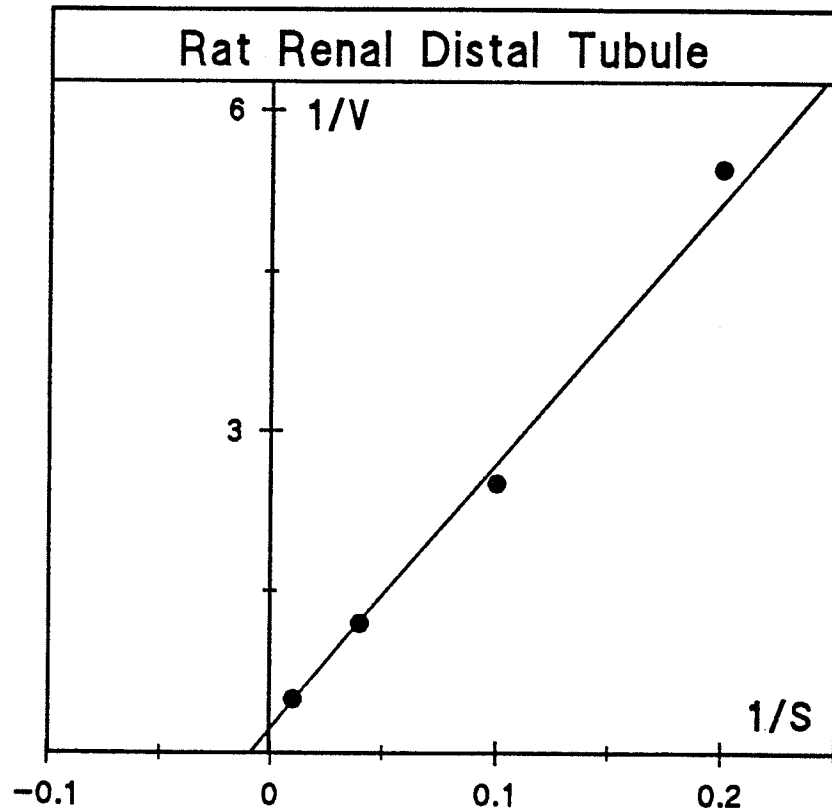


Figure R-10. Representative Lineweaver-Burk transformation of control amantadine uptake values in isolated rat distal tubules. Velocity of accumulation (V) is expressed in $\mu\text{mol amantadine/mg slice wet weight/minute}$, and amantadine concentration (S) is in micromolar amounts. Apparent K_m is calculated from the negative reciprocal of the abscissa intercept ($78 \mu\text{M}$), whereas apparent V_{max} is the reciprocal of the ordinate intercept ($3.5 \text{ nmol/mg tubule protein/minute}$).

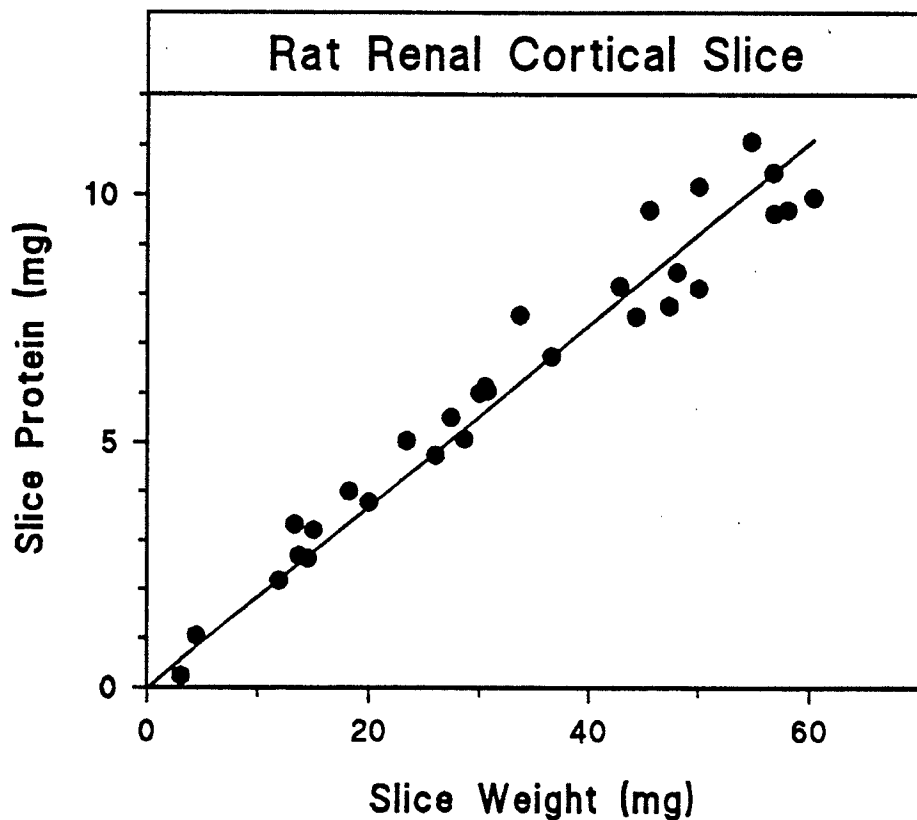


Figure R-11. Conversion of rat renal cortical slice wet weight to cortical slice protein. Each slice was weighed and dissolved in 1 ml 0.5 M sodium hydroxide. Protein concentration was determined by the Biuret analysis. Gradient generated by linear regression (through origin) is 0.184 ± 0.008 ($N=30$, $r^2 = 0.95$).

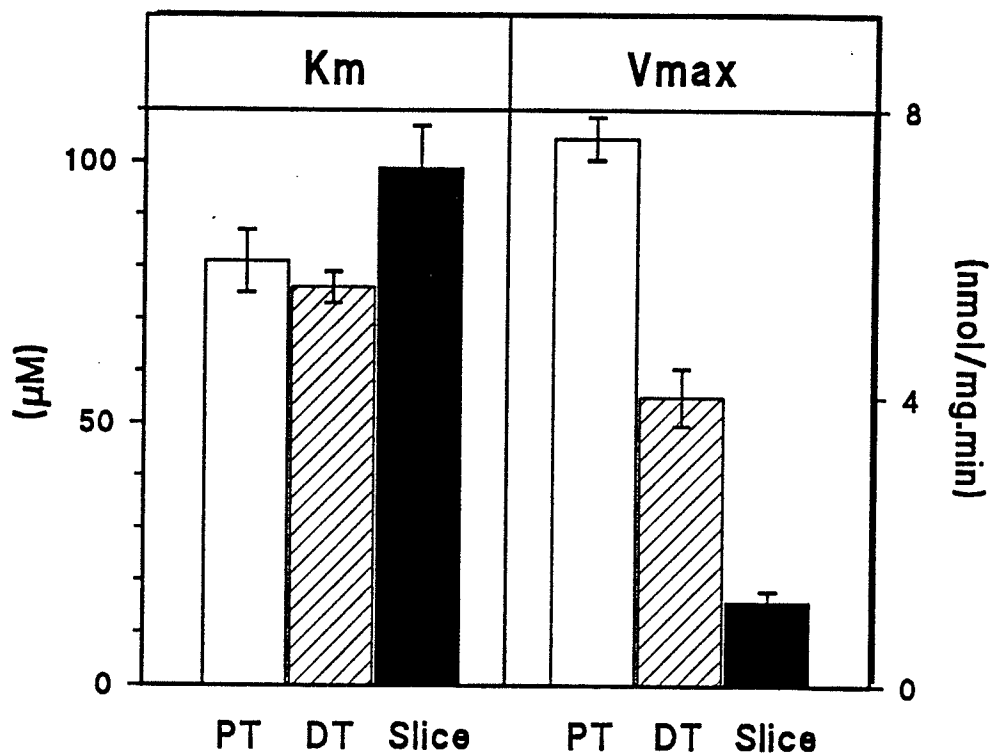


Figure R-12. Michaelis-Menten kinetic parameters for rat renal cortical slices, isolated proximal tubules and distal tubules. Apparent K_m is expressed in micromolar, and V_{max} is expressed in *nmol* amantadine/*mg* tubule protein (measured or estimated)/minute. Data are reported as mean \pm SEM from 4 separate determinations.

parallel kinetic analysis of the time-corrected 4-minute uptake data generated comparable Michaelis-Menten kinetic parameters to those obtained using 30-second initial uptake velocity values (Table R-A).

Control Amantadine Efflux. Efflux of [³H]amantadine from preloaded proximal tubules under control conditions was observed to be linear for the first minute (Figure R-13), and initial efflux rate of amantadine was 64 ± 14 pmol/mg tubule protein/30 seconds (n=3). The incorporation of 100 μ M unlabelled amantadine into the efflux incubation medium significantly promoted initial efflux of [³H]amantadine from preloaded proximal tubules to 233 ± 15 pmol/mg tubule protein/30 seconds ($p = 0.013$ as determined by the paired Student's *t*-test). Rate of amantadine egress in cortical slices was observed to be evidently slower than that in isolated tubules (Figure R-14). Efflux remained relatively linear for the first minute, and initial efflux rate was approximated to be 24 pmol/mg estimated proximal tubule protein/30 seconds.

Uptake Inhibition by Quinine & Quinidine. The incorporation of either diastereoisomer into the incubation medium elicited inhibition of amantadine uptake in all three preparations (Figures R-15, R-16 and R-17). The type of inhibition was attributed to direct competition between substrates for common carrier(s). Apparent K_m for amantadine uptake was increased significantly by quinine and quinidine whereas V_{max} was unaltered (Table R-B).

Inhibitory constant (K_i) values for quinine and quinidine were calculated using the Cheng-Prusoff or Dixon analyses (Figures R-16 to R-21). In renal cortical slices and isolated proximal tubules, the inhibitory potency of the 8S, 9R(-)-isomer, quinine, was observed to be two- to three-fold greater than that for the 8R, 9S(+)-isomer, quinidine. However, corresponding K_i values were approximately ten-fold

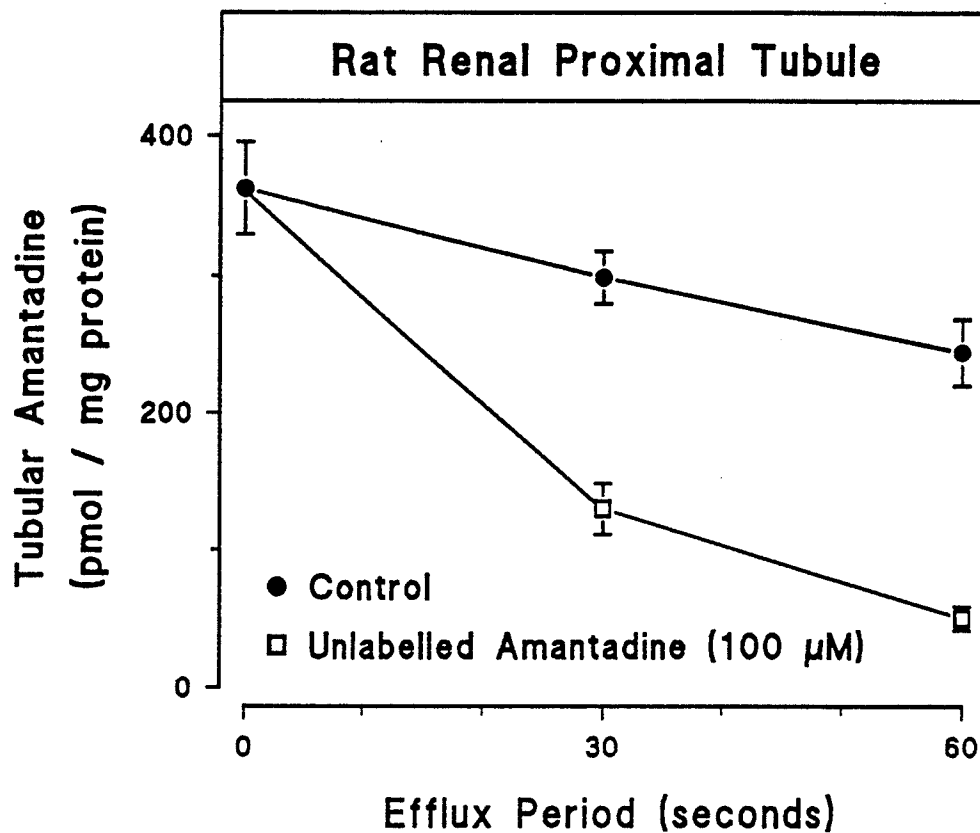


Figure R-13. Effects of unlabelled amantadine on [³H]amantadine efflux from rat renal proximal tubules. Tubules were preloaded in 200 μ l medium with [³H]amantadine for 30 seconds and efflux was subsequently initiated by a dilution of the incubation medium with KHS \pm unlabelled amantadine to 3330 μ l. Final amantadine concentrations in efflux media were 100 μ M. All data points are represented as mean \pm SEM from 4 separate determinations.

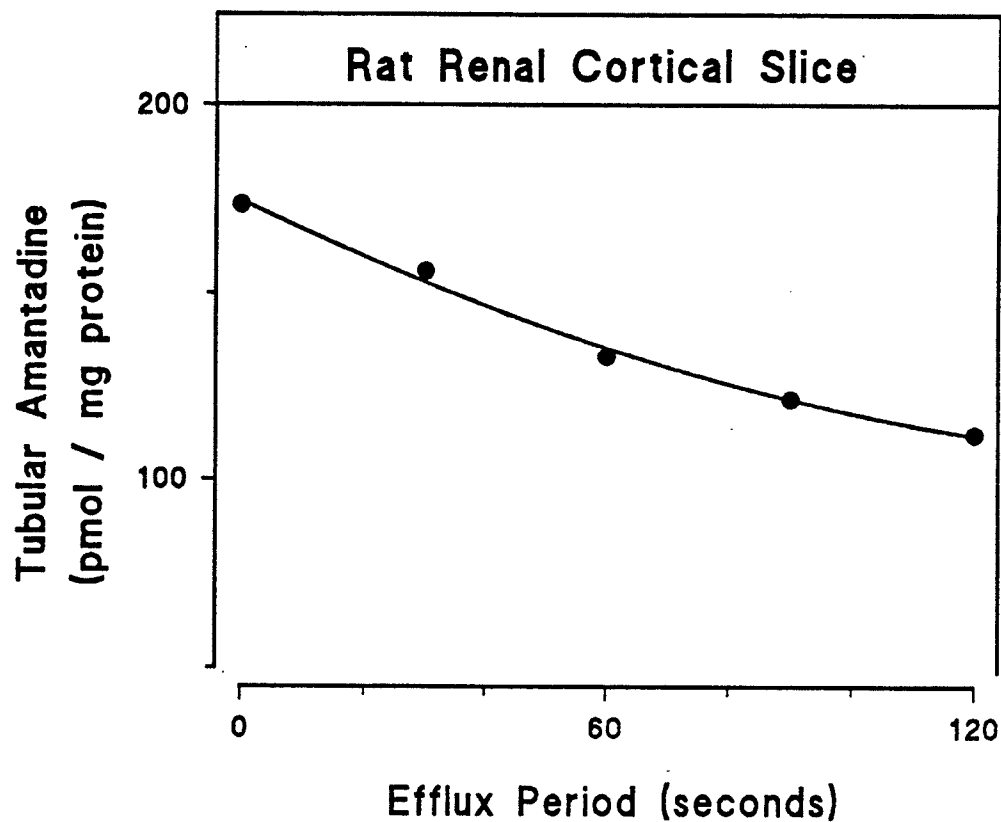


Figure R-14. Representative experiment showing [³H]amantadine efflux from rat renal cortical slices from 0 - 2 minutes. Each slice was preloaded in incubation medium (3 ml) containing 10 μ M amantadine, and efflux was initiated by rapid relocation of the slice into 3 ml KHS for a predetermined egress period. Initial efflux rate was 1.8 μ mol/mg slice wet weight/30 seconds or 24 μ mol/mg estimated proximal tubule protein/30 seconds with protein conversion.

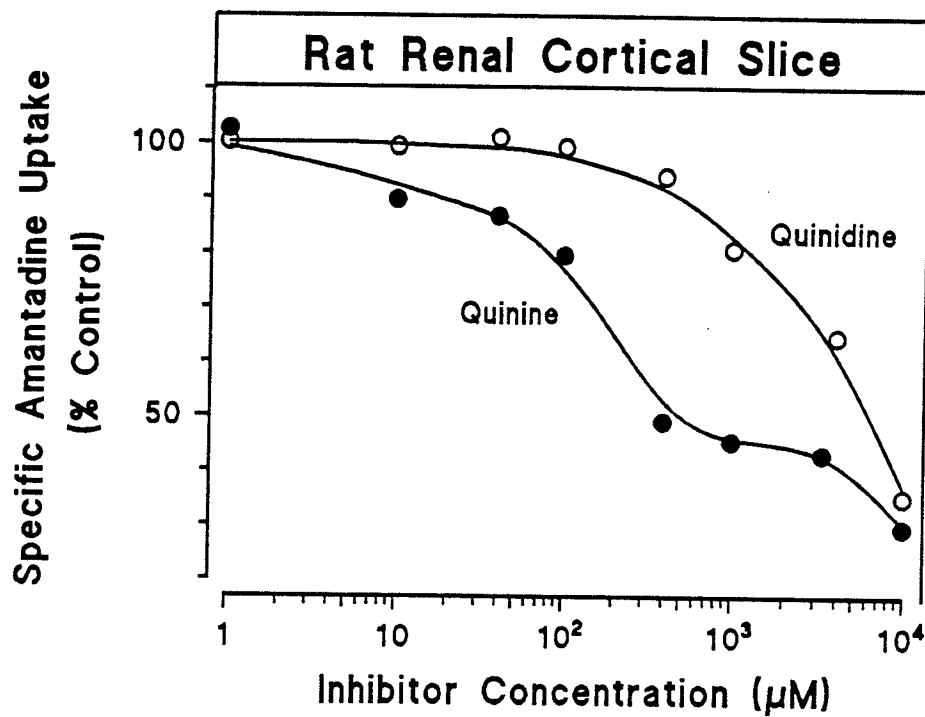


Figure R-15. A representative experiment showing the effects of quinine and quinidine on amantadine accumulation into rat renal cortical slices. Incubation medium (3.0 ml) contained 10 μM amantadine \pm quinine or quinidine (1 μM - 10 mM) with approximately 30 mg of renal cortical slice.

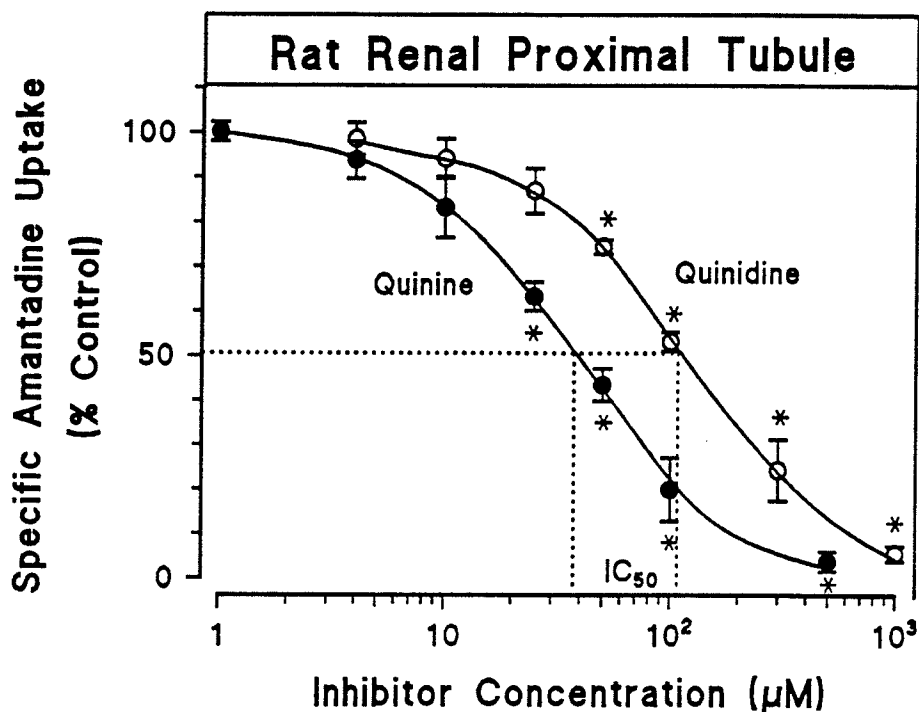


Figure R-16. Effects of quinine and quinidine on amantadine accumulation into rat renal proximal tubules. Incubation medium (200 μ l) contained 10 μ M amantadine \pm quinine or quinidine with approximately 0.4 mg tubular protein. Data points are reported as mean \pm SEM from 4 separate determinations. Inhibitory Constant (K_i) values were calculated individually in each experiment using the Cheng-Prusoff analysis, and were 36 ± 4 and 100 ± 8 μ M for quinine and quinidine, respectively (mean \pm SEM, n=4). * Denotes a significant difference from control at $p < 0.05$ as determined by repeated measures ANOVA followed by Tukey's HSD and Newman-Keuls tests.

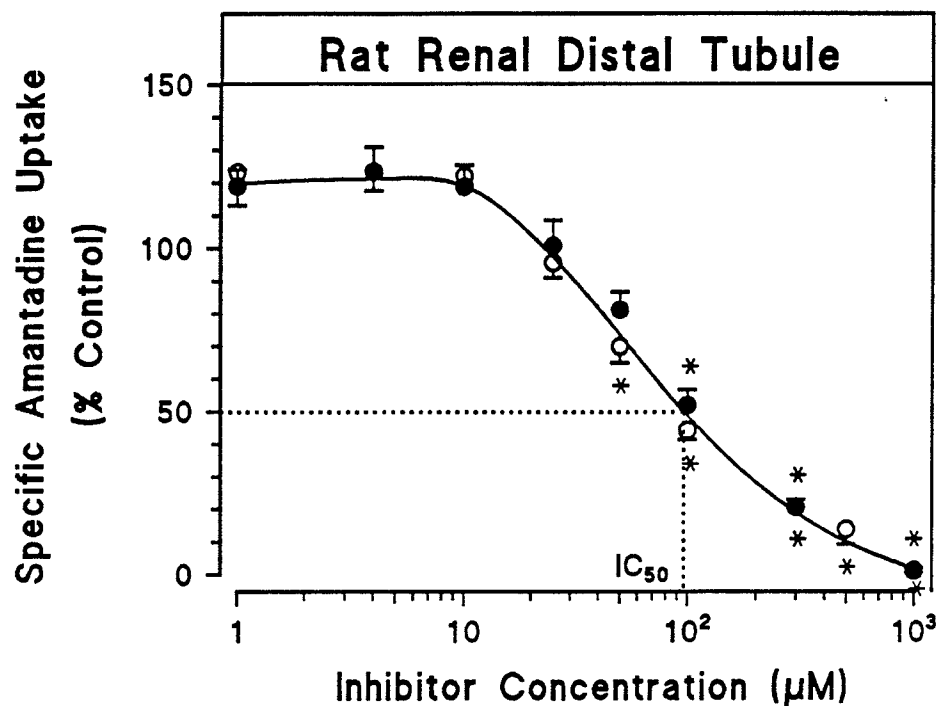


Figure R-17. Effects of quinine and quinidine on amantadine accumulation into rat renal distal tubules. Incubation medium (200 μ l) contained 10 μ M amantadine \pm quinine (●) or quinidine (○) with approximately 0.4 mg tubular protein. Data points are reported as mean \pm SEM from 4 separate determinations. Inhibitory Constant (K_i) values were calculated individually in each experiment using Cheng-Prusoff analysis, and were 87 ± 8 and 78 ± 8 μ M for quinine and quinidine, respectively (mean \pm SEM, $n=4$). * Denotes a significant difference from control at $p < 0.05$ as determined by repeated measures ANOVA followed by Tukey's HSD and Newman-Keuls tests.

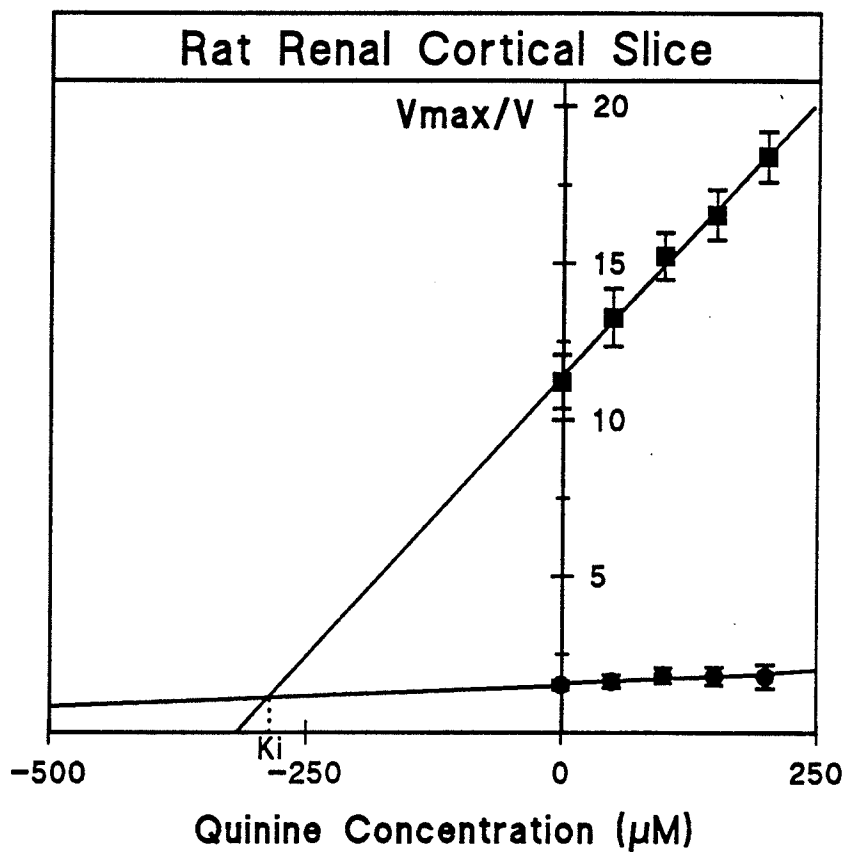


Figure R-18. Dixon analysis for [^3H]amantadine uptake by rat renal cortical slices in the presence of quinine. Amantadine concentrations were 10 (\blacksquare) and 100 μM (\bullet), and mean K_i (\pm SEM) for quinine determined individually from 4 experiments was $288 \pm 21 \mu\text{M}$. Velocity of accumulation (V) is expressed in $\text{pmol amantadine/mg tubular protein/minute}$.

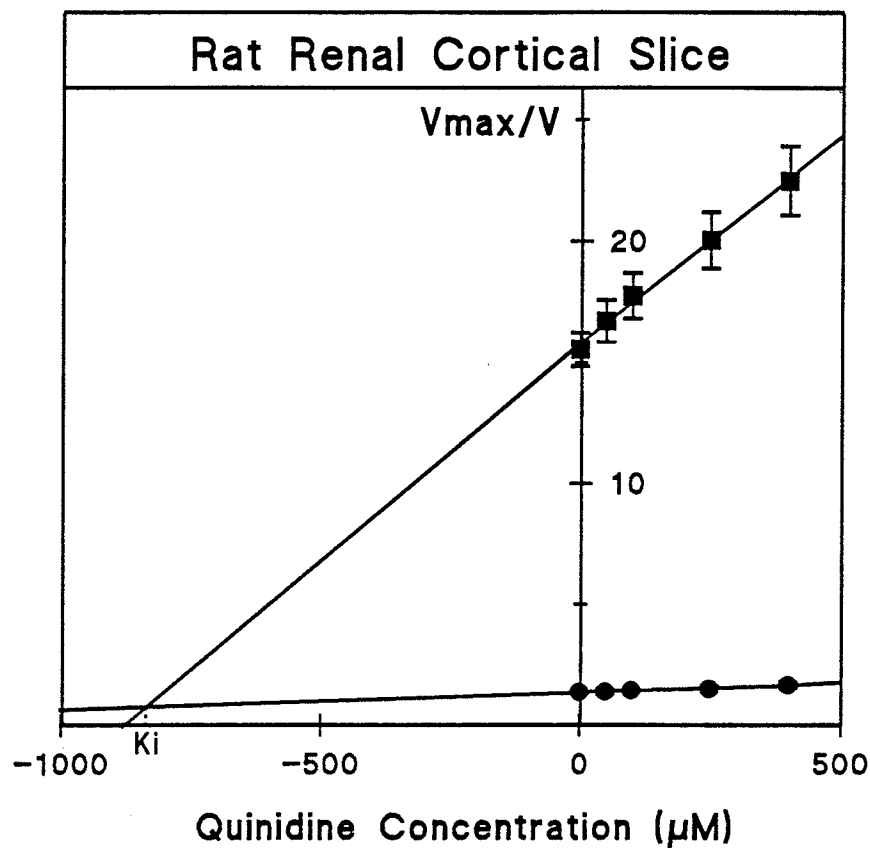


Figure R-19. Dixon analysis for [^3H]amantadine uptake by rat renal cortical slices in the presence of quinidine. Amantadine concentrations were 10 μM (■) and 100 μM (●), and mean K_i (\pm SEM) for quinidine determined individually from 4 experiments was $861 \pm 79 \mu\text{M}$. Velocity of accumulation (V) is expressed in $\text{pmol amantadine}/\text{mg tubular protein}/\text{minute}$.

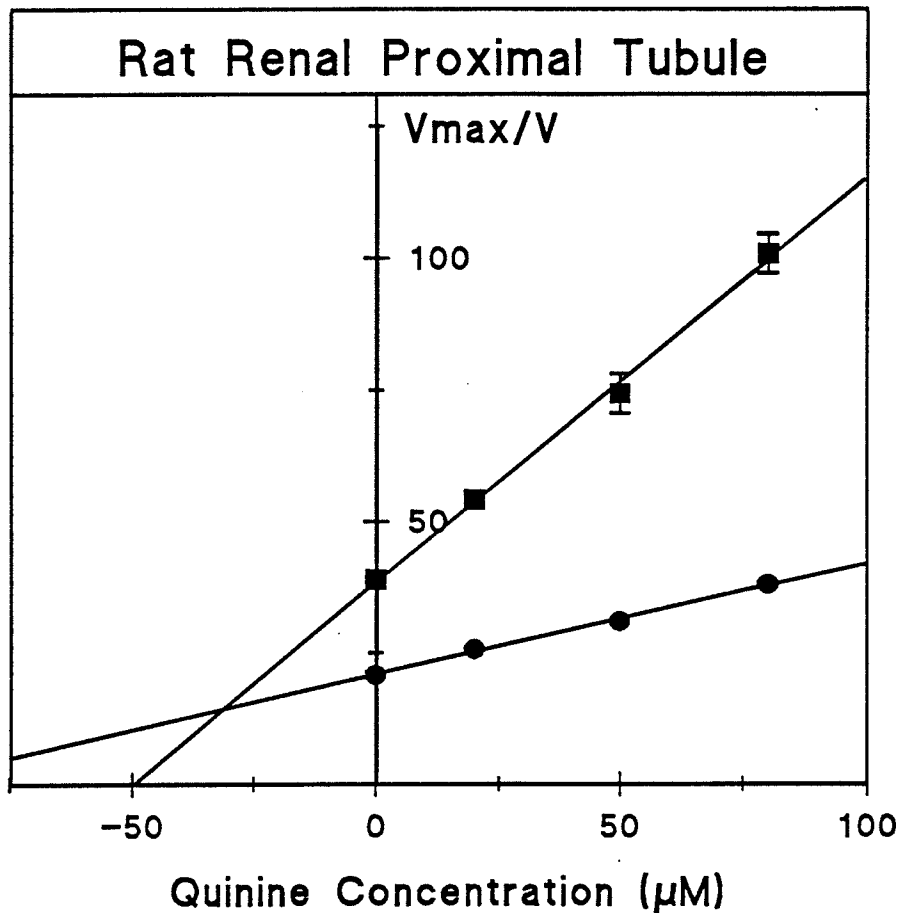


Figure R-20. Dixon analysis for [^3H]amantadine uptake by rat renal proximal tubules in the presence of quinine. Amantadine concentrations were 2.3 μM (■) and 4.5 μM (●), and mean K_i (\pm SEM) for quinine determined individually from 4 experiments was 32.1 ± 3.4 . Velocity of accumulation (V) is expressed in pmol amantadine/ mg tubular protein/ minute .

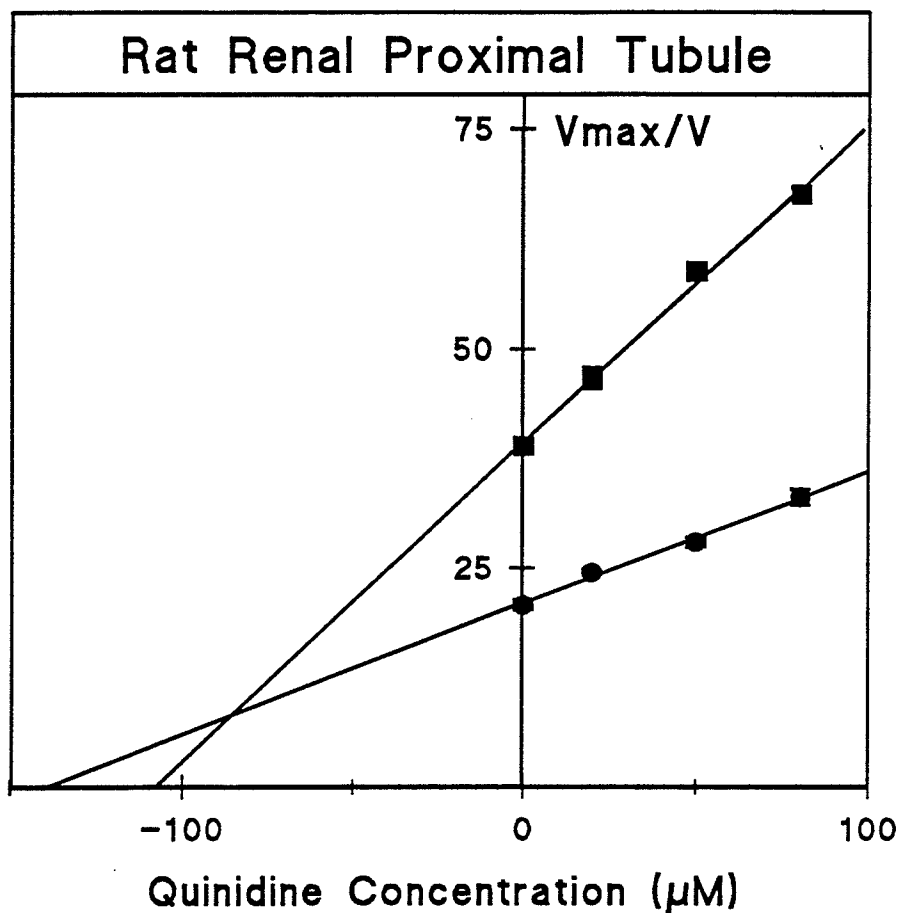


Figure R-21. Dixon analysis for $[^3\text{H}]$ amantadine uptake by rat renal proximal tubules in the presence of quinidine. Amantadine concentrations were (■) $2.3 \mu\text{M}$ and (●) $4.5 \mu\text{M}$, and mean K_i for quinidine (\pm SEM) determined individually from 4 experiments was $83.5 \pm 11.1 \mu\text{M}$. Velocity of accumulation (V) is expressed in $\text{pmol amantadine}/\text{mg tubular protein}/\text{minute}$.

TABLE R-A

[³H]Amantadine accumulation by rat renal proximal tubules using 30 second and 4 minute incubation times.

Amantadine concentrations used in each experiment were 2.3, 4.5, 9.0, 15.0 and 30.0 μ M. Values are reported as mean \pm S.E.M. from 4 separate determinations. Statistical significance was assessed using the unpaired Student's *t*-test.

Incubation time	V_{\max} (nmol/mg/minute)	K_m (μ M)
30 seconds	7.6 \pm 0.3	81 \pm 6
4 minutes	8.0 \pm 0.2	85 \pm 2
	(<i>p</i> > 0.1)	(<i>p</i> > 0.1)

TABLE R-B

Inhibition of [³H]amantadine accumulation into rat renal proximal tubules and cortical slices by quinine and quinidine.

Amantadine concentrations used in each experiment were: 2.3, 4.5, 9.0, 15.0 and 30.0 μ M in the proximal tubule preparation and 1, 5, 10, 50 and 100 μ M in the cortical slice preparation. Values are reported as mean \pm S.E.M. from 4 separate determinations. Statistical significance was assessed using unpaired Student's t-test for cortical slice data, and repeated measures ANOVA with Tukey's HSD test for proximal and distal tubule data.

Tissue	Inhibitor	V_{max} (nmol/mg/minute)	K_m (μ M)
	Control	1.34 ± 0.08	89 ± 9
	Quinine (200 μ M)	1.39 ± 0.11 ($p > 0.1$)	131 ± 15 ($p < 0.1$)
Slices :	Control	1.23 ± 0.03	87 ± 5
	Quinidine (500 μ M)	1.30 ± 0.04 ($p > 0.1$)	141 ± 18 ($p < 0.05$)
	Control	6.9 ± 0.4	81 ± 4
	Quinine (50 μ M)	6.9 ± 0.5 ($p > 0.1$)	198 ± 14 ($p < 0.05$)
Proximal Tubules :	Control	6.9 ± 0.4	81 ± 4
	Quinidine (100 μ M)	6.5 ± 0.4 ($p > 0.1$)	222 ± 33 ($p < 0.05$)
	Control	4.0 ± 0.4	76 ± 3
	Quinine (50 μ M)	3.7 ± 0.2 ($p > 0.1$)	163 ± 25 ($p < 0.1$)
Distal Tubules :	Control	4.0 ± 0.4	76 ± 3
	Quinidine (50 μ M)	3.5 ± 0.1 ($p > 0.1$)	170 ± 20 ($p < 0.05$)

higher in the cortical slice preparation. Stereoselective inhibition was not observed in distal tubules.

Human Renal Cortical Slices. Human renal tissue was obtained from 8 patients (6 males and 2 females, age 61 ± 4 years) who underwent unilateral nephrectomy. Patient demography is represented in Table M-A in the *Materials & Methods* section. Control uptake of amantadine ($5 \mu\text{M}$) by human cortical slices as a function of time is presented in Figure R-22 (patient 8). In comparison to the rat renal cortical slice data, uptake remained linear for up to 3 minutes (V_i) and thereafter attained saturation. At $10 \mu\text{M}$ amantadine, the slice/medium ratio for a 30-second incubation was 0.6 ± 0.1 ($n=4$). Figure R-23 displays a representative experiment with tissue from patient 7 showing the classical hyperbolic profile of amantadine accumulation at varying initial drug concentrations ($1 - 400 \mu\text{M}$). Lineweaver-Burk transformation of the data yielded an apparent K_m value for control amantadine uptake into the cortical slices of $198 \mu\text{M}$. V_{\max} was $0.17 \text{ nmol/mg slice wet weight/minute}$ (Figure R-24). The conversion of slice wet weight to estimated proximal tubule protein (Figure R-25) correspondingly modified control V_{\max} to $2.49 \text{ nmol/mg estimated proximal tubule protein/minute}$. Individual kinetic parameters for all experiments are reported in Table R-C.

The inclusion of either isomer, quinine or quinidine, in the incubation medium inhibited amantadine accumulation by the cortical slices. The type of inhibition was observed to be competitive, as indicated by representative Dixon plots for patients 5 and 4 (Figures R-26 and R-27). Inhibitory constant (K_i) values for quinine and quinidine were 301 and $543 \mu\text{M}$ respectively, and reiterates the greater inhibitory potency for the (-) isomer, quinine, over the (+) isomer, quinidine. All K_i values are presented in Table R-C.

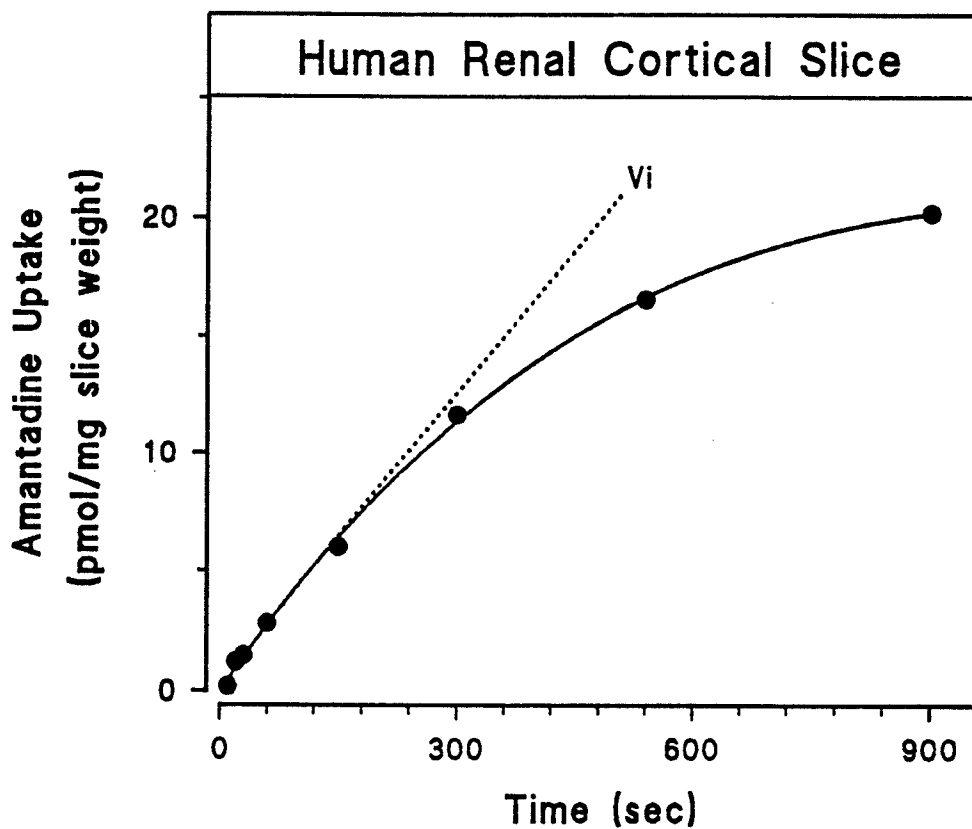


Figure R-22. Accumulation of [^3H]amantadine by human renal cortical slices as a function of time ranging from 0-900 seconds. Incubation medium (3 ml) contained 5 μM amantadine and 20-40 mg of a cortical slice from the right kidney of a 76 year-old male patient (patient 8). The dotted line represents the extrapolated initial linear phase of uptake (V_i).

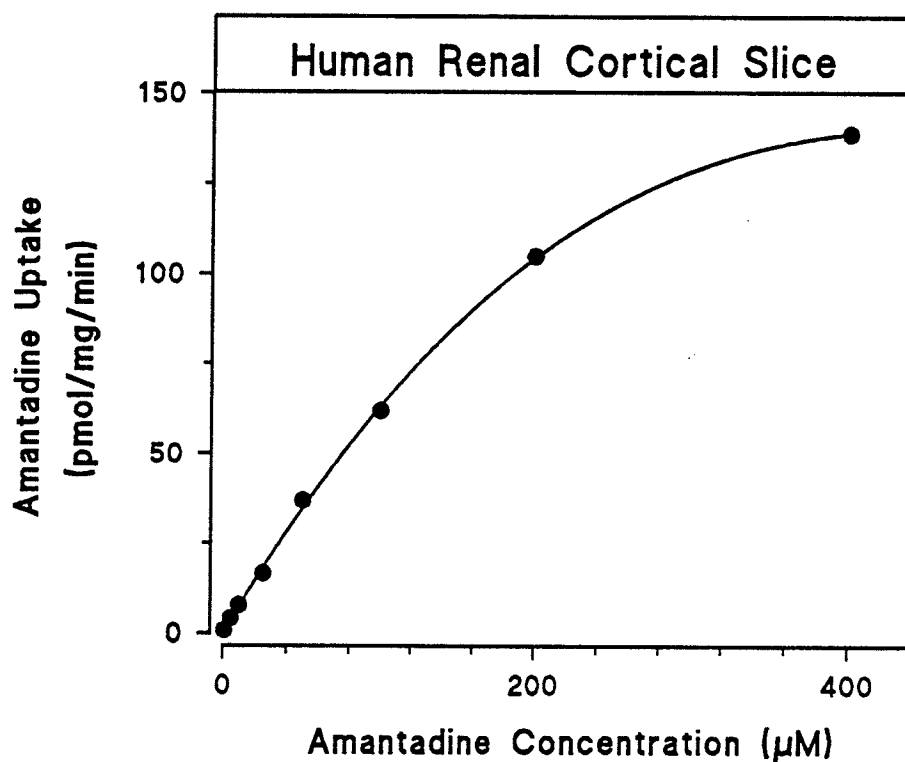


Figure R-23. Representative saturation isotherm for active amantadine accumulation by human cortical slices. Tissue was obtained from the left kidney of a 70 year-old female patient (patient 7). Incubation medium (3 ml) contained 1 - 400 μM amantadine and 20-40 mg of a cortical slice.

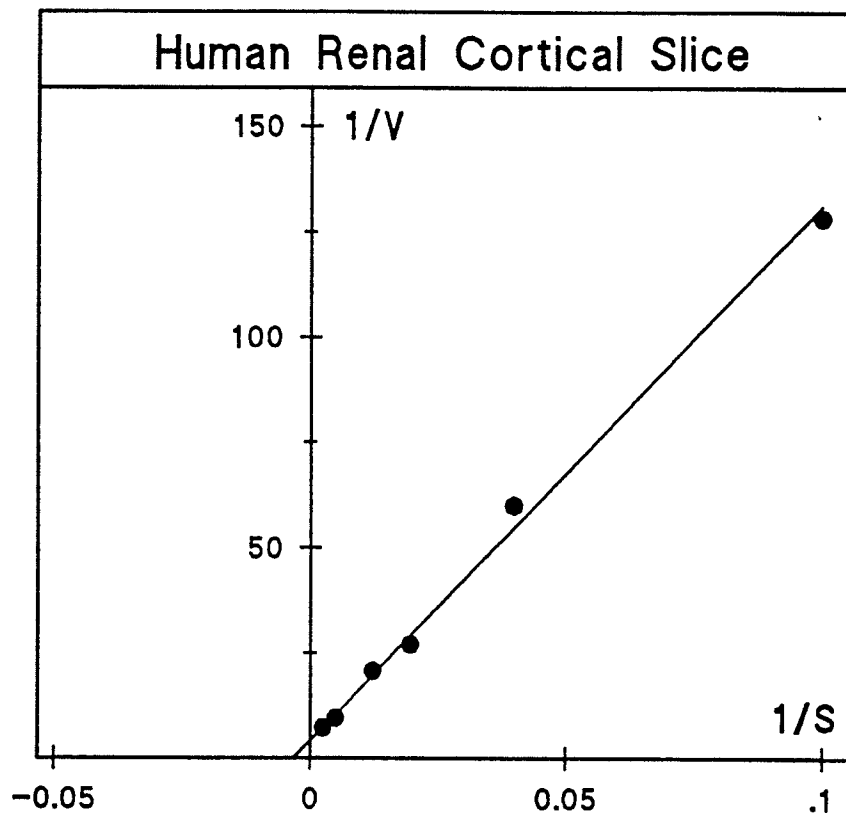


Figure R-24. Lineweaver-Burk transformation of control amantadine uptake values in human renal cortical slices (patient 7). Velocity of accumulation (V) is expressed in $\mu\text{mol amantadine}/\text{mg slice wet weight}/\text{minute}$, and amantadine concentration (S) is in micromolar. Apparent K_m is calculated from the negative reciprocal of the abscissa intercept to be $198 \mu\text{M}$, whereas apparent V_{max} is the reciprocal of the ordinate intercept ($0.17 \text{ nmol}/\text{mg slice wet weight}/\text{minute}$).

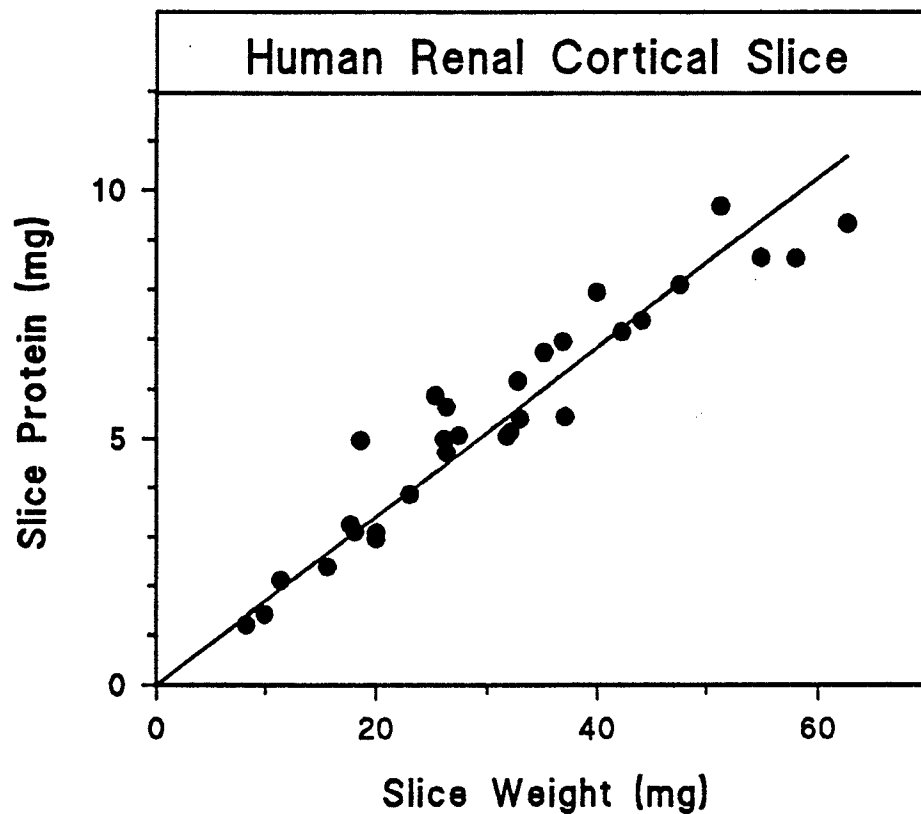


Figure R-25. Conversion of human renal cortical slice wet weight to cortical slice protein. Untreated slices from all kidneys were individually weighed and dissolved in 1 ml 0.5 M sodium hydroxide. Protein concentration was determined by the Biuret analysis. Gradient generated by linear regression (through origin) is 0.171 ± 0.004 (N=30, $r^2 = 0.90$)

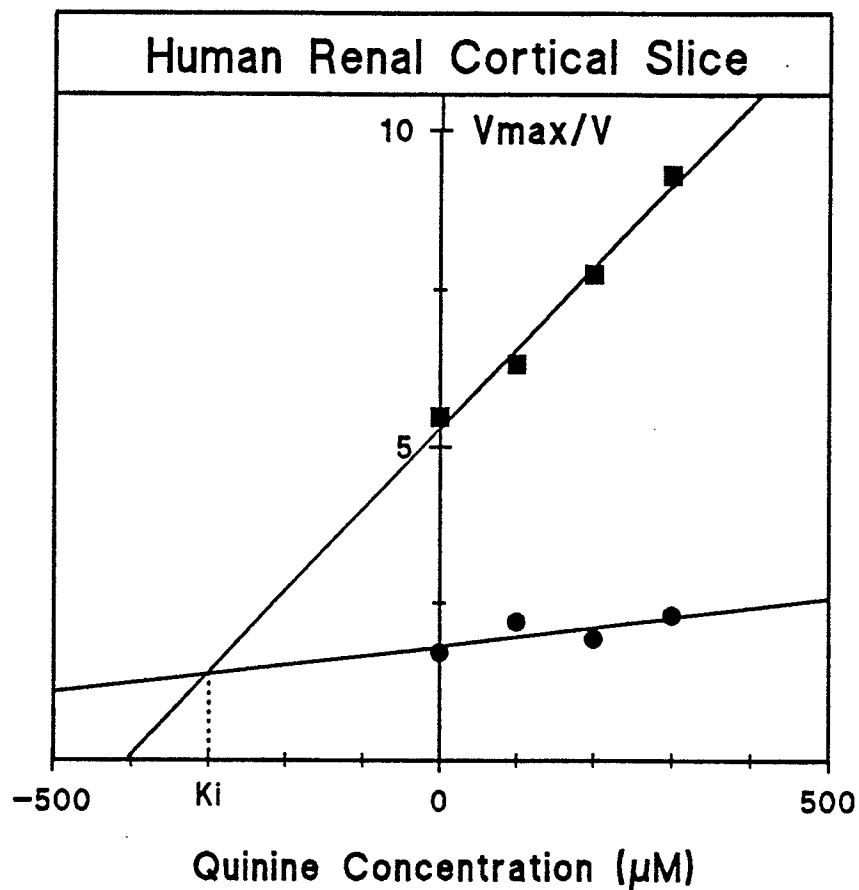


Figure R-26. Dixon analysis for inhibition of [^3H]amantadine uptake by human renal proximal tubules by quinine (patient 5). Amantadine concentrations were $10 \mu\text{M}$ (\blacksquare) and $80 \mu\text{M}$ (\bullet). Velocity of accumulation (V) is expressed in pmol amantadine/ mg estimated proximal tubule protein/ minute , and K_i for quinine is estimated to be $301 \mu\text{M}$.

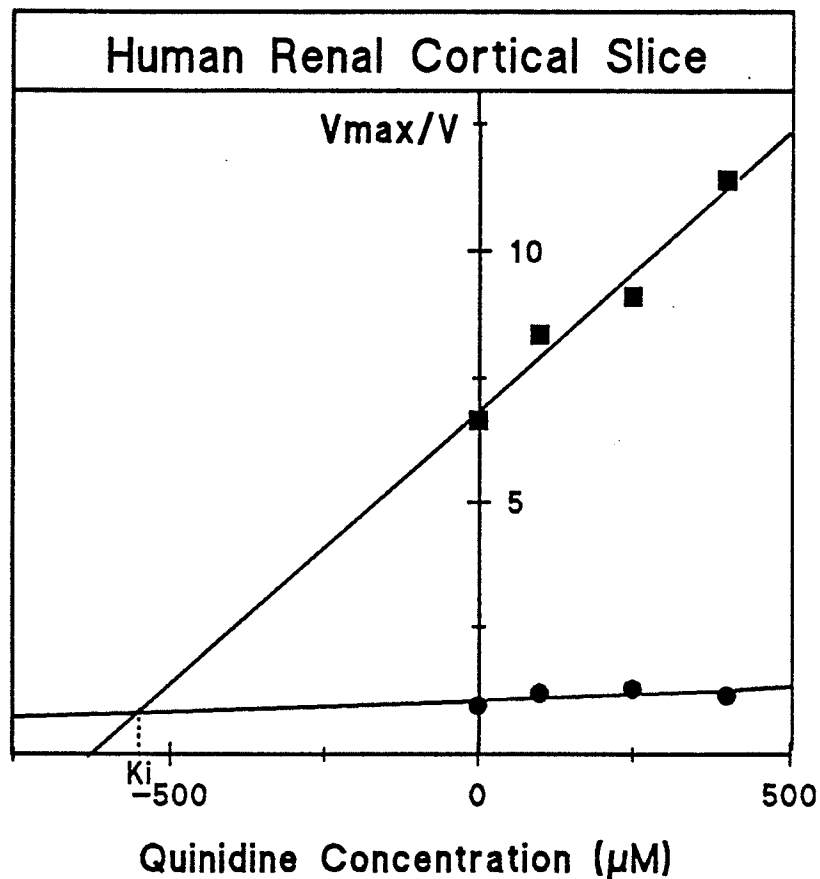


Figure R-27. Dixon analysis for inhibition of [^3H]amantadine uptake by human renal proximal tubules by quinidine (patient 4). Amantadine concentrations were 10 μM (■) and 80 μM (●). Velocity of accumulation (V) is expressed in μmol amantadine/ mg estimated proximal tubule protein/minute, and K_i for quinidine is estimated to be 543 μM .

TABLE R-C

Michaelis-Menten and Dixon kinetic parameters for control [³H]amantadine accumulation by human renal cortical slices using 30 second incubation.

Amantadine concentrations used in each control experiment were 10, 25, 50, 80 and 200 μ M. V_{max} values are expressed in $nmol$ amantadine/ mg estimated proximal tubule protein/minute. In inhibition studies, amantadine concentrations employed were 10 and 80 μ M. *ND* abbreviates for *Not Determined* due to limited tissue availability. * Denotes a significant difference between K_i values of quinine and quinidine at $p < 0.05$ using the unpaired Student's *t*-test.

Patient No.	K_m (μ M)	V_{max} ($nmol/mg/min$)	K_i (μ M)	
			Quinine	Quinidine
1	165	2.69	232	495
2	<i>ND</i>	<i>ND</i>	<i>ND</i>	720
3	170	2.93	154	<i>ND</i>
4	<i>ND</i>	<i>ND</i>	<i>ND</i>	543
5	<i>ND</i>	<i>ND</i>	301	<i>ND</i>
6	213	5.54	358	<i>ND</i>
7	198	2.49	<i>ND</i>	<i>ND</i>
Mean \pm SEM	187 \pm 11	3.4 \pm 0.7	261 \pm 44*	586 \pm 68*

II. Pharmacological Congeners & Renal Organic Cation Transport:

Control Uptake of Amantadine. Under control conditions, [³H]amantadine was transported actively by renal cortical slices, and isolated proximal and distal tubules. For a 30-second incubation, slice/medium ratio was 0.4 ± 0.03 (10 μ M amantadine, n=8). Apparent K_m and V_{max} values for amantadine uptake by cortical slices were $94 \pm 5 \mu$ M and $1.3 \pm 0.1 \text{ nmol/mg}$ estimated proximal tubule protein/minute respectively (n=10). In proximal and distal tubules, tubule/medium ratios were 35 ± 1 and 19 ± 2 respectively (10 μ M amantadine, 30-second incubation, n=8). Apparent K_m and V_{max} values were $87 \pm 4 \mu$ M and $7.2 \pm 0.4 \text{ nmol/mg}$ tubule protein/minute in proximal tubules (n=8), and $84 \pm 6 \mu$ M and $3.5 \pm 0.1 \text{ nmol/mg}$ tubule protein/minute in distal tubules (n=8).

Mixed Effects of Cimetidine. In cortical slices, low concentrations of cimetidine (10 and 25 μ M) significantly enhanced amantadine accumulation, whereas higher concentrations ($\geq 50 \mu$ M) produced a bimodal attenuation of accumulation (Figure R-28).

The addition of cimetidine (1 μ M to 10 mM) in proximal tubules solely augmented amantadine uptake by decreasing apparent K_m without affecting V_{max} (Table R-D and Figure R-29). Such an enhancement of uptake was of greater prominence than that observed in the cortical slices. Plateau was reached at approximately 100 μ M cimetidine, and uptake values subsequently declined back towards the basal level.

In distal tubules, cimetidine did not facilitate amantadine accumulation, and only produced competitive inhibition of uptake at millimolar concentrations (Table R-D and Figure R-29).

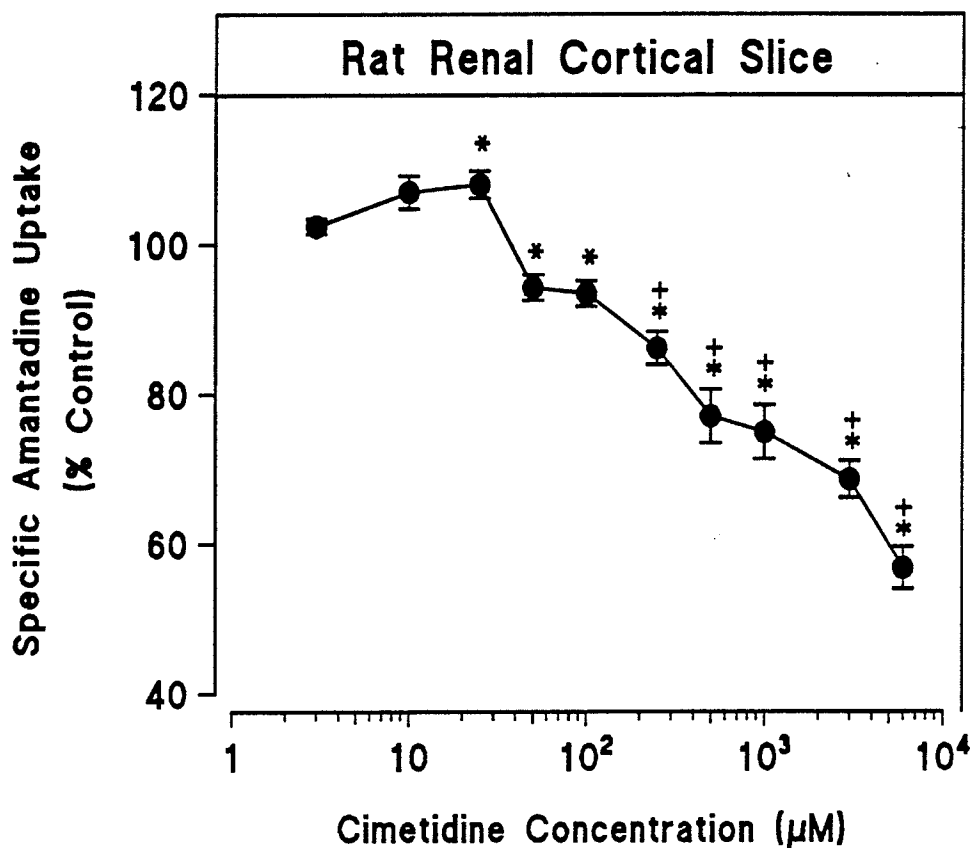


Figure R-28. Effects of cimetidine on amantadine accumulation into rat renal cortical slices. Incubation medium (3.0 ml) contained 10 μ M amantadine \pm cimetidine (3-6000 μ M) with approximately 30 mg of renal cortical slice. Slice/medium ratio (30-second incubation, n=4) for control specific uptake was 0.5 ± 0.03 . Data points are reported as mean \pm SEM from 4 separate determinations. * and + Denotes a significant difference from control at $p < 0.05$ as determined by repeated measures ANOVA followed by Tukey's HSD and Newman-Keuls tests respectively.

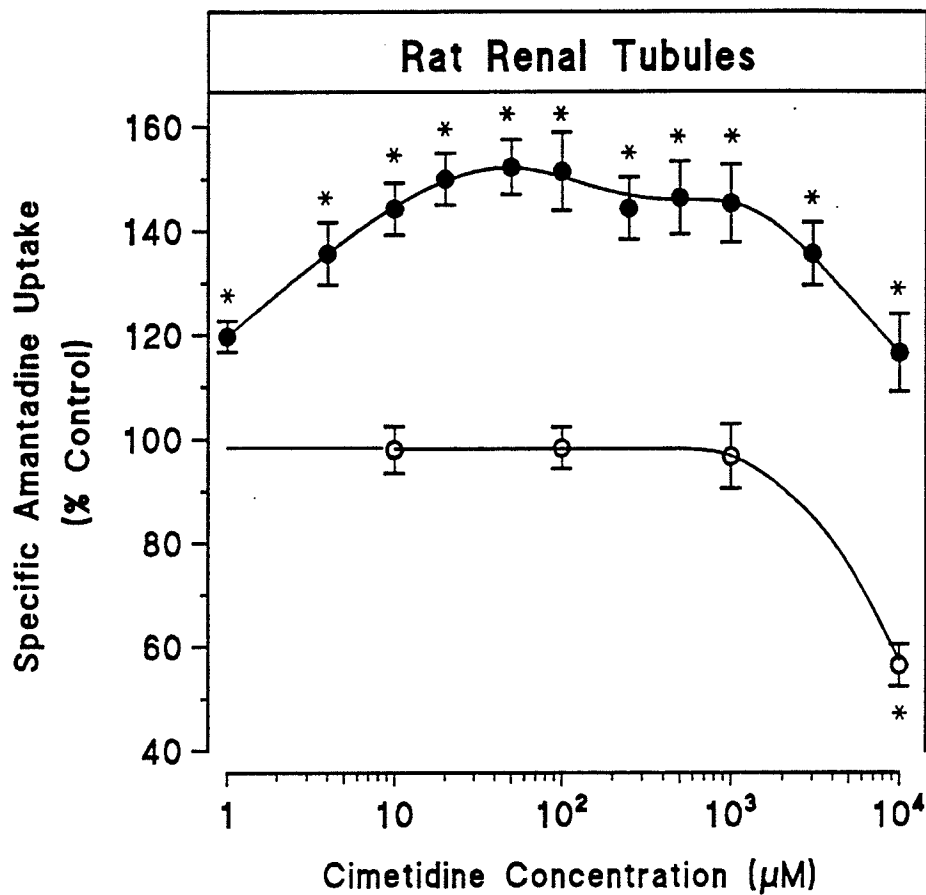


Figure R-29. Effects of cimetidine on amantadine accumulation into rat renal proximal (●) and distal (○) tubules. Incubation medium (200 μ l) contained 10 μ M amantadine \pm cimetidine with approximately 0.4 mg tubular protein. Tissue/medium ratio (30-second incubation, n=8) for control specific uptake is 35 ± 1 in proximal tubules and 19 ± 2 in distal tubules. Data points are reported as mean \pm SEM from 4 separate determinations. * Denotes a significant difference from control at $p < 0.05$ as determined by repeated measures ANOVA followed by Tukey's HSD and Newman-Keuls tests.

TABLE R-D

Effects of cimetidine and ranitidine on amantadine accumulation into rat renal proximal and distal tubules.

Amantadine concentrations used in each experiment were: 10, 15, 25, 50 and 100 μ M. Tissue/medium ratios were calculated using uptake data (10 μ M amantadine \pm histamine receptor antagonist) after 30 seconds incubation. All values reported represent mean \pm SEM from 4 separate experiments. P.T. and D.T. represent proximal and distal tubules respectively. Statistical significance was determined using unpaired Student's *t*-test.

Tissue	Experiment	T/M Ratio	V_{max}	K_m
			(nmol/mg/min)	(μ M)
P.T.	Control	33 \pm 1	6.8 \pm 0.5	88 \pm 5
	Cimetidine (20 μ M)	41 \pm 2 (<i>p</i> < 0.003)	5.8 \pm 0.6 (<i>p</i> < 0.195)	55 \pm 3 (<i>p</i> < 0.002)
D.T.	Control	21 \pm 0.5	3.4 \pm 0.1	71 \pm 4
	Cimetidine (10 mM)	13 \pm 0.1 (<i>p</i> < 0.001)	3.5 \pm 0.3 (<i>p</i> < 0.711)	131 \pm 13 (<i>p</i> < 0.005)
P.T.	Control	37 \pm 2	8.9 \pm 0.7	86 \pm 7
	Ranitidine (10 mM)	24 \pm 2 (<i>p</i> < 0.007)	7.9 \pm 0.8 (<i>p</i> < 0.369)	121 \pm 8 (<i>p</i> < 0.015)
D.T.	Control	15 \pm 2	4.3 \pm 0.1	95 \pm 5
	Ranitidine (10 mM)	9 \pm 2 (<i>p</i> < 0.083)	3.8 \pm 0.2 (<i>p</i> < 0.171)	160 \pm 10 (<i>p</i> < 0.001)

Inhibition by Ranitidine. In contrast to cimetidine, therapeutic low concentrations of ranitidine did not alter amantadine uptake in any preparation examined. Higher ranitidine concentrations (millimolar range) elicited inhibition of uptake in a competitive manner (Table R-D, Figures R-30 and R-31).

Effects of Imidazole & Guanidine. Figure R-32 displays a representative experiment showing the individual effects of the two major functional groups in cimetidine, imidazole and guanidine, on control specific amantadine uptake by isolated proximal tubules.

III. Nicotine and Cotinine & Renal Organic Cation Transport:

Control Uptake in Tubules. Consistent with results reported in previous sections, [³H]amantadine (10 μ M) was again accumulated by both proximal and distal segments with tubule/medium ratio values of 32 ± 1 (n=14) and 18 ± 1 (n=13) respectively. Both tubule fractions again exhibited similar apparent affinity with K_m values of 78 ± 2 and 76 ± 5 μ M (n=4 and 5) respectively, and V_{max} in distal tubules was 3.4 ± 0.5 in comparison to 6.6 ± 0.1 nmol/mg tubule protein/minute in proximal tubules.

(-) & (+) Nicotine on Amantadine Uptake. Amantadine accumulation in renal proximal tubules was significantly enhanced by the addition of (-) nicotine (n=5) and (+) nicotine (n=6) in a bimodal fashion (Figure R-33). Apparent K_m for amantadine uptake was decreased by (-) and (+) nicotine (0.4 μ M) from 78 ± 2 to 52 ± 2 and 61 ± 5 μ M respectively, whereas V_{max} was not altered significantly (6.6 ± 0.1 to 6.3 ± 0.1 and 6.5 ± 0.2 nmol/mg tubule protein/minute).

In distal tubules, clinically relevant concentrations of nicotine (0.1 - 0.3 μ M)

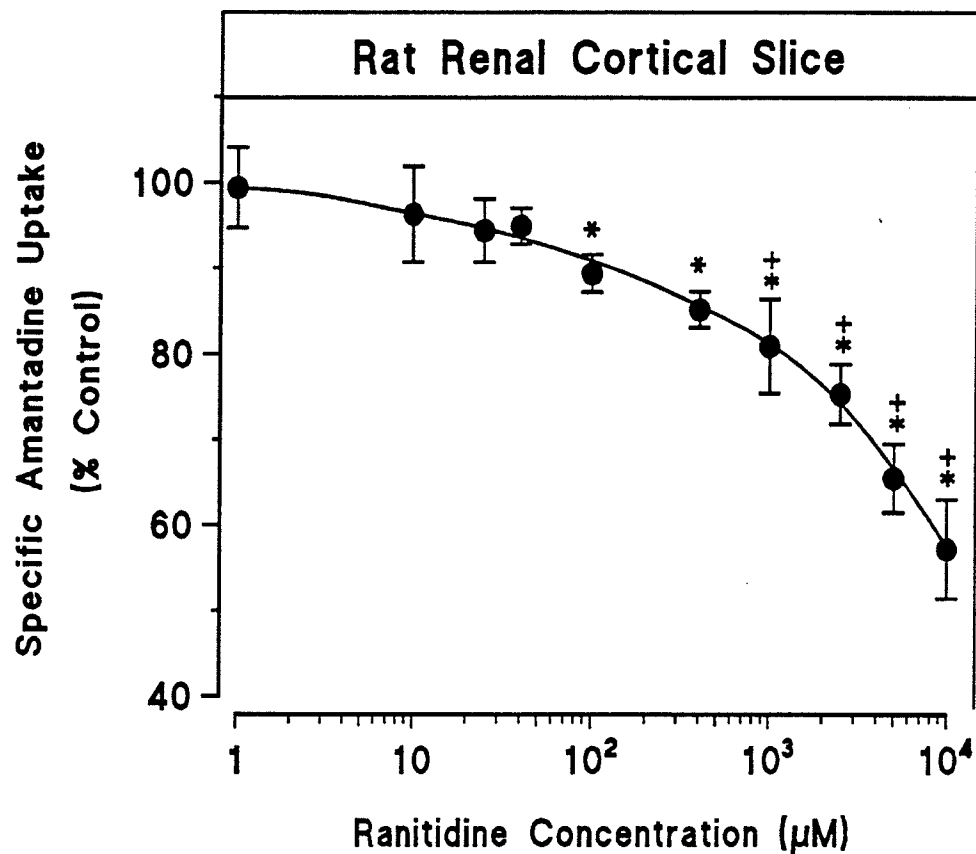


Figure R-30. Effects of ranitidine on amantadine accumulation into rat renal cortical slices. Incubation medium (3.0 ml) contained 10 μ M amantadine \pm ranitidine (1-10000 μ M) with approximately 30 mg of renal cortical slice. Slice/medium ratio (30-second incubation, n=4) for control specific uptake was 0.4 ± 0.04 . Data points are reported as mean \pm SEM from 5 separate determinations. * and + Denotes a significant difference from control at $p < 0.05$ as determined by repeated measures ANOVA followed by Tukey's HSD and Newman-Keuls tests respectively.

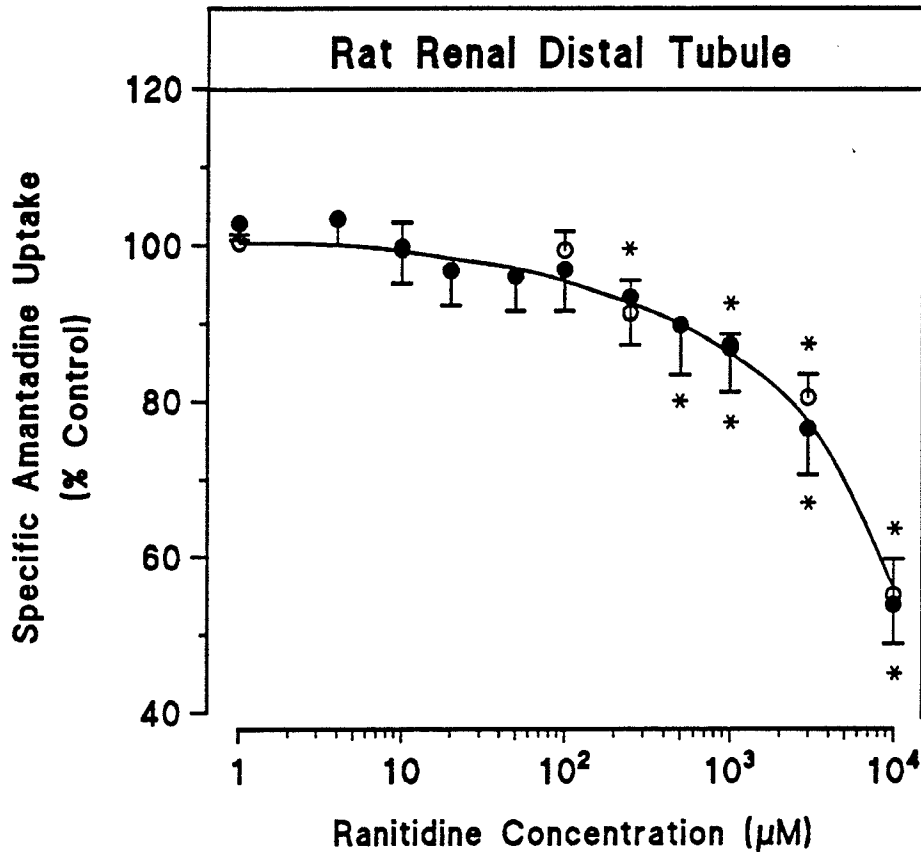


Figure R-31. Effects of ranitidine on amantadine accumulation into rat renal proximal (●) and distal (○) tubules. Incubation medium (200 μ l) contained 10 μ M amantadine \pm ranitidine with approximately 0.4 mg tubular protein. Tissue/medium ratio (30-second incubation, n=8) for control specific uptake is 35 ± 1 in proximal tubules and 19 ± 2 in distal tubules. Data points are reported as mean \pm SEM from 4 separate determinations. * Denotes a significant difference from control at $p < 0.05$ as determined by repeated measures ANOVA followed by Tukey's HSD and Newman-Keuls tests.

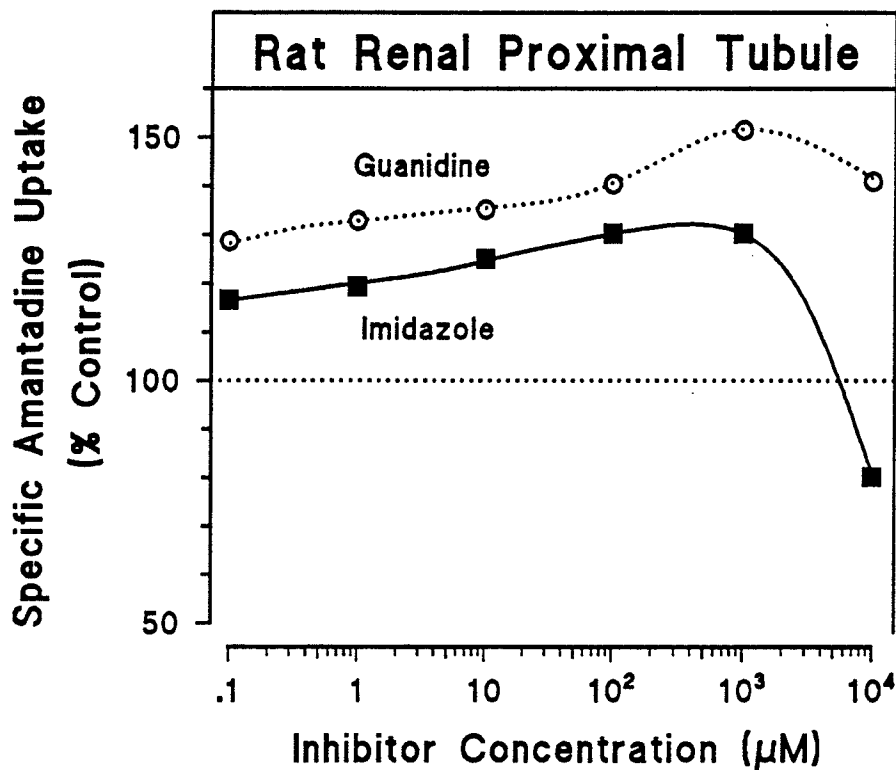


Figure R-32. A representative experiment demonstrating the effects of imidazole and guanidine on amantadine accumulation into rat renal proximal tubules. Incubation medium (200 μ l) contained 10 μ M amantadine \pm imidazole or guanidine (0.1 μ M - 10 mM) with approximately 0.4 mg tubular protein. After 30-second incubation, tubule/medium ratio was 3.0.

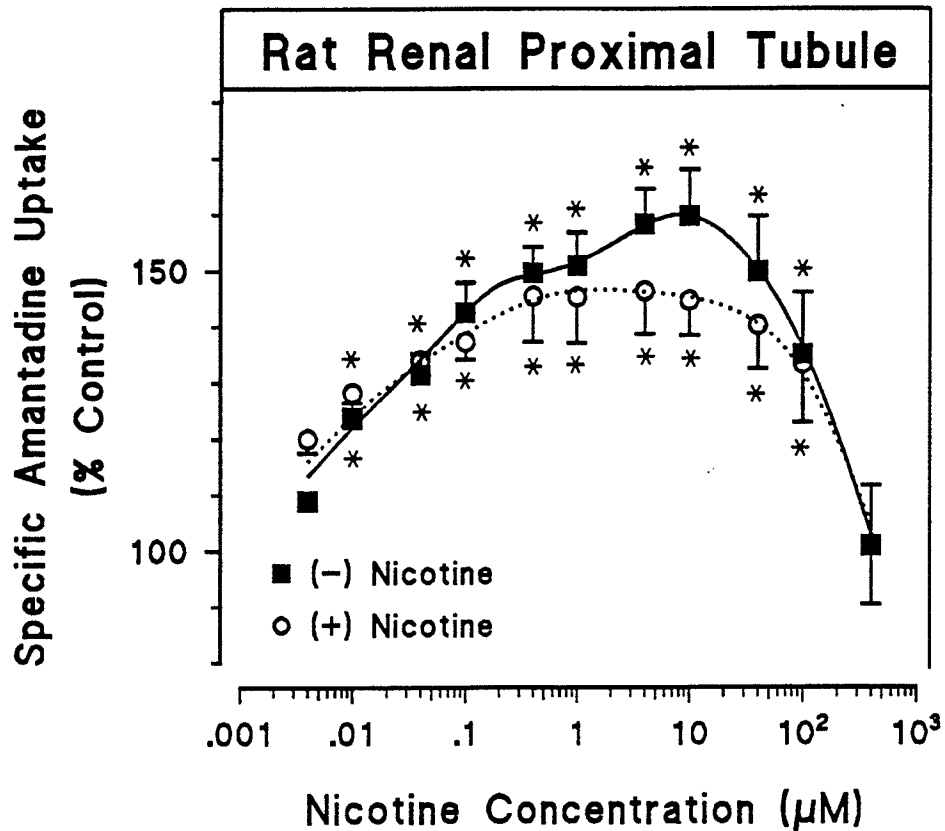


Figure R-33. Effects of (-) and (+) nicotine on amantadine accumulation into rat renal proximal tubules. Incubation medium (200 μl) contained 10 μM amantadine \pm nicotine (4 nM - 400 μM). Tubule/medium ratio (30-second incubation) for control specific uptake (100 %) is 32 ± 1 . Data points are reported as mean \pm SEM from 5 and 6 separate determinations for (-) and (+) nicotine respectively. * Denotes a significant difference from control at $p < 0.05$ as determined by repeated measures ANOVA followed by Tukey's HSD and Newman-Keuls tests.

did not affect amantadine uptake. However, higher nicotine concentrations of ≥ 40 μM produced inhibition of uptake (Figure R-34). K_m for amantadine uptake was increased by (-) and (+) nicotine (400 μM) from 76 ± 5 to 124 ± 9 and 116 ± 17 μM respectively, and V_{max} was moderately, but significantly, decreased from 3.4 ± 0.5 to 3.0 ± 0.4 and 3.0 ± 0.4 nmol/mg/minute .

Nicotine on Amantadine Efflux. Efflux of amantadine from both tubule preparations under control conditions was observed to be linear for the first minute (Figures R-35 (a-d)). Initial efflux rates of amantadine from proximal and distal tubules were 58 ± 6 (n=8) and 27 ± 7 (n=4) $\text{pmol/mg tubule protein/30 seconds}$ respectively. The incorporation of 0.4 μM (-) or (+) nicotine into the efflux incubation medium significantly attenuated initial efflux of amantadine from preloaded proximal tubules from 51 ± 4 to 32 ± 8 and 27 ± 4 $\text{pmol/mg tubule protein/30 seconds}$ (Figure R-35a).

However, a higher concentration of (-) or (+) nicotine (400 μM) significantly stimulated initial efflux of amantadine from 66 ± 11 to 200 ± 23 and 208 ± 28 $\text{pmol/mg tubule protein/30 seconds}$ (Figure R-35b). The addition of cimetidine (10 μM) did not significantly affect amantadine efflux (64 ± 10 to 77 ± 4 $\text{pmol/mg tubule protein/30 seconds}$) (Figure R-35c).

In preloaded distal tubules, 400 μM (-) or (+) nicotine also promoted amantadine efflux from 27 ± 7 to 75 ± 8 and 70 ± 10 $\text{pmol/mg/30 seconds}$ respectively (Figure R-35d).

(-) Cotinine on Amantadine Uptake. The addition of (-) cotinine moderately stimulated amantadine uptake in isolated proximal tubules. Although statistical significance from control was achieved with cotinine concentrations of 0.4 to 100 μM , maximal enhancement of uptake was comparatively lower than that produced

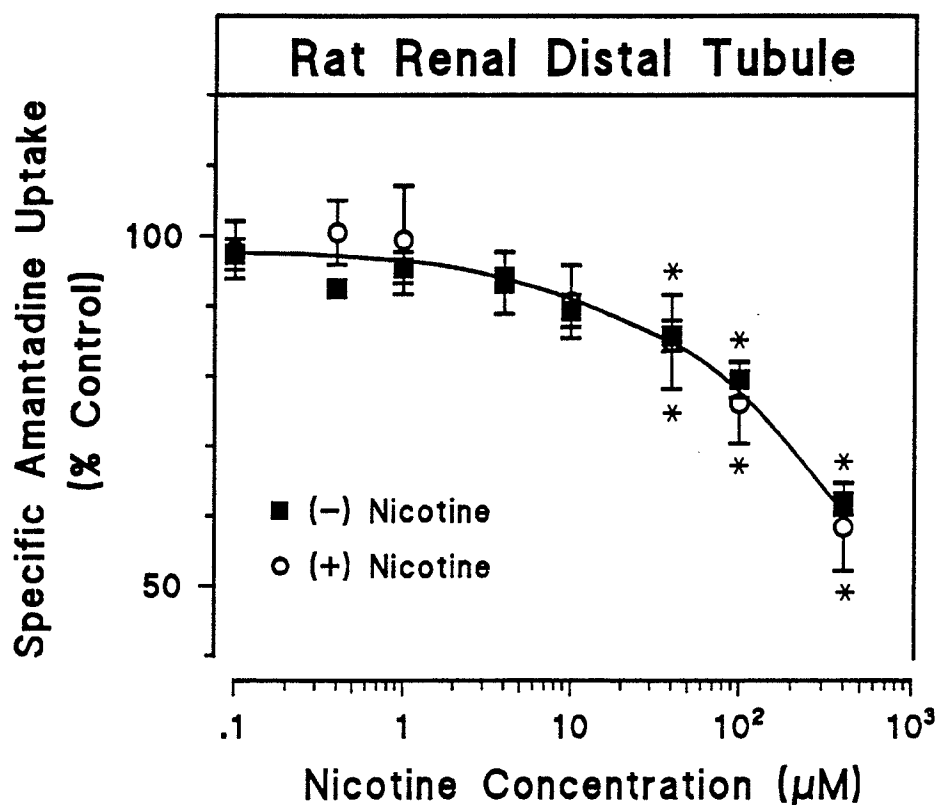
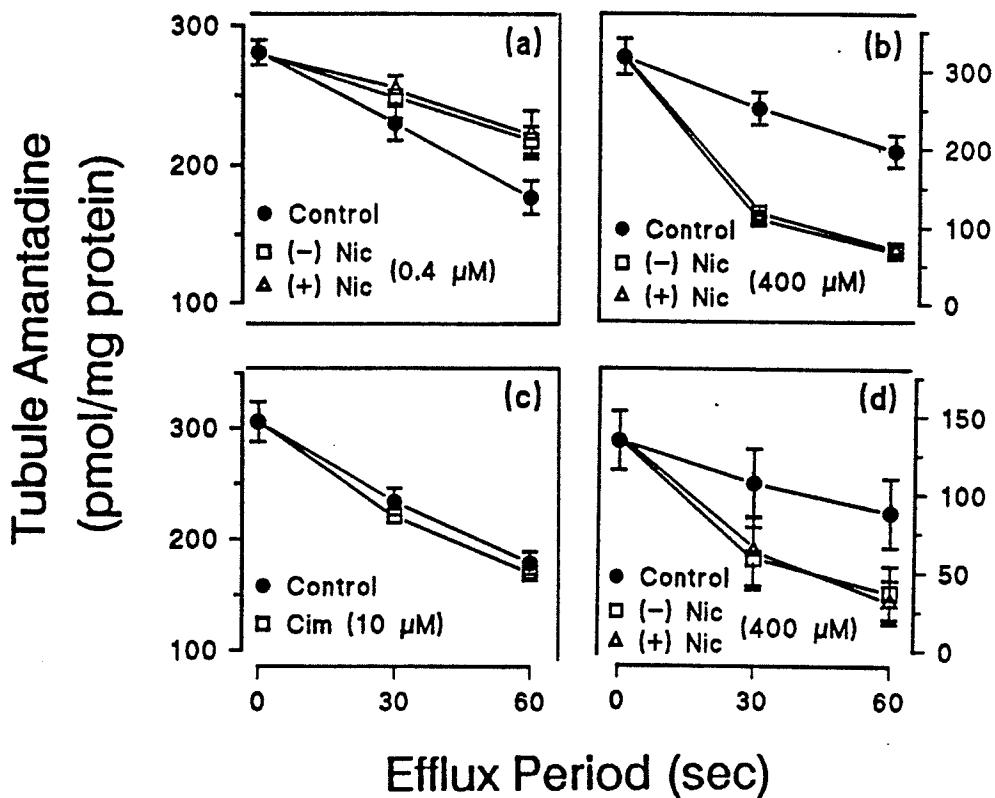


Figure R-34. Effects of (-) and (+) nicotine on amantadine accumulation into rat renal distal tubules. Incubation medium (200 μl) contained 10 μM amantadine \pm nicotine (100 nM - 400 μM). Tubule/medium ratio (30-second incubation) for control specific uptake (100 %) is 18 ± 1 . Data points are reported as mean \pm SEM from 4 separate determinations. * Denotes a significant difference from control at $p < 0.05$ as determined by repeated measures ANOVA followed by Tukey's HSD and Newman-Keuls tests.



Figures R-35. Effects of (-) & (+) nicotine and cimetidine on amantadine efflux from rat renal proximal tubules (a, b & c) and distal tubules (d). Tubules were preloaded in 200 μ l medium with [3 H]amantadine for 30 seconds and efflux was subsequently initiated by a dilution of the incubation medium with KHS \pm (-) or (+) nicotine or cimetidine to 3330 μ l. Final nicotine concentrations in efflux media were 0.4 μ M (a) and 400 μ M (b & d), whereas concentration of cimetidine was 10 μ M (c). All data points are represented as mean \pm SEM from 4 separate determinations.

by its parent compound nicotine (Figure R-36 versus Figure R-33). In distal tubules, all concentrations of (-) cotinine examined did not significantly alter uptake.

Rat Renal Cortical Slices. [³H]Amantadine (10 μ M) was accumulated by rat cortical slices with a slice/medium ratio of 0.33 ± 0.04 (30-second incubation). In contrast to that observed in isolated proximal tubules, the addition of 0.01 - 40 μ M (-) nicotine did not significantly enhance amantadine accumulation, and only the higher concentrations ($\geq 100 \mu$ M) produced low-affinity inhibition of uptake (Figure R-37).

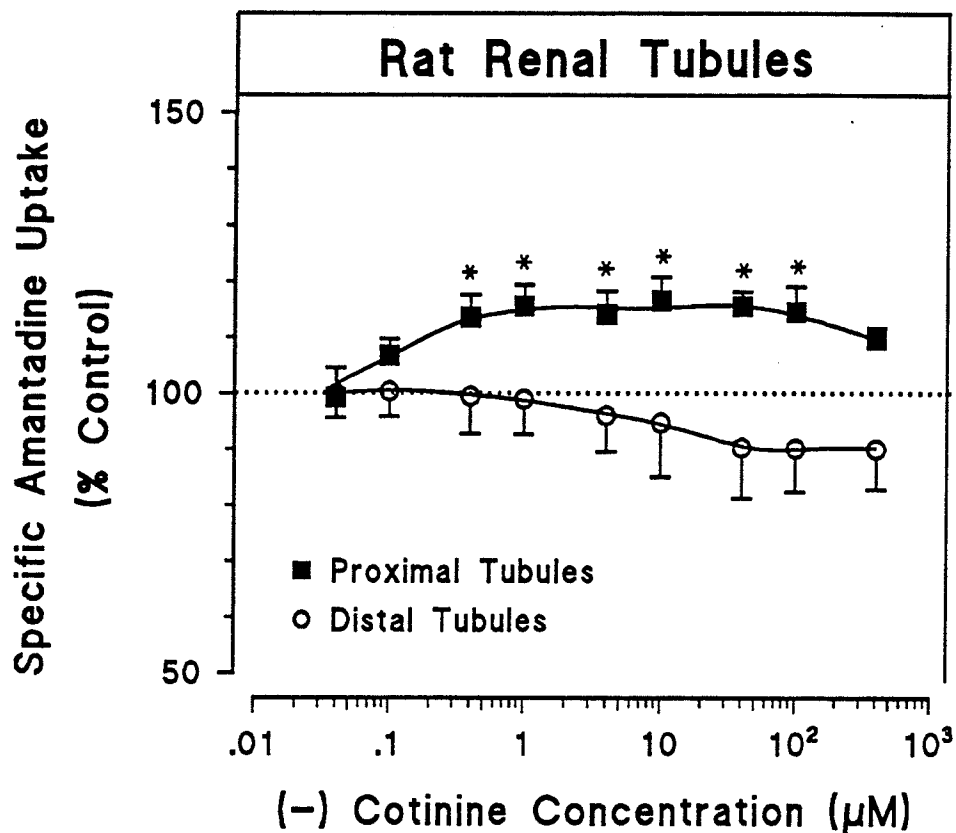


Figure R-36. Effects of (-) cotinine on amantadine accumulation into rat renal proximal (■) and distal tubules (○). Incubation medium (200 μ l) contained 10 μ M amantadine \pm cotinine (40 nM - 400 μ M). Tubule/medium ratio (30-second incubation) for control specific uptake (100 %) is 34 ± 2 in proximal tubules and 18 ± 3 in distal tubules. Data points are reported as mean \pm SEM from 4 separate determinations. * Denotes a significant difference from control at $p < 0.05$ as determined by repeated measures ANOVA followed by Tukey's HSD and Newman-Keuls tests.

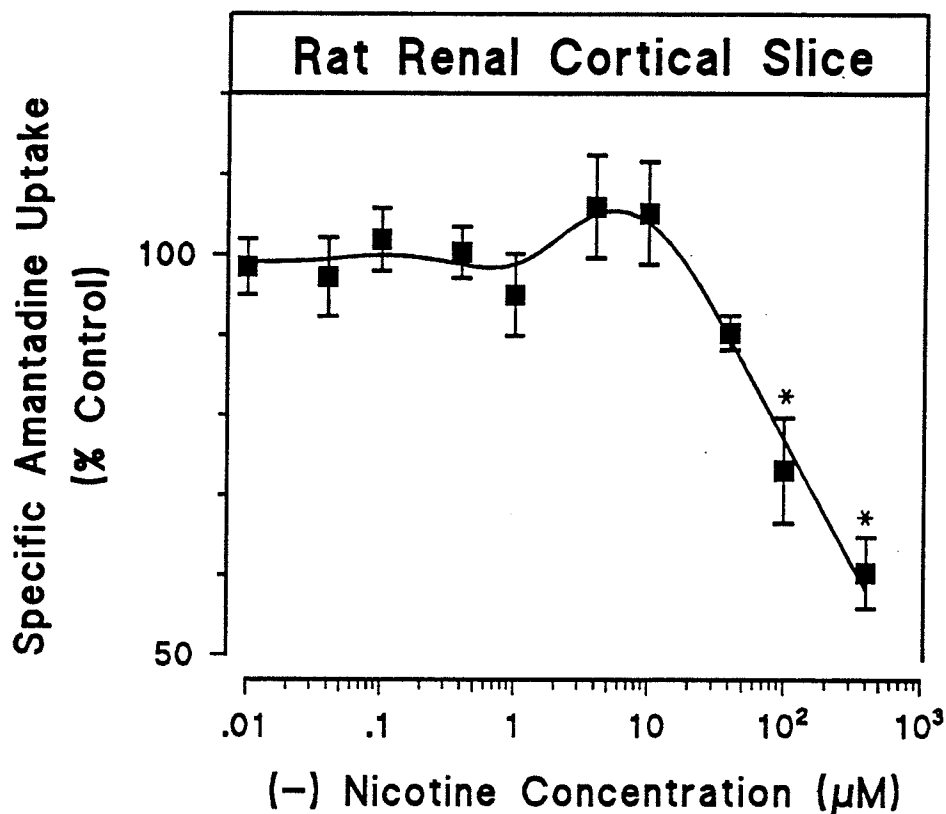


Figure R-37. Inhibition of (-) nicotine on amantadine accumulation in rat renal cortical slices. Incubation medium (3.0 ml) contained 10 μ M amantadine \pm nicotine (10 nM - 400 μ M) with approximately 30 mg of renal cortical slice. Slice/medium ratio (30-second incubation) for control specific uptake was 0.33 ± 0.04 . Data points are reported as mean \pm SEM from 4 separate determinations. * Denotes a significant difference from control at $p < 0.05$ as determined by repeated measures ANOVA followed by Tukey's HSD and Newman-Keuls tests.

DISCUSSION

Amantadine as a Marker Organic Cation. The present investigation has established the contemporary use of amantadine as a chemical probe in the examination of renal organic cation transport in the mammalian kidney *in vitro*. In recapitulation, the availability of incontrovertible and clinically applicable organic cation probes is limited, and the major advantages behind the use of this particular organic cation include its therapeutic relevance, homogeneous and achiral chemical properties, and limited metabolism in mammalian species.

General experimental precautions taken to diminish potential artefactual interference are as follows. In order to minimize potential contamination with medullary segments in the present tubule and slice preparations, excessive tissue from the cortico-medullary junction was discarded. Henceforth, such an omission of the *juxtamedullary nephrons* has consequently rendered the applicability of the current observations to confine within *superficial cortical* and *midcortical nephrons*. Possible hypoxia leading to tissue degradation during incubation was alleviated by the use of a verified physiological incubation environment, and a lower incubation temperature of 25 °C. In conjunction, a relatively shorter incubation period of 30 seconds was employed to minimize potentially significant intratubular metabolism of competing substrates (Table D-A), and to provide initial linear transport velocity values for the valid use of the Lineweaver-Burk analysis of data. The absence of physiological levels of plasma proteins from the current incubation media was of subordinate concern from other investigators within this field, and such a potentially confounding issue is evaded by the fact that active carrier-mediated transfer of organic solutes is the primary focus of the present study. In comparison to renal glomerular filtration *in vivo*, this latter process involves an isosmotic movement of solute, with water, into the glomerular filtrate. It does not disturb the equilibrium

Table D-A. Pharmacokinetic data for cationic drugs employed. Values are obtained from: Bowman & Rand (1980), Ochs *et al.* (1980), Gugler *et al.*, 1981; White (1985), Aoki & Sitar (1988), Grant *et al.* (1989).

Drug	Half Life (Hours)	Clinically Relevant Plasma Concentration (μ M)	Protein Binding In Plasma (%)
Amantadine	16	1.5 - 5.0	67
Quinine	11	20 - 40	90 - 95
Quinidine	6	5 - 15	85 - 90
Cimetidine	2	1.5 - 2.5	19
Ranitidine	2	0.3 - 1.0	15
Nicotine	2	0.1 - 0.3	5

between free and bound solute in the plasma, and the rate of solute clearance by filtration is directly proportional to the free fraction of the solute. Conversely, in the case of active tubular transport, solute transfer by the carrier is unaccompanied by water. The decline in free plasma concentration of the solute would in turn cause a net dissociation of bound solute from the protein, and effectively all of the solute (bound and free) is available to the carrier. As reference, approximate percentage values for plasma protein binding of the organic cations employed are listed Table D-A.

Under control conditions, the marker organic cation, amantadine, was concentrated by rat renal cortical slices, isolated proximal tubules and distal tubules. Transport was observed to be saturable with increasing substrate concentrations and 2,4-dinitrophenol-sensitive, which supports the interpretation of a carrier-mediated transport process and its dependency upon oxidative phosphorylation (Farah & Rennick, 1956; Peters, 1960; Berndt, 1976 & 1981; Kinsella *et al.*, 1979a; Holohan & Ross, 1980 & 1981; Rennick, 1981; Ross & Holohan, 1983; Grantham & Chonko, 1986 & 1991; Somogyi, 1987; van Ginneken & Russel, 1989; Sokol & McKinney, 1990). The presently demonstrated *cis*-competitive inhibition of amantadine uptake by quinine and quinidine, and self-induced *trans*-stimulation of amantadine efflux, further reinforced the current proposition of a carrier-mediated phenomenon (Wilbrandt & Rosenberg, 1961; Sokol *et al.*, 1989). The addition of two prototypic organic cations, tetraethylammonium or guanidine, into the incubation medium both interacted significantly with control amantadine transport *in vitro*, and supported their common pathway(s) *via* the customary organic cation transport system (Rennick, 1981; Miyamoto *et al.*, 1989).

Conventionally, the predominant site of renal organic cation transport is believed to be located exclusively in the proximal tubules. Nevertheless, current experimentation has also demonstrated active accumulation of the organic cation,

amantadine, in renal distal tubules for the first time. In prolepsis, although the inward-negative electrochemical gradient would explain such an accumulation of the cationic amantadine by the distal tubule cells, the possibility of contamination of the distal tubule fraction with proximal tubules was of primary concern. The purity of both fractions was confirmed by microscopic and enzymatic examination. The observed heterogeneity in tubule morphology and enzyme distribution between the two fractions is in concordance with previous reports (Scholer & Edelman, 1979; Guder & Ross, 1984; Gesek *et al.*, 1987). Furthermore, the clear distinctions observed between patterns of interference by a given competing organic cation in the two tubule fractions represent further evidence for their purity. Examples of which include the total absence of uptake facilitation by cimetidine, and the loss of stereoselectivity in inhibition by quinine and quinidine, in the distal tubule fraction.

In the renal cortical slice, rate or velocity of amantadine accumulation was perceived to be considerably slower than that in either tubule preparation (Burg & Orloff, 1969; Sheikh & Möller, 1970; Möller & Sheikh, 1983). Although all three preparations expressed similar apparent affinities (K_m) for amantadine, the apparent capacity (V_{max}) was the lowest in the slice system despite slice weight to estimated tubule protein conversion. The basis for such a difference in the latter may include an incomplete penetration of amantadine and/or metabolic substrates into deeper regions of the cortical slices during the relatively short incubation time period (Wedeen & Weiner, 1973b; Berndt, 1976), and/or the presence of additional amantadine transport sites with lower capacity with the remaining segments of the cortical nephron within the slice preparation. Moreover, possible directional differences in amantadine uptake between preparations should also be considered. The accessibility of the tubule lumina during incubation in isolated tubules and cortical slices is currently controversial. Tubule lumina in the cortical slices are believed preponderantly to be in a collapsed state, whereas lumina in isolated renal

tubules have been reported to be dilated and patent for substrate exchange (Foulkes & Miller, 1959; Wedeen & Weiner, 1973a; Berndt, 1976; Wedeen & Vyas, 1978; Möller & Sheikh, 1983; Chahwala & Harpur, 1986; Gesek *et al.*, 1987). These postulates are supported by the present efflux experimental series in which the rate of amantadine egress from preloaded cortical slices was observed to be significantly lower than that from preloaded proximal tubules (Murthy & Foulkes, 1967). Therefore, luminal exchange of amantadine is proposed to be attenuated in the cortical slice (closed-lumen) preparation, and net uptake is primarily reflective of the secretory influx of amantadine across the basolateral membrane. Conversely in isolated tubules, basolateral substrate influx may be supplemented by a luminal reabsorptive process, which may perchance represent common pathway(s) for amino acid reabsorption (Foulkes, 1972; Berndt, 1976; Jessen & Sheikh, 1990).

Diastereoisomers & Organic Cation Transport. The incorporation of either quinine or quinidine during incubation inhibited competitively the accumulation of amantadine in all three preparations, which supports the possibility of common transport sites shared amongst the non-chiral amantadine and the two diastereoisomers. However, observed K_i values for the two diastereoisomers varied considerably between the three preparations. Stereoselective inhibition was observed in isolated proximal tubules with an apparent inhibitory potency of the 8S, 9R-(-)-isomer, quinine, being approximately two to three-fold greater than that of the 8R, 9S-(+)-isomer, quinidine. In distal tubules, both diastereoisomers exhibited equipotent inhibition of amantadine uptake with no apparent stereoselectivity. As renal cortical tissue consists primarily of proximal and distal tubules (Berndt, 1976; Vinay *et al.*, 1981; Gesek *et al.*, 1987), experimentation with the cortical slices sustained a composite representation of proximal and distal phenomena. The addition of quinine or quinidine produced competitive inhibition of amantadine

uptake by cortical slices, of which approximately one half of the net accumulation was perceived to be stereoselective for quinine and represented proximal tubular uptake. However, the apparent inhibitory potency for quinine and quinidine in the cortical slices (closed-lumen preparation) was proportionately ten-fold lower than that observed in isolated tubules, and infers the potential for such a phenomenon to be a luminal event.

In comparison to the previously reported stereoselectivity in human renal clearance for quinidine over quinine by Notterman and co-workers in 1986, the apparent inversion of stereoselectivity *in vitro* may be attributed to the possibility of species differences in renal tubular secretion of chiral organic cations between human and rat (McIsaac, 1965 & 1969; Grantham & Chonko, 1991). In order to pursue such a hypothesis, the conjunctive examination of this phenomenon in human renal cortical slices was implemented.

It is evident that species differences in biomedical research represent a major issue in regard to the extrapolation of phenomena observed from animal data. The use of human tissue unequivocally resolves such a concern. However, one common question is the viability of the tissue following its excision from the donor. Previous systematic studies using several human tissues, including renal proximal tubule cells, had demonstrated durations of viability to be one to two hours when tissue was stored at body temperature. When storage temperature was reduced, survival times increased considerably to over 24 hours (Trump & Harris, 1979; Trifillis *et al.*, 1985). In the present study using human renal cortical slices, the immediate rapid processing and utilization of the human renal tissue subsequent to its excision conforms with such limitations, and supports the validity of our current preparation *in vitro*.

The marker organic cation, amantadine, was concentrated by human renal cortical slices in a comparable manner to that observed in the corresponding rat

preparation. Accumulation was saturable and was inhibited by pretreatment of the tissue with a metabolic inhibitor, 2,4-dinitrophenol. Kinetic characteristics, such as the apparent affinity and maximal capacity of the transport sites involved, are also in proximate correlation with those documented for rat slices. Experimentation with the two diastereoisomers confirmed the greater inhibitory potency of quinine (8S, 9R-(-)-isomer) as observed in the rat, thus providing primary evidence for the elimination of species differences as an explanation for the present apparent discrepancy between *in vivo* and *in vitro* data.

Alternative mechanisms include a predominant secretion of the achiral amantadine molecule *via* quinine-preferring transport sites, and/or stereoselective *cis*-inhibition of amantadine reabsorption or *trans*-stimulation of amantadine efflux *via* luminal counterports across the luminal membrane by quinine over quinidine. A schematic model consisting of the tentative sites of interaction between amantadine and the two diastereoisomers in the renal proximal tubule cell is represented in figure D-1.

Previous literature had also documented a dissociation between the rate of tubular secretion of a competitive inhibitor of organic cation transport and its ability to produce inhibition (Rennick *et al.*, 1956; Grantham & Chonko, 1991). The basic cyanine dye no. 863 was observed to inhibit potently the renal tubular excretion *in vivo* of two prototypic organic cation markers, tetraethylammonium (TEA) and N¹-methylnicotinamide (NMN), whilst itself was absolutely or relatively refractory to excretion by the transport system. Therefore, a greater inhibitory potency of quinine on renal transport of another organic cation does not necessitate a correspondingly higher renal clearance for this isomer.

In view of the similarity between the inhibitory constant for quinine in the isolated proximal tubule preparation and its mean therapeutic plasma concentration (Table D-A), potentially important clinical interactions at the renal level are

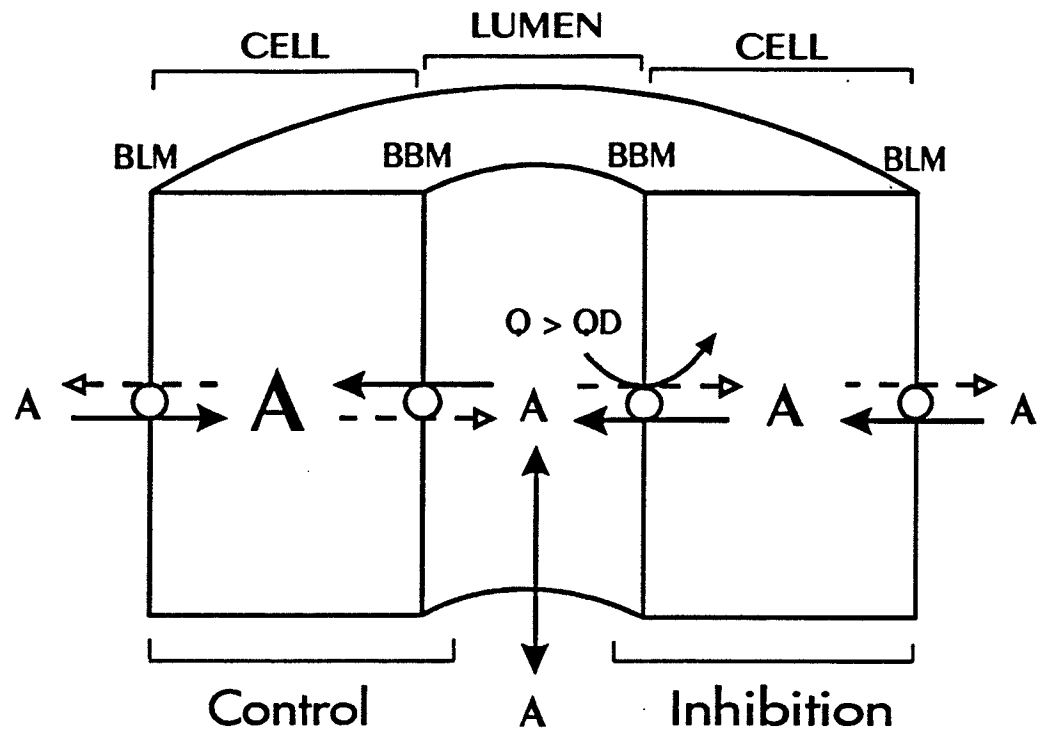


Figure D-1. Putative sites of interaction between the diastereoisomers and amantadine in isolated rat renal proximal tubule. Control amantadine transport and its interference by quinine and quinidine are represented in the left and right cell compartments respectively. BLM and BBM denote basolateral and brush-border membranes respectively. Lumen of the tubule is believed to be patent and luminal content is assumed to be in equilibrium with that of the incubation medium. The addition of quinine or quinidine stereoselectively competed for amantadine reabsorption and/or facilitated luminal amantadine efflux. Stereoselectivity was not observed in the distal tubule.

implicated during concomitant administration *in vivo*. The ten-fold higher apparent K_i values for quinine and quinidine in the cortical slice preparation are vindicated to represent quantitatively inaccurate assessments of their true inhibitory potency, as the suspected competition at the luminal membrane is believed to be attenuated in a preparation with collapsed lumina. Therapeutic implications of the compounds have been mentioned (*vide supra*). Briefly, amantadine is clinically employed to alleviate symptoms associated with Parkinson's syndrome, in addition to its documented value in both the treatment and prophylaxis against Influenza A viral infection. In general, quinine has been superseded by less toxic and more effective antimalarial agents. However, the occurrence of substantial resistance to these drugs has left a place for quinine in malaria chemotherapy, and it remains currently as the parenteral antimalarial of choice. Furthermore, the value of quinine in the treatment of nocturnal leg cramps and *Myotonia Congenita* has recently been appreciated (Webster, 1990).

Extension of the present *in vitro* work included the implementation of a clinical investigation in which potential alterations in amantadine disposition by co-administered quinine or quinidine were determined in healthy human volunteers (Gaudry *et al.*, 1990; Sitar *et al.*, 1990). In this randomized three-limbed crossover study, significant reductions in amantadine renal clearance by quinine and quinidine were observed in male, but not in female subjects. Such a disparity between genders was not ascribed to metabolic contributions, as pharmacokinetic profiles for quinine and quinidine were found to be equitable in male and female subjects. Hence, this adjunct study not only confirmed the present extrapolation of the preliminary observations from animal studies to the clinical situation, but the potential significance of gender differences in renal organic solute transport was also reinstated (Harvey & Malvin, 1965; Kleinman *et al.*, 1966; Bowman & Hook, 1972).

Pharmacological Congeners & Organic Cation Transport. In the second experimental series, effects of two histamine H₂-receptor antagonists on renal tubular organic cation transport were investigated and compared. The antecedent compound, cimetidine (N^{''}-cyano-N-methyl-N[']-{2[[[(5-methyl-1H-imidazol-4-yl)methyl]thio]-ethyl]-guanidine (Tagamet[®])), has been documented extensively to be a potent inhibitor of both cytochrome P450 metabolic function and renal tubular excretion of organic cations (*vide supra*). It was recently proposed to assume the role as a prototypic inhibitor of renal organic cation secretion in an analogous manner to probenecid and renal organic anion secretion (Somogyi, 1987). Henceforth, newer antagonists with lesser interfering capabilities were developed and introduced, and the previously exclusive market for cimetidine was annexed significantly by such agents (Schunack, 1989). Ranitidine (N-{2-[[[5'-(dimethylaminomethyl)-2-furanyl]methyl]thio]ethyl}-N1-methyl-2-nitro-1,1-ethenediamine (Zantac[®])) is an example of the latter category of agents. It is a structural analogue of cimetidine with a relatively greater potency in the suppression of basal and stimulated gastric acid secretion (Daly *et al.*, 1981; Brater *et al.*, 1982). The substitution of the five-membered, nitrogen-containing, imidazole ring by a six-membered furan moiety is postulated to be the primary basis behind the reduced ability of ranitidine to inhibit cytochrome P450 function (Murray, 1987), but its potential effects on renal tubular drug secretion at the cellular level had not been examined. In view of the higher *pK_a* value of ranitidine (hence greater proportion of ionization at physiological *pH*) than that of cimetidine, it did not seem unbecoming to anticipate a correspondingly higher incidence of interaction at the renal level.

Prior to the determination for potential ability of the newer congener to affect renal tubular organic cation transport, characteristics of the documented interference by cimetidine was examined and established in our present renal

preparations *in vitro*.

In renal cortical slices, low concentrations of cimetidine elicited marginal facilitation of amantadine accumulation, whereas competitive inhibition was produced by higher cimetidine concentrations. The enhancing component was determined to be confined within the proximal tubules, whereas the lower-affinity competition was evident within both tubule fractions. At first glance, the apparent facilitation of amantadine uptake invoked by therapeutic concentrations of a potential prototypic transport inhibitor appeared to be anomalous. However, with reference to the previously documented biphasic mixture of facilitation and inhibition of renal tubular organic cation excretion *in vivo* (Acara & Rennick, 1972; Acara *et al.*, 1975; Acara & Rennick, 1976), the present observations *in vitro* offer additional insight into the cellular mechanism(s) underlying such a phenomenon. Possible explanations for the high-affinity enhancement of uptake include the following: Although a combination of the present proximal and distal tubular data may explain in part the trimodality of the cortical slice data, the minimal transport facilitation observed in the latter preparation (with collapsed lumina) insinuated a luminal phenomenon. The apparent increase in amantadine uptake may have resulted from an increase in influx *via* a shift in the rate limiting step of concern or a direct allosteric effect produced by cimetidine. Conversely, an inhibition of luminal amantadine efflux by intracellular cimetidine would have also actuated an apparent increase in accumulation. Efflux experimentation with cimetidine at a concentration which produced enhancement of uptake did not alter significantly the rate of amantadine egress from preloaded proximal tubules, and purged the postulate of both *cis*- and *trans*- effects by cimetidine on amantadine efflux. Nonetheless, a *cis*- or *trans*- stimulation by cimetidine on luminal amantadine influx (reabsorption) remains to be compatible with the previously proposed inhibitory property of cimetidine on the renal elimination of organic cations (Somogyi, 1987).

In comparison to the tissue specificity of high-affinity stimulation, the corresponding lower-affinity inhibition of uptake was readily demonstrable in the cortical slice and both isolated tubule preparations. The mechanism underlying such a phenomenon was ascribed to a direct competition between amantadine and cimetidine for common influx site(s), and its ubiquitous occurrence between preparations suggests the probability of a basolateral event. In essence, the tentative sites of interaction between amantadine and cimetidine are represented diagrammatically in Figure D-2.

Despite the complexity in relation to the high-affinity stimulation and low-affinity inhibition of amantadine uptake elicited by cimetidine, low therapeutically-relevant concentrations of ranitidine did not affect uptake in renal cortical tissue. However, the low-affinity inhibitory component was again observed to be omnipresent in all preparations examined. The potential site of interaction with ranitidine is therefore suspected to be located on the basolateral membrane of either the proximal or distal tubule cell, and that the absence of luminal competition between amantadine and ranitidine is a feasible explanation for the sole inhibitory effect of ranitidine (Figure D-2).

An ancillary question of interest concerns the differences in molecular structure between cimetidine and ranitidine, and whether the substitution of the imidazole (to furan) ring or the cyanoguanidine (to ethenediamine) moiety contributed to the eradication of the ability of ranitidine to interfere with renal organic cation transport. Experimentation using either functional moiety in cimetidine (imidazole nucleus or guanidine side chain) as the competing organic cation revealed their equitable abilities in interfering with amantadine transport in renal proximal tubules, and deduced the necessity for their concurrent replacement in the constitution of the lesser interactive compound at the renal level.

In conclusion, the differential effects of the two histamine receptor

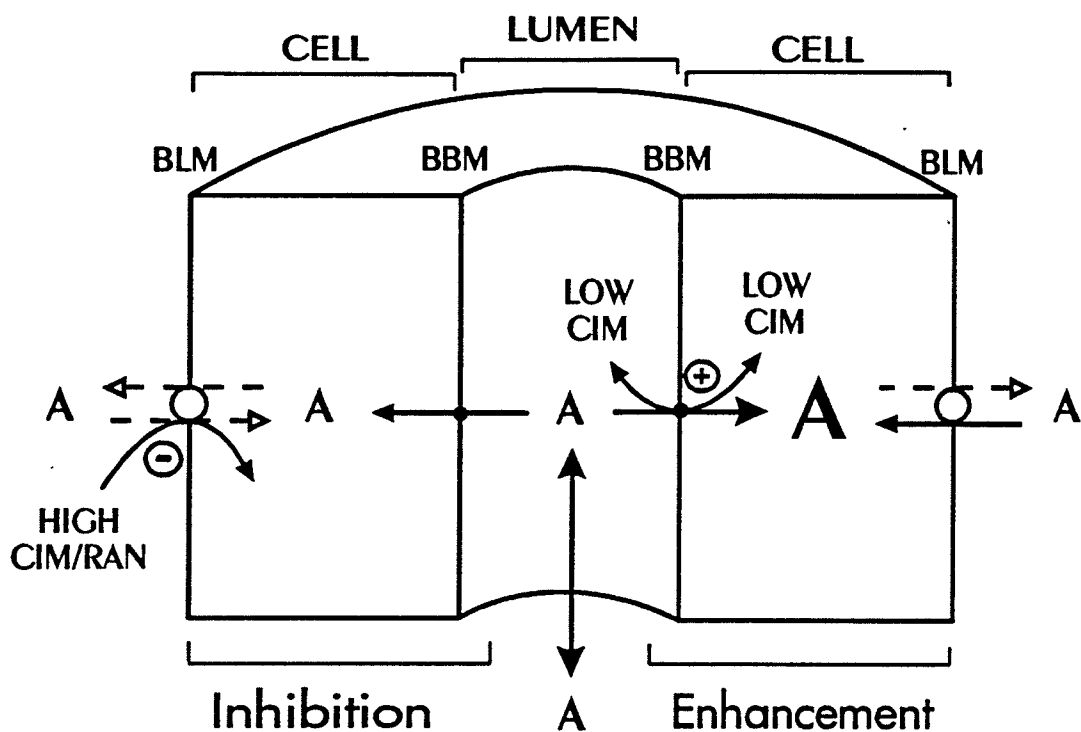


Figure D-2. Putative sites of interaction between histamine H₂-receptor antagonists and amantadine in isolated rat renal tubules. High-affinity enhancement produced by low concentrations of cimetidine (low cim) and low-affinity inhibition by high cimetidine or ranitidine concentrations (high cim / ran) are represented in the right and left cell compartments respectively. BLM and BBM denote basolateral and brush-border membranes respectively. Lumen of the tubule is believed to be patent and luminal content is assumed to be in equilibrium with that of the incubation medium. A negative sign signifies *cis*-inhibition of amantadine transport in the direction as indicated (basolateral influx), whereas a positive sign indicates the presently undetermined *cis*- or *trans*- stimulation of luminal amantadine reabsorption. Luminal amantadine efflux was not affected by cimetidine.

antagonists on the renal accumulation of amantadine suggest disparate rate limiting steps and/or transport pathways involved in their renal excretion. Although the mean therapeutic plasma concentration of ranitidine is lower than that of cimetidine (Table D-A) (Grant *et al.*, 1989; Benet & Williams, 1990), the relatively inert nature of the lower ranitidine concentrations on amantadine uptake by the renal preparations *in vitro* suggests a lower incidence of interaction with cationic drugs in the kidney than its predecessor, cimetidine (Rodvold *et al.*, 1987; Baciewicz *et al.*, 1989; Bendayan *et al.*, 1990b).

Nicotine & Organic Cation Transport. The final series of investigation examined the potential interference of renal tubular handling of organic cations by a clinically and environmentally relevant substance, nicotine. Nicotine accounts for approximately 95 % of the total alkaloid content in tobacco smoke, and its plasma concentration is maintained at fairly constant levels in habitual tobacco users (Russell, 1978; McMorro & Foxx, 1983; Benowitz & Jacob, 1985; Benowitz *et al.*, 1988; Bowman & Rand, 1980; Jaffe, 1990). Elimination of nicotine has been documented to involve extensive metabolism by the cytochrome P450 enzyme system with cotinine being a major metabolite, and both of these compounds are excreted renally *via* glomerular filtration and active tubular transport (Nwosu *et al.*, 1988; Bendayan *et al.*, 1990b; Kyerematen *et al.*, 1990; Kyerematen & Vesell, 1991). In view of the cationic properties of the nicotine molecule, the latter process is anticipated to partake pathways within the organic cation transport system. The primary criterion behind the choice of nicotine and cotinine concentrations in the present investigation was to mimic *in vitro* the approximate concentrations of these compounds presented chronically to the renal tubules in habitual tobacco users. In addition, S-(-) and R-(+) nicotine were pursued individually in order to further determine the enantiomeric preferences of the tubular carriers under examination.

The incorporation of either isomer of nicotine significantly altered amantadine accumulation in cortical slices and isolated tubules. High-affinity enhancement of uptake in proximal tubules was readily demonstrable with low concentrations of S-(-) or R-(+) nicotine, and maximum enhancement was observed at concentrations equivalent to those found in the plasma of habitual tobacco smokers. With increasing nicotine concentrations, low-affinity inhibition of amantadine uptake was observed in both proximal and distal tubule preparations. Such an ability to elicit the present dichotomy of high-affinity enhancement and lower-affinity inhibition of amantadine uptake in isolated renal tubules appeared to be parallel to that described for the potential prototypic organic cation transport inhibitor, cimetidine, with the exception that the observed potency of nicotine was comparatively greater. In the cortical slice preparation, the high-affinity stimulatory component was perceived to be negligible, which again suggests a luminal site of interaction.

Possible mechanisms underlying the apparent increase of amantadine uptake in proximal tubules may again be attributed to an actual increase of luminal amantadine influx into proximal tubule cells *via* an allosteric symport or counterport system (Wilbrandt & Rosenberg, 1961; Holm, 1972), and/or a decreased efflux of amantadine across the luminal membrane. Despite the fact that this latter possibility is supported by the demonstrated significant hindrance of amantadine efflux by a low concentration of nicotine, the addition of cimetidine at a concentration which enhanced amantadine uptake did not affect egress (*vide supra*). Therefore, an attenuation of amantadine egress may only account in part for such an apparent facilitation of accumulation, and the former concept involving an increase of amantadine influx should not be disregarded.

A schematic model consisting of the tentative sites of interaction in the renal proximal tubule cell is represented in Figure D-3. The high-affinity enhancement

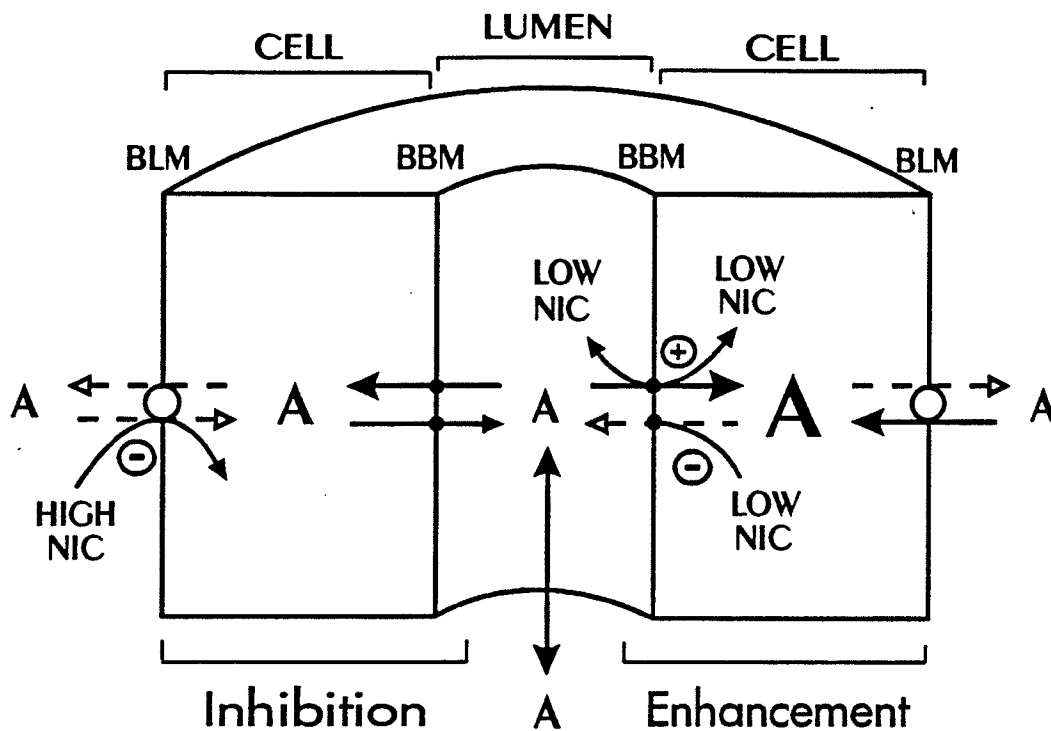


Figure D-3. Putative sites of interaction between nicotine and amantadine in isolated rat renal proximal tubule. High-affinity enhancement produced by low concentrations of nicotine (low nic) and low-affinity inhibition by higher nicotine concentrations (high nic) are represented in the right and left cell compartments respectively. BLM and BBM denote basolateral and brush-border membranes respectively. Lumen of the tubule is believed to be patent and luminal content is assumed to be in equilibrium with that of the incubation medium. A negative sign signifies *cis*-inhibition of amantadine transport in the direction as indicated (basolateral influx or luminal efflux), whereas a positive sign indicates the presently undetermined *cis*- or *trans*-stimulation of luminal amantadine reabsorption.

elicited by nicotine or cimetidine is suspected to be mediated at brush-border membrane secretory and/or reabsorptive sites, whereas the lower-affinity inhibition produced by nicotine in isolated proximal and distal tubules can be attributed largely to a direct competition between substrates for common transport site(s). Present lines of evidence for the latter include a prominent increase of apparent K_m for amantadine by nicotine with minimally altered V_{max} , and counter-stimulation of amantadine efflux by high nicotine concentrations. Moreover, as this low-affinity inhibition was also apparent in the renal cortical slice (closed-lumen preparation), potential sites of competition are deduced to be located within the basolateral membrane of the tubule cell. Nevertheless, such a highly toxic and even lethal nicotine level at which inhibition was observed is achieved rarely in clinical situations and its significance remains indefinite at present.

With regard to the issue of chiral preference in renal organic cation transport, stereoselective inhibition of amantadine uptake by quinine (8S, 9R(-) isomer) > quinidine (8R, 9S(+) isomer) was demonstrated in the first experimental series. However, anticipated chirality-related differences between S(-) and R(+) nicotine were neither associated with the high-affinity enhancement nor low-affinity inhibition of amantadine transport observed at present. Such an absence of stereoselectivity is indicative of disparate mechanisms of interaction between the two nicotine isomers and quinine / quinidine, owing perchance to variations in the degree of isomerism and/or individual functional moieties between these compounds.

The potentially significant alteration in amantadine transport by a major metabolite of nicotine, cotinine, was also considered. S(-) Cotinine, a metabolite of S(-) nicotine, was examined as the representative isomer. As observed with the parent compound, amantadine uptake into proximal tubules was significantly facilitated by the addition of S(-) cotinine at concentrations of approximate

equivalence to those observed with S-(-) nicotine. However, maximal enhancement elicited (plateau) was comparatively lower than that produced by S-(-) nicotine. In addition, the present use of the short 30-second incubation period in relation to the documented lengthy plasma half-life values for amantadine and nicotine (of approximately 16 and 2 hours respectively) renders intracellular metabolism during incubation, hence contribution by metabolites, to be minimal in our experimental settings *in vitro* (Russell, 1978; Aoki & Sitar, 1988; Bjercke *et al.*, 1990; Jaffe, 1990).

In conclusion, the demonstrated potent interference of renal tubular amantadine transport by both nicotine and cotinine at concentrations equivalent to those documented in the plasma of habitual tobacco smokers suggests the probability of clinically significant alterations in the disposition and elimination of therapeutic organic cations with predominant renal clearance in these subjects.

Synopsis. In summary, the present pursuit in the investigation of renal tubular organic cation transport has advocated the following issues:

1. With the continual development and introduction of novel organic cationic therapeutic agents, properties of a desirable marker compound should include a homogeneous organic cation with predominant renal clearance and minimal adversaries *in vivo*. The present study proposed and established the suitability of amantadine for such a role *in vitro*, and corresponding clinical studies by our laboratory have endorsed its safety in human volunteers (Gaudry *et al.*, 1990; Sitar *et al.*, 1990; Hoff *et al.*, 1991).
2. In the renal proximal tubule, interaction profiles between the organic cations examined suggest a high-affinity transport process involved at the luminal or brush-border membrane, whereas lower-affinity carrier(s) are predominant in the basolateral membrane. These postulates are in agreement with earlier or concurrent documentations by established

- investigators in this field of research (Kinsella *et al.*, 1979a; Holohan & Ross, 1980; Wright & Wunz, 1987; Bendayan *et al.*, 1990a; Chatton *et al.*, 1990; Sokol, 1990; Sokol & Gates, 1990; Griffiths *et al.*, 1991).
3. Active carrier-mediated renal tubular transport of the organic cation, amantadine, was also demonstrated in the distal tubule. Interactions in the distal tubule were observed to involve primarily low-affinity basolateral transport site(s), which may be associated with a relatively underdeveloped brush-border membrane in comparison to that of the proximal tubule.
 4. The adequacy in relation to the use of the renal cortical slice preparation in examination of renal tubular transport and metabolic processes has been under debate, and remains currently to be controversial (Cross & Taggart, 1950; Foulkes & Miller, 1959, Berndt, 1976; Rose *et al.*, 1985). A majority of previous experimentation with renal cortical slices had employed prolonged incubation periods, and the viability of both tissue integrity and kinetic analyses (where applicable) are in question. The present use of a relatively shorter incubation, at which rate of uptake remained within the initial linear uptake phase, has circumvented such apprehensions. However, the current comparison with observations in isolated renal tubules has disclosed significant discrepancies, and that the use of cortical slices may have masked the true potency and efficacy of lumenally interactive organic cations. Such an underestimation may render this preparation to be an unrealistic model for the study of phenomena *in vivo*.
 5. The current data *in vitro* incite the consideration for potentially significant or insignificant interactions between organic cations at the renal level in the clinical setting. A proportion of the predictions have been confirmed by our laboratory using human volunteers or reflected insofar by the general literature. The potential interaction between nicotine and amantadine is

undetermined at present, and is worthwhile of mention. Although such a seemingly obvious notion had been previously unperceived, it is not improbable for an interaction at the renal level to be overlooked owing to concurrent confounding effect(s) of tobacco usage upon mammalian drug metabolism. It is hoped that the persistent development and usage of organic cationic therapeutic agents with predominant renal clearance will accentuate the anticipated significance of the present interaction.

Further Investigations. With regard to the implications of the current data and observations, further extension of the present endeavor is bidirectional:

Firstly, more intricate preparations *in vitro* may be utilized to confirm the proposed sites of interactions within the tubule segments. Current choices include isolated antiluminal (basolateral (BLMV)) and luminal (brush-border (BBMV)) membrane vesicles from specific nephron segments, isolated perfused or nonperfused nephron segments, and renal tubule cell cultures.

The common objective for the nomination of these preparations is to isolate and focus upon individual events in relation to the two membranes of the renal tubule. Henceforth, their kinetic characteristics, substrate specificity and association with cellular metabolism may be delineated individually, and such acquisition would improve our present ability to extrapolate into the therapeutic setting. Analogous advancements from the previous extensive research on renal organic anion transport have ensued the introduction of "loop" or "high-ceiling" diuretic agents, in addition to the uricosuric agents in the treatment of gout (*vide supra*). In renal organic cation transport research, a current focus with potential therapeutic significance pertains to its linkage with P-glycoprotein as the transporter underlying Multidrug Resistance (MDR) in chemotherapy (Nelson, 1988; Chatton *et al.*, 1990; Horio *et al.*, 1990; Griffiths *et al.*, 1991; Gutierrez *et al.*, 1991; Ichikawa *et*

al., 1991).

Additional aspects of investigation involve the identification and isolation of homogeneous populations of specific carrier proteins (Hori *et al.*, 1987; Hysu & Giacomini, 1987; Ott & Giacomini, 1991; Zimmerman *et al.*, 1991). Determination of the protein sequences would eventuate insight into the corresponding genome attributes, and facilitate the concept of artificial modulation of carrier synthesis.

In consideration of the individual experimental preparations mentioned above, isolation of renal membrane vesicles is comparatively the most extensively documented and employed procedure. In the late 1960s, Fitzpatrick and co-workers isolated basolateral and brush-border plasma membranes from the rat kidney by differential centrifugation (Fitzpatrick *et al.*, 1969). The differences in polarity of the membranes were then recognized, and purification was improved by free-flow electrophoresis (Heidrich *et al.*, 1972). Thereafter, variations and combinations of the above-mentioned procedures have evolved, in addition to a "preferential sedimentation" technique using divalent inorganic cations (Booth & Kenny, 1974; Turner & Silverman, 1977; Kinsella *et al.*, 1979b; Malathi *et al.*, 1979; Reynolds *et al.*, 1980; Inui *et al.*, 1981; Boumendil-Podevin & Podevin, 1983; Ross & Holohan, 1983; McKinney & Kunnemann, 1985; Grassl & Aronson, 1986; Grassl *et al.*, 1987).

Fundamentally, one should be aware of the advantages and disadvantages associated with the use of renal membrane vesicles. The advantages include: (i) vesicles are relatively free of metabolic reactions, (ii) intra- and extra-vesicular environment is readily controlled, and (iii) transport properties of the two membranes can be investigated separately. Disadvantages are: (i) relatively lengthy preparation may facilitate tissue degradation, (ii) purity and orientation of the vesicles are often heterogeneous, (iii) essential endogenous regulating factors are obviated, and (iv) the existence of a transport process in isolated vesicles does not necessitate a prominent physiological role *in vivo*.

With regard to the homogeneity of the vesicles within each preparation, the following should be considered. Firstly, as whole renal cortical tissue is used in general for preparation, it is imperative to stress that such preparations do not distinguish between proximal and distal tubular phenomena. Membrane vesicles isolated from pre-separated proximal or distal tubule suspensions would circumvent such an inconclusion, but corresponding tissue yield and viability may be further compromised. Secondly, the purity of basolateral or brush border membrane vesicle fractions is of primary consideration, and it may be ascertained by the determination of appropriate enzyme markers (Guder & Ross, 1984). Thirdly, the orientation or sidedness of brush border (luminal) membrane vesicles are conceived to be uniformly rightside-out (due to steric hindrance by brush border microvilli). However, the polarity of basolateral membrane vesicles are often regarded to be relatively more heterogeneous (Möller & Sheikh, 1983; Ramachandran & Brunette, 1989). Such a variance may be monitored by exploiting the facts that diffusion of adenosine triphosphate (ATP) and ouabain across cell membranes is limited, and they have opposite sidedness of action. The ATP-catalytic unit is located exclusively on the cytoplasmic surface of the cell membrane, whereas its inhibitor, ouabain, binds only to the exterior of the cell. Deductively, one would not expect to perceive Na /K -ATPase activity in rightside-out vesicles, whereas such enzymatic activity would be expressed in inside-out vesicles in an ouabain-insensitive manner. Moreover, ouabain-sensitive Na /K -ATPase activity would only be expressed in disrupted membrane sheets or leaky vesicles. Further intricate details on exact experimental procedures have been documented by Boumendil-Podevin & Podevin (1983).

An alternative experimental approach with lesser limitation involves the use of isolated perfused or nonperfused segments of the nephron (Schäli & Roch-Ramel, 1980; Schäli *et al.*, 1983; Lapointe *et al.*, 1986; Dantzler & Brokl, 1987;

Schild & Roch-Ramel, 1988; Besseghir *et al.*, 1990 a & b; Dantzler, 1989; Beck *et al.*, 1991; Chatton & Roch-Ramel, 1991). Techniques for perfusion studies using single isolated tubules were pioneered by Burg and co-workers (1966). Tubule fragments are dissected manually from the mammalian renal nephron under microscopic guidance. Each end of the tubule segment is cannulated with a micropipette for fluid perfusion and collection, and the preparation is immersed subsequently in medium corresponding to the fluid bathing the basolateral membrane. Procedures have also been developed to focus upon basolateral events by filling the tubule lumen with inert oil which limits luminal accessibility (Burg *et al.*, 1966; Burg & Orloff, 1968). Specific advantages associated with use of microdissected tubule segments include the assurance in their morphology and origin, and that both basolateral and luminal contents are readily regulated. Rate of luminal substrate perfusion also represents a controlled experimental variable in the perfusion model, and potential flow rate dependency of substrate transfer may be evaluated.

The ability of mammalian epithelial cells to form a monolayer of cellular membrane on firm support provides adequate means of examining transport processes within a geometrically simple system. Previous reports have documented extensively the use of both animal and human renal tubule cells in culture or as immortal cell lines (Hull *et al.*, 1976; Handler *et al.*, 1980; Chung *et al.*, 1982; Detrisac *et al.*, 1984; Trifillis *et al.*, 1985; Blackburn *et al.*, 1988; McKinney *et al.*, 1988; Fouda *et al.*, 1990; Trifillis & Kahng, 1990). More recent development of renal tubule cell cultures grown on permeable membrane filters have further permitted the differentiation of media exposed to each side of the cell, thereby facilitating the examination of directional transepithelial solute transport (Ford *et al.*, 1990). Liabilities in the use of such cultures include the possibility of contamination with unrelated cells (such as fibroblasts), and the potential for cell dedifferentiation during the course of cell passage (primarily in long-term cultures

and immortal cell lines). The former notion of contamination has been reported to be alleviated by substitution of specific constituents in the culture medium (Boogaard *et al.*, 1990). However, routine microscopic and enzymatic examination of the cultures is imperative to devoid the potential for artefactual interference due to cell dedifferentiation.

In summary of the proposed experimentation *in vitro*, it is of paradoxical concern to omit the use of the isolated membrane vesicle preparations for quantitative purposes. The rationalization behind such a bias includes the controversial polarity of the basolateral membrane vesicles, in addition to their limited tissue yield, which ultimately attenuates comparative cost effectiveness.

The alternative extension of the current experimental status involves the extrapolation of the present observations to potentially significant drug interactions in the clinical setting. Previous investigation by our laboratory has confirmed the anticipated renal interaction between therapeutic doses of amantadine and quinine during concurrent administration in healthy human volunteers (*vide supra*). In addition, such a phenomenon was associated with prominent gender variations. In view of the potent interference of amantadine transport by nicotine *in vitro*, the consequent pursuit is to compare amantadine renal clearance in habitual tobacco smokers with control subjects (absolute abstainers). Such a non-randomized study is designed to involve the administration of a low therapeutic dose of amantadine (at 3 mg/kg) to evenly distributed groups consisting of male and female tobacco smokers and non-smokers. Regular samples of blood and urine will be collected up to 54 hours (approximately four half-lives), and extracted amantadine will be determined using gas chromatography. Renal and plasma amantadine clearances will be calculated and compared between tobacco smokers and abstainers, males and females. Creatinine clearance will also be estimated in order to calibrate renal function in the subjects.

The acute administration of amantadine hydrochloride (Symmetrel[®]) to healthy human volunteers has been performed on numerous previous occasions by this laboratory (representative studies: E83.05, E86.206 and E89.87). No adverse reactions to this compound were observed in any of the investigations.

Possible confounding factors in this proposed study include differences in relation to the chronicity of nicotine exposure, with which autoregulation of renal carriers may become significant. Moreover, concurrent synergistic and/or antagonistic actions of other constituents in tobacco smoke and their metabolites should also be considered.

REFERENCES

- ACARA, M., KOWALSKI, M. AND RENNICK, B.: Renal tubular excretion of triethylcholine (TEC) in the chicken: Enhancement and inhibition of renal excretion of choline and acetylcholine by TEC. *Br. J. Pharmacol.* **54**: 41-48, 1975.
- ACARA, M. AND RENNICK, B.: Renal tubular transport of acetylcholine and atropine: Enhancement and inhibition. *J. Pharmacol. Exp. Ther.* **182**: 11-26, 1972.
- ACARA, M. AND RENNICK, B.: The biphasic effect of organic cations on the excretion of other organic cations. *J. Pharmacol. Exp. Ther.* **199**: 32-40, 1976.
- ALEXANDER, F., GOLD, H. AND KATZ, L. N.: The relative value of synthetic quinidine, dihydroquinidine, commercial quinidine and quinine in the control of cardiac arrhythmias. *J. Pharmacol. Exp. Ther.* **90**: 191-201, 1947.
- AOKI, F. Y. AND SITAR, D. S.: Clinical pharmacokinetics of amantadine hydrochloride. *Clin. Pharmacokinet.* **14**: 35-51, 1988.
- ARIENS, E. J.: Stereoselectivity in bioactive agents: general aspects. *In Stereochemistry and biological activity of drugs*, ed. by E. J. Ariens, W. Soudijn and P. B. Timmermans, pp. 11-32, Blackwell Scientific Publications, Boston, 1983.
- ARIENS, E. J.: Chirality in bioactive agents and its pitfalls. *Trends Pharmacol. Sci.* **7**: 200-205, 1986.
- BACIEWICZ, A. M. AND BACIEWICZ, F. A.: Effect of cimetidine and ranitidine on cardiovascular drugs. *Am. Heart J.* **118**: 144-154, 1989.

- BAILIE, M. D., BARBOUR, J. A. AND HOOK, J. B.: Effects of indomethacin on furosemide-induced changes on renal blood flow. *Proc. Soc. Exp. Biol. Med.* **148**: 1173-1175, 1975.
- BARBIERI, R. L., YORK, C. M., CHERRY, M. L. AND RYAN, K. J.: The effects of nicotine, cotinine and anabasine on rat adrenal 11β -hydroxylase and 21 -hydroxylase. *J. Steroid Biochem.* **28**: 25-28, 1987.
- BECK, J. S., BRETON, S., LAPRADE, R. AND GIEBISCH, G.: Volume regulation and intracellular calcium in the rabbit proximal convoluted tubule. *Am. J. Physiol.* **260**: F861-F867, 1991.
- BEEUWKES, R. III: The vascular organization of the kidney. *Ann. Rev. Physiol.* **42**: 531-542, 1980.
- BENDAYAN, R., SELLERS, E. M. AND SILVERMAN, M.: Inhibition kinetics of cationic drugs on N1-methylnicotinamide uptake by brush-border membrane vesicles from the dog kidney cortex. *Can. J. Physiol. Pharmacol.* **68**: 467-475, 1990a.
- BENDAYAN, R., SULLIVAN, J. T., SHAW, C., FRECKER, R. C. AND SELLERS, E. M.: Effect of cimetidine and ranitidine on the hepatic and renal elimination of nicotine in humans. *Eur. J. Clin. Pharmacol.* **38**: 165-169, 1990b.
- BENET, L. Z. AND WILLIAMS, R. L.: Design and optimization of dosage regimens: Pharmacokinetics data. *In The Pharmacological Basis of Therapeutics*, 8th edition, ed. by A. G. Gilman, T. W. Rall, A. S. Wies and P. Taylor, pp. 1650-1735, Pergamon Press, Inc., New York, 1990.
- BENOWITZ, N. L. AND JACOB, P. III: Nicotine renal excretion rate influences nicotine intake during cigarette smoking. *J. Pharmacol. Exp. Ther.* **234**: 153-155, 1985.

- BENOWITZ, N. L., PORCHET, H., SHEINER, L. AND JACOB, P. III: Nicotine absorption and cardiovascular effects with smokeless tobacco use: Comparison with cigarettes and nicotine gum. *Clin. Pharmacol. Ther.* **44**: 23-28, 1988.
- BERNDT, W. O.: Use of the tissue slice technique for evaluation of renal transport processes. *Environ. Health. Perspect.* **15**: 73-88, 1976.
- BERNDT, W. O.: Organic base transport: a comparative study. *Pharmacology* **22**: 251-262, 1981.
- BESSEGHIR, K., PEARCE, L. B. AND RENNICK, B.: Renal tubular transport and metabolism of organic cations by the rabbit. *Am. J. Physiol.* **241**: F308-F314, 1981.
- BESSEGHIR, K., MOSIG, D. AND ROCH-RAMEL F.: Transport of the organic cation N-methylnicotinamide by the rabbit proximal tubule. I. Accumulation in the isolated non-perfused tubule. *J. Pharmacol. Exp. Ther.* **253**: 444-451, 1990a.
- BESSEGHIR, K., CHATTON, J.-Y. AND ROCH-RAMEL, F.: Transport of the organic cation N-methylnicotinamide by the rabbit proximal tubule. II. Reabsorption and secretion in the isolated perfused tubule. *J. Pharmacol. Exp. Ther.* **253**: 452-460, 1990b.
- BEYER, K. H.: Functional characteristics of renal transport mechanisms. *Pharmacol. Rev.* **2**: 227-280, 1950.
- BEYER, K. H., PAINTER, R. H. AND WIEBELHAUS, V. D.: Enzymatic factors in renal tubular secretion of phenol red. *Am. J. Physiol.* **161**: 259-267, 1950.

BEYER, K. H., PETERS, L., WOODWARD, R. AND VERWEY, W. F.: The enhancement of the physiological economy of penicillin in dog by the simultaneous administration of para-aminohippuric acid II. *J. Pharmacol. Exp. Ther.* **82**: 310-323, 1944.

BJERCKE, R. J., HAMMOND, D. K., STROBEL, H. W. AND LANGONE, J. J.: Interaction of cotinine with rat hepatic microsomal P-450: Comparison with metyrapone and immunomodulation of cotinine and metyrapone binding by monoclonal anti-cotinine antibodies. *Drug Metab. Dispos.* **18**: 759-764, 1990.

BLACKBURN, J. G., HAZEN-MARTIN, D. J., DETRISAC, C. J. AND SENS, D. A.: Electrophysiology and ultrastructure of cultured human proximal tubule cells. *Kidney Int.* **33**: 508-516, 1988.

BOOGAARD, P. J., ZOETEWELJ, J. P., VAN BERKEL, T. J. C., VAN'T NOORDENDE, J. M., MULDER, G. J. AND NAGELKERKE, J. F.: Primary culture of proximal tubular cells from normal rat kidney as an in vivo model study mechanisms of nephrotoxicity. *Biochem. Pharmacol.* **39**: 1335-1345, 1990.

BOOTH, A. G. AND KENNY, A. J.: A rapid method for the preparation of microvilli from rabbit kidney. *Biochem. J.* **142**: 575-581, 1974.

BOSS, G. R. AND SEEGMILLER, J. E.: Hyperuricemia and gout: Classification, complications and management. *N. Eng. J. Med.* **300**: 1459-1468, 1979.

BOUMENDIL-PODEVIN, E. F. AND PODEVIN, R. A.: Isolation of basolateral and brush-border membranes from the rabbit kidney cortex. Vesicle integrity and membrane sidedness of the basolateral fraction. *Biochim. Biophys. Acta.* **735**: 86-94, 1983.

- BOURKE, E., FRINDT, G., PREUSS, H., ROSE, E., WEKSLER, M. AND SCHREINER, G. E.: Studies with uraemic serum on the renal transport of hippurates and tetraethylammonium in the rabbit and rat: Effect of oral neomycin. *Clin. Sci.* **38**: 41-48, 1970.
- BOWMAN, H. M. AND HOOK, J. B.: Sex differences in organic ion transport by rat kidney. *Proc. Soc. Exp. Biol. Med.* **141**: 258-262, 1972.
- BOWMAN, W.: On the structure and use of the malpighian bodies of the kidney, with observations on the circulation through the gland. *Philos. Trans. R. Soc. Lond.* **132**: 57-80, 1842.
- BOWMAN, W. C. AND RAND, M. J.: Social pharmacology: Drug use for nonmedical purposes: Drug dependence. *In* *Textbook of Pharmacology*, 2nd edition, pp. 42.25-42.40, Blackwell Scientific Publications, Oxford, 1980.
- BRADSHAW, J. BRITAIN, R. T., CLITHEROW, J. W., DALY, M. J., JACK, D., PRICE, B. J. AND STABLES, R.: Ranitidine (AH 19065): a new potent, selective histamine H₂-receptor antagonist. *Br. J. Pharmacol.* **66**: 464P, 1979.
- BRÄNDLE, E. AND GREVEN, J.: Transport of cimetidine across the basolateral membrane of rabbit kidney proximal tubules: Characterization of transport mechanisms. *J. Pharmacol. Exp. Ther.* **258**: 1038-1045, 1991.
- BRATER, D. C.: Pharmacodynamic considerations in the use of diuretics. *Ann. Rev. Pharmacol. Toxicol.* **23**: 45-62, 1983.
- BRATER, D. C., PETERS, M. N., ESHELMAN, F. N. AND RICHARDSON, C. T.: Clinical comparison of cimetidine and ranitidine. *Clin. Pharmacol. Ther.* **32**: 484-489, 1982.

- BULGER, R. E. AND DOBYAN, D. C.: Renal advances in renal morphology. *Ann. Rev. Physiol.* **44**: 147-179, 1982.
- BURG, M. B., GRANTHAM, J., ABRAMOW, M. AND ORLOFF, J.: Preparation and study of fragments of single rabbit nephrons. *Am. J. Physiol.* **210**: 1293-1298, 1966.
- BURG, M. B., ISAACSON, L., GRANTHAM, J. AND ORLOFF, J.: Preparation and study of fragments of single rabbit nephrons. *Am. J. Physiol.* **210**: 1293-1298, 1966.
- BURG, M. B. AND ORLOFF, J.: Effect of strophanthidin on electrolyte content and PAH accumulation. *Am. J. Physiol.* **202**: 565-571. 1962.
- BURG, M. B. AND ORLOFF, J.: Control of fluid reabsorption in the rat proximal tubule. *J. Clin. Invest.* **47**: 2016-2024, 1968.
- BURG, M. B. AND ORLOFF, J.: *p*-Aminohippurate uptake and exchange by separated renal tubules. *Am. J. Physiol.* **217**: 1064-1068, 1969.
- CACINI, W., KELLER, M.B. AND GRUND, V.R.: Accumulation of cimetidine by kidney cortex slices. *J. Pharmacol. Exp. Ther.* **221**: 342-346, 1982.
- CARAFOLI, E. AND SCARPA, A.: Transport ATPases. *In Annals of the New York Academy of Sciences*, vol. 42, New York Academy of Sciences, New York, 1982.
- CEDARBAUM, J. M.: Clinical pharmacokinetics of anti-Parkinsonian drugs. *Clin. Pharmacokinet.* **13**: 141-178, 1987.
- CHAHWALA, S. B. AND HARPUR, E. S.: The use of renal tubule fragments isolated from the rat to investigate aspects of gentamycin nephrotoxicity. *J. Pharmacol. Methods* **15**: 21-34, 1986.

- CHAIN, E. B.: The development of bacterial chemotherapy. *Antibiot. Chemother.* **4**: 215-241, 1954.
- CHAMBERS, R. AND KEMPTON, R. T.: The elimination of neutral red by the frog's kidney. *J. Cell. Comp. Physiol.* **10**: 199-221, 1937.
- CHATTON, J.-Y., ODONE, M., BESSEGHIR, K. AND ROCH-RAMEL, F.: Renal secretion of 3'-azido-3'-deoxythymidine by the rat. *J. Pharmacol. Exp. Ther.* **255**: 140-145, 1990.
- CHATTON, J.-Y. AND ROCH-RAMEL, F.: Passive permeability of salicylic acid in renal proximal S2 and S3 tubules. *J. Pharmacol. Exp. Ther.* **256**: 1112-1118, 1991.
- CHENG, Y.-C. AND PRUSOFF, W. H.: Relationship between the inhibition constant (K_i) and the concentration of inhibitor which causes 50 percent inhibition (I_{50}) of an enzymatic reaction. *Biochem. Pharmacol.* **22**: 3099-3108, 1973.
- CHO, K. C. AND CAFRUNY, E. J.: Renal tubular reabsorption of *p*-aminohippuric acid (PAH) in the dog. *J. Pharmacol. Exp. Ther.* **173**: 1-12, 1970.
- CHUNG, S. D., ALAVI, N., LIVINGSTONE, D., HILLER, S. AND TAUB, M.: Characterization of primary rabbit kidney cultures which express proximal tubule functions in hormonally-defined medium. *J. Cell. Biol.* **95**: 118-126, 1982.
- CLARK, A. J.: General pharmacology. *In Handbuch der experimentellen pharmakologie, Band IV* (reprinted, 1973), Springer-Verlag, Berlin, 1937.
- CLELAND, W. W.: Computer programmes for processing enzyme kinetic data. *Nature* **4879**: 463-465, 1963.

CORNISH-BOWDEN, A.: Practical considerations. *In* Fundamentals of enzyme kinetics, pp. 39-58, Camelot Press, Southampton, 1979.

CRANE, R. K.: Intestinal absorption of sugars. *Physiol. Rev.* **40**: 789-825, 1960.

CRANE, R. K.: Hypothesis of mechanism of intestinal active transport of sugars. *Fed. Proc.* **21**: 891-895, 1962.

CRANE, R. K.: The gradient hypothesis and other models of carrier-mediated active transport. *Rev. Physiol. Pharmacol.* **78**: 99-159, 1977.

CROSS, R. J. AND TAGGART, J. V.: Renal tubular transport: Accumulation of *p*-aminohippurate by rabbit kidney slices. *Am. J. Physiol.* **161**: 181-190, 1950.

DALY, M. J., HUMPHRAY, J. M. AND STABLES R.: Some *in vitro* and *in vivo* actions of the new histamine H₂-receptor antagonist, ranitidine. *Br. J. Pharmacol.* **72**: 49-54, 1981.

DANTZLER, W. H.: Organic acid (or anion) and organic base (or cation) transport by renal tubules of non-mammalian vertebrates. *J. Exp. Zool.* **249**: 247-257, 1989.

DANZLER, W. H. AND BROKL, O. H.: NMN transport by snake renal tubules: Choline effects, countertransport, H⁺-NMN exchange. *Am. J. Physiol.* **253**: F656-F663, 1987.

DAWSON, G. W. AND VESTAL, R. E.: Smoking and drug metabolism. *Pharmacol. Ther.* **15**: 207-221, 1982.

- DETRISAC, C. J., SENS, M. A., GARVIN, A. J., SPICER, S. S. AND SENS, D. A.: Tissue culture of human kidney epithelial cells of proximal tubule origin. *Kidney Int.* **25**: 383-390, 1984.
- DIXON, M.: The determination of enzyme inhibitor constants. *Biochem. J.* **55**: 170-171, 1953.
- DRAYER, D. E.: Pharmacodynamic and pharmacokinetic differences between drug enantiomers in humans: An overview. *Clin. Pharmacol. Ther.* **40**: 125-133, 1986.
- EADIE, G. S.: The inhibition of cholinesterase by physostigmine and prostaglandin. *J. Biol. Chem.* **146**: 85-93, 1942.
- FARAH, A. AND RENNICK, B. R.: Studies on the renal tubular transport of tetraethylammonium ion in renal slices of the dog. *J. Pharmacol. Exp. Ther.* **117**: 478-487, 1956.
- FITZPATRICK, D. F., DAVENPORT, G. R., FORTE, L. AND LANDON, E. J.: Characterization of plasma membrane proteins in mammalian kidney. *J. Biol. Chem.* **244**: 3561-3569, 1969.
- FLAMENBAUM, W. AND FRIEDMAN, R.: Pharmacology, therapeutic efficacy, and adverse effects of bumetanide, a new "loop" diuretic. *Pharmacotherapy* **2**: 213-222, 1982.
- FLEMING, A.: History and development of penicillin. *In Penicillin: Its practical application*, ed. by A. Fleming, pp. 1-33, The Blakiston Company, Philadelphia, PA, 1946.
- FLOREY, H. W.: The use of microorganisms for therapeutic purposes. *Yale J. Biol. Med.* **19**: 101-118, 1946.

- FORD, S. M., WILLIAMS, P. D., GRASSL, S. AND HOLOHAN, P. D.: Transepithelial acidification by cultures of rabbit proximal tubules grown on filters. *Am. J. Physiol.* **259**: C103-C109, 1990.
- FORSTER, R. P. AND COPENHAVER, J. H.: Intracellular accumulation as an active process in mammalian renal transport system *in vitro*. Energy dependence and competitive phenomena. *Am. J. Physiol.* **186**: 167-171, 1956.
- FOUDA, A.-K., FAUTH, C. AND ROCH-RAMEL, F.: Transport of organic cations by kidney epithelial cell line LLC-PK1. *J. Pharmacol. Exp. Ther.* **252**: 286-292, 1990.
- FOULKES, E. C.: Cellular localization of amino acid carriers in renal tubules. *Proc. Soc. Exp. Biol. Med.* **139**: 1032-1033, 1972.
- FOULKES, E. C.: Movement of *p*-aminohippurate between lumen and cells of renal tubule. *Am. J. Physiol.* **232**: F424-F428, 1977.
- FOULKES, E. AND MILLER, B. F.: Steps in *p*-aminohippurate transport in kidney slices. *Am. J. Physiol.* **196**: 86-92, 1959.
- GAUDRY, S., SITAR, D. S., SMYTH, D. D., MCKENZIE, J. K. AND AOKI, F. Y.: The effect of quinine and quinidine on the renal excretion of amantadine in man. *Clin. Invest. Med.* **13**: B15 (82), 1990.
- GECK, P AND HEINZ, E.: Secondary active transport: Introductory remarks. *Kidney Int.* **36**: 334-341, 1989.
- GESEK, F. A., WOLFF, D. W. AND STRANDHOY, J. W.: Improved separation method for rat proximal and distal tubules. *Am. J. Physiol.* **253**: F358-F365, 1987.

- GISCLON, L. G., BOYD, R. A., WILLIAMS, R. L. AND GIACOMINI, K. M.: The effect of probenecid on the renal elimination of cimetidine. *Clin. Pharmacol. Ther.* **45**: 444-452, 1989.
- GORNALL, A. G., BARDAWILL, C. J. AND DAVID, M. M.: Determination of serum proteins by means of the Biuret reaction. *J. Biol. Chem.* **177**: 751-766, 1949.
- GRANT, S. M., LANGTRY, H. D. AND BROGDEN, R. N.: Ranitidine. An updated review of its pharmacodynamic and pharmacokinetic properties and therapeutic use in peptic ulcer disease and other allied diseases. *Drugs* **37**: 801-870, 1989.
- GRANTHAM, J. J. AND CHONKO, A. M.: Renal handling of organic anions and cations; metabolism and excretion of uric acid. *In* The kidney, 3rd edition, ed. by B. M. Brenner and F. C. Rector, pp. 663-700, W. B. Saunders Company, Philadelphia, PA, 1986.
- GRANTHAM, J. J. AND CHONKO, A. M.: Renal handling of organic anions and cations; excretion of uric acid. *In* The kidney, 4th edition, ed. by B. M. Brenner and F. C. Rector, pp. 483-509, W. B. Saunders Company, Philadelphia, PA, 1991.
- GRASSL, S. M. AND ARONSON, P. S.: Na⁺/HCO₃⁻ co-transport in basolateral membrane vesicles isolated from rabbit renal cortex. *J. Biol. Chem.* **261**: 8778-8783, 1986.
- GRASSL, S. M., HOLOHAN, P. D. AND ROSS, C. R.: HCO₃⁻ transport in basolateral membrane vesicles isolated from rat renal cortex. *J. Biol. Chem.* **262**: 2682-2687, 1987.
- GRIFFITHS, D. A., HALL, S. D. AND SOKOL, P. P.: Interaction of 3'-azido-3'-deoxythymidine with organic ion transport in rat renal basolateral membrane vesicles. *J. Pharmacol. Exp. Ther.* **257**: 149-155, 1991.

- GUDER, W. G. AND ROSS, B. D.: Enzyme distribution along the nephron. *Kidney Int.* **26**: 101-111, 1984.
- GUGLER, R., FUCHS, G., DIECKMANN, M. AND SOMOGYI, A. A.: Cimetidine plasma concentration-response relationships. *Clin. Pharmacol. Ther.* **29**: 744-748, 1981.
- GUTIERREZ, M. M., BRETT, C. M., OTT, R. J. AND GIACOMINI, K. M.: Characterization of the Na⁺-nucleoside transporter in the human renal brush border membrane [abstract PPDM 8391]. *Pharm. Res.* **8** (10): 5323, 1991.
- GUTMAN, A. B.: The past four decades of progress in the knowledge of gout, with an assessment of the present status. *Arthritis Rheum.* **16**: 431-445, 1973.
- HABERLE, D.: Influence of glomerular filtration rate on the rate of para-aminohippurate secretion by the rat kidney: Micropuncture and clearance studies. *Kidney Int.* **7**: 385-396, 1975.
- HANDLER, J. S., PERKINS, F. M. AND JOHNSON, J. P.: Studies on renal cell function using cell culture techniques. *Am. J. Physiol.* **238**: F1-F9, 1980.
- HARVEY, A. M. AND MALVIN, R. L.: Comparison of creatinine and inulin clearances in male and female rats. *Am. J. Physiol.* **209**: 849-852, 1965.
- HAYMAN, J. M. JR.: Malpighi's "Concerning the structure of the kidneys." *Ann. Med. Hist.* **7**: 242-263, 1925.
- HEDMAN, A., ANGELIN, B., ARVIDSSON, A., DAHLQVIST, R. AND NILSSON, B.: Interactions in the renal and biliary elimination of digoxin: Stereoselective difference between quinine and quinidine. *Clin. Pharmacol. Ther.* **47**: 20-26, 1990.

- HEIDRICH, H. G., KINNE, R., SAFFRON-KINNE, R. AND HANNIG, K.: The polarity of the proximal tubule cell in rat kidney. *J. Cell Biol.* **54**: 232-235, 1972.
- HEINZ, E., GECK, P. AND WILBRANDT, W.: Coupling in secondary active transport. Activation of transport by co-transport and/or counter-transport. *Biochim. Biophys. Acta.* **255**: 442-461, 1972.
- HOFF, H. R., SITAR, D. S. AND AOKI, F. Y.: Sulfapyridine determined acetylator phenotype does not predict amantadine acetylation in humans. *Clin. Res.* **39**: 787A, 1991.
- HOFFMAN, J. F. AND FORBUSH, B.: Structure, mechanism, and function of the Na/K pump. *In* Current topics in membranes and transport, vol. 19, Academic Press, Inc., New York, 1983.
- HOFSTEE, B. H. J.: On the evaluation of the constants V_m and K_m in enzyme reactions. *Science* **116**: 329-331, 1952.
- HOLM, J.: The stimulating and inhibitory effect of monoquaternary ammonium compounds on decamethonium uptake by rat kidney cortex slices. *Biochem. Pharmacol.* **21**: 2021-2030, 1972.
- HOLOHAN, P. D. AND ROSS, C. R.: Mechanisms of organic cation transport in kidney plasma membrane vesicles: 1. Countertransport studies. *J. Pharmacol. Exp. Ther.* **215**: 191-197, 1980.
- HOLOHAN, P. D. AND ROSS, C. R.: Mechanisms of organic cation transport in kidney plasma membrane vesicles: 2. δ pH studies. *J. Pharmacol. Exp. Ther.* **216**: 294-298, 1981.

- HOOK, J. B. AND MUNRO, J. R.: Specificity of the inhibitory effect of "uremic" serum on *p*-aminohippurate transport. *Proc. Soc. Exp. Biol. Med.* **127**: 289-292, 1968.
- HOOK, J. B. AND WILLIAMSON, H. E.: Influence of probenecid and alterations in acid-base balance of the saluretic activity of furosemide. *J. Pharmacol. Exp. Ther.* **149**: 404-408, 1965.
- HOPFER, U., NELSON, K., PERROTTO, J AND ISSELBACHER, K. J.: Glucose transport in isolated brush border membrane from rat small intestine. *J. Biol. Chem.* **248**: 25-32, 1973.
- HORI, R., MAEGAWA, H., OKANO, T., TAKANO, M. AND INUI, K.: Effects of sulfhydryl reagents on tetraethylammonium transport in rat renal brush border membrane vesicles. *J. Pharmacol. Exp. Ther.* **241**: 1010-1016, 1987.
- HORIO, M., PASTAN, I., GOTTESMAN, M. M. AND HANDLER, J. S.: Transepithelial transport of vinblastine by kidney-derived cell lines. Application of a new kinetic model to estimate *in situ* K_m of the pump. *Biochim. Biophys. Acta* **1027**: 116-122, 1990.
- HOWARD, J. M., CHREMOS, A. N., AND COLLEN, M. J.: Famotidine. A new potent, long-lasting histamine H_2 -receptor antagonist - comparison with cimetidine and ranitidine in the treatment of Zollinger-Ellison syndrome. *Gastroenterology* **88**: 1026-1033, 1985.
- HOWELLS, R. E.: Advances in chemotherapy. *Br. Med. Bull.* **38**: 193-199, 1982.
- HSYU, P. H. AND GIACOMINI, K. M.: Stereoselective clearance of pindolol in humans. *J. Clin. Invest.* **76**: 1720-1726, 1985.

- HSYU, P. H. AND GIACOMINI, K. M.: Essential tyrosine residues in transport of organic cations in renal BBMV. *Am. J. Physiol.* **252**: F1065-F1072, 1987.
- HSYU, P. H., GISCLON, L. G., HUI, A. C. AND GIACOMINI, K. M.: Interactions of organic anions with the organic cation transporter in renal BBMV. *Am. J. Physiol.* **254**: F56-F61, 1988.
- HULL, R. N., CHERRY, W. R. AND WEAVER, G. W.: The origin and characteristics of a pig kidney cell line LLC-PK. *In Vitro* **12**: 670-677, 1976.
- ICHIKAWA, M., YOSHIMURA, A., SUMIZAWA, T., SHUDO, N., KUWAZURU, Y., FURAKAWA, T. AND AKIYAMA, S.: Interaction of organic chemicals with P-glycoprotein in the adrenal gland, kidney, and a multidrug-resistant KB cell. *J. Biol. Chem.* **266**: 903-908, 1991.
- IMAI, M.: Effect of bumetanide and furosemide on the thick ascending limbs of Henle's loop of rabbits and rats perfused *in vitro*. *Eur. J. Pharmacol.* **41**: 409-416, 1977.
- INOTSUME, N., NISHIMURA, M., NAKANO, M., FUJIYAMA, S. AND SATO, T.: The inhibitory effect of probenecid on renal excretion of famotidine in young, healthy volunteers. *J. Clin. Pharmacol.* **30**: 50-56, 1990.
- INUI, K.-I., OKANO, T., TAKANO, M., KITAZAWA, S. AND HORI, R.: A simple method for the isolation of basolateral plasma membrane vesicles from rat kidney cortex. Enzyme activities and some properties of glucose transport. *Biochim. Biophys. Acta* **647**: 150-154, 1981.

- JAFFE, J. H.: Drug addiction and drug abuse. *In* The Pharmacological Basis of Therapeutics, 8th edition, ed. by A. G. Gilman, T. W. Rall, A. L. Nies and P. Taylor, pp. 522-573, Pergamon Press, Inc., New York, 1990.
- JAHNCHEN, E. AND MULLER, W. E.: Stereoselectivity in protein binding and drug disposition. *In* Topics in pharmaceutical sciences, ed. by D. D. Breimer and P. Speiser, pp. 109-117, Elsevier Science Publishers, New York, 1983.
- JESSEN, H. AND SHEIKH, I.: Renal transport of taurine in luminal membrane vesicles from rabbit proximal tubule. *Biochim. Biophys. Acta* **1064**: 189-198, 1990.
- JUSKO, W. J.: Influence of cigarette smoking on drug metabolism in man. *Drug Metab. Rev.* **9**: 221-236, 1979.
- KEMPTON, R. T.: Differences in the elimination of neutral red and phenol red by the frog kidney. *J. Cell. Comp. Physiol.* **14**: 73-81, 1939.
- KINSELLA, J. L., HOLOHAN, P. D., PESSAH, N. I. AND ROSS, C. R.: Transport of organic ions in renal cortical luminal and antiluminal membrane vesicles. *J. Pharmacol. Exp. Ther.* **209**: 443-450, 1979a.
- KINSELLA, J. L., HOLOHAN, P. D., PESSAH, N. I. AND ROSS, C. R.: Isolation of luminal and antiluminal membranes from dog kidney cortex. *Biochim. Biophys. Acta.* **552**: 468-477, 1979b.
- KIRCH, W., HOENSCH, H. AND JANISCH, H. D.: Interactions and non-interactions with ranitidine. *Clin. Pharmacokinet.* **9**: 493-510, 1984.
- KLEINMAN, L. I., LOEWENSTEIN, M. S. AND GOLDSTEIN, L.: Sex difference in the transport of *p*-aminohippurate by the rat kidney. *Enzymology* **78**: 403-406, 1966.

- KLUS, H. AND KUHN, H.: A study of the optical activity of smoke nictines. *Fachliche. Mitt. Oesterr. Tabakregie* **17**: 331-336, 1977.
- KOPPEL, C. AND TENCZER, J. A.: A revision of the metabolic disposition of amantadine. *Biomed. Mass. Spectrom.* **12**: 499-501, 1985.
- KRIZ, W. AND BANKIR, L.: A standard nomenclature for structures of the kidney. *Am. J. Physiol.* **254**: F1-F8, 1988.
- KYEREMATEN, G. A., MORGAN, M. L., CHATTOPADHYAY, B., DEBETHIZY, D. AND VESELL, E. S.: Disposition of nicotine and eight metabolites in smokers and nonsmokers: Identification in smokers of two metabolites that are longer lived than cotinine. *Clin. Pharmacol. Ther.* **48**: 641-651, 1990.
- KYEREMATEN, G. A. AND VESELL, E. S.: Metabolism of nicotine. *Drug metab. Rev.*, **23**: 3-41, 1991.
- LAM, Y. W. F., BOYD, R. A., CHIN, S. K., CHANG, D. AND GIACOMINI, K. M.: Effect of probenecid on the pharmacokinetics and pharmacodynamics of procainamide. *J. Clin. Pharmacol.* **31**: 429-432, 1991.
- LAPOINTE, J. Y., LAPRADE, R. AND CARDINAL, J.: Characterization of the apical membrane ionic permeability of the rabbit proximal convoluted tubule. *Am. J. Physiol.* **250**: F339-F347, 1986.
- LINWEAVER, H. AND BURK, D.: The determination of enzyme dissociation constants. *J. Am. Chem. Soc.* **56**: 658-666, 1934.

- MALATHI, P., PREISER, H., FAIRCLOUGH, P., MALLETT, P. AND CRANE, R. K.: A rapid method for the isolation of kidney brush border membranes. *Biochim. Biophys. Acta* **554**: 259-263, 1979.
- MALPIGHI, M.: De viscerum structura. *In Opera Omnia*, pp. 87-100, Scott, London, 1666.
- MARSHALL, E. K., JR.: The secretion of phenol red by the mammalian kidney. *Am. J. Physiol.* **99**: 77-86, 1931.
- MARSHALL, E. K. JR. AND CRANE, M. M.: The secretory function of the renal tubules. *Am. J. Physiol.* **70**: 465-488, 1924.
- MARSHALL, E. K. AND GRAFFLIN, A. L.: The function of the proximal convoluted segment of the renal tubules. *J. Cell. Comp. Physiol.* **1**: 161-176, 1932.
- MARSHALL, E. K., JR., AND VICKER, J. L.: The mechanism of the elimination of phenolsulphonephthalein by the kidney - A proof of secretion by the convoluted tubules. *Bull. Johns Hopkins Hosp.* **34**: 1-7, 1923.
- McISAAC, R. J.: The uptake of hexamethonium-C¹⁴ by kidney slices. *J. Pharmacol. Exp. Ther.* **150**: 92-98, 1965.
- McISAAC, R. J.: The binding of organic bases to kidney cortex slices. *J. Pharmacol. Exp. Ther.* **168**: 6-12, 1969.
- McKINNEY, T. D.: Heterogeneity of organic base secretion by proximal tubules. *Am. J. Physiol.* **243**: F404-F407, 1982.

McKINNEY, T. D., DELEON, C. AND SPEEG, K. V. JR.: Organic cation uptake by a cultured renal epithelium. *J. Cell. Physiol.* **137**: 513-520, 1988.

McKINNEY, T. D. AND KUNNEMANN, M. E.: procainamide transport in rabbit renal cortical brush border membrane vesicles. *Am. J. Physiol.* **249**: F532-F541, 1985.

McKINNEY, T. D., MYERS, P. AND SPEEG, K. V., JR.: Cimetidine secretion by rabbit renal tubules *in vitro*. *Am. J. Physiol.* **241**: F69-F76, 1981.

McKINNEY, T. D. AND SPEEG, K. V., JR.: Cimetidine and procainamide secretion by proximal tubules *in vitro*. *Am. J. Physiol.* **242**: F672-F680, 1982.

McMORROW, M. J. AND FOXX, R. M.: Nicotine's role in smoking: An analysis of nicotine regulation. *Psychol. Bull.* **93**: 302-327, 1983.

MICHAELIS, L.: Die permeabilität von membranen. *Naturwissenschaften* **14**: 33-42, 1926.

MICHAELIS, L. AND MENTEN, M. L.: Die kinetik der invertinwirkung. *Biochem. Z.* **49**: 333-369, 1913.

MITCHELL, P.: Molecular group and electron translocation through natural membranes. *Biochem. Soc. Symp.* **22**: 142-168, 1963.

MIYAMOTO, Y., TIRUPPATHI, C., GANAPATHY, V. AND LEIBACH, F. H.: Multiple transport systems for organic cations in renal brush-border membrane vesicles. *Am. J. Physiol.* **256**: F540-F548, 1989.

- MÖLLER, J. V. AND SHEIKH, M. I.: Renal organic anion transport system: Pharmacological, physiological and biochemical aspects. *Pharmacol. Rev.* **34**: 315-358, 1983.
- MUIRHEAD, M., ROLAN, P., BOCHNER, F. AND SOMOGYI, A.: Renal and hepatic interaction between cimetidine and triamterene in man. *Clin. Exp. Pharmacol. Physiol.* **9** (suppl.): 53, 1985.
- MURRAY, M.: Mechanisms of the inhibition of cytochrome P-450-mediated drug oxidation by therapeutic agents. *Drug Metab. Rev.* **18**: 55-81, 1987.
- MURTHY, L. AND FOULKES, E. C.: Movements of solutes across luminal cell membranes in kidney tubules of the rabbit. *Nature* **213**: 180-181, 1967.
- NELSON, J. A.: A physiological function for multidrug-resistant membrane proteins: A hypothesis regarding the renal organic cation-secretory system [letter]. *Cancer Chemother. Pharmacol.* **22**: 92-93, 1988.
- NOTTERMAN D. A., DRAYER, D. E., METAKIS, L. AND REIDENBERG, M. M.: Stereoselective renal tubular secretion of quinidine and quinine. *Clin. Pharmacol. Ther.* **40**: 511-517, 1986.
- NWOSU, C. G., GODIN, C. S., HOUDI, A. A., DAMANI, L. A. AND CROOKS, P. A.: Enantioselective metabolism during continuous administration of S(-)- and R-(+)-nicotine isomers to guinea-pigs. *J. Pharm. Pharmacol.* **40**: 862-869, 1988.
- OCHS, H. R., GREENBLATT, D. J. AND WOO, E.: Clinical pharmacokinetics of quinidine. *Clin. Pharmacokinet.* **5**: 150-168, 1980.

- ODLIND, B.: A modified Sperber technique for direct estimation of true renal tubular excretion fraction. *Acta. Physiol. Scand.* **103**: 404-412, 1978.
- OTT, R. J. AND GIACOMINI, K. M.: The organic cation transport in the brush border membrane of opossum kidney (OK) cells is an N-linked glycosylated protein [abstract PPDM 8390]. *Pharm. Res.* **8** (10): 5323, 1991.
- OTT, R. J., HAI, A. C. AND GIACOMINI, K. M.: Mechanisms of interactions between organic anions and the organic cation transporter in renal brush-border membrane vesicles. *Biochem. Pharmacol.* **40**: 659-661, 1990.
- VERTON, E.: Über die allgemeinen osmotischen Eigenschaften der Zelle, ihre vermutlichen Ursachen und ihre Bedeutung für die Physiologie. *Vjschr. Naturf. Ges. Zürich* **44**: 88-135, 1899.
- VERTON, E.: Beiträge zur allgemeinen Muskel- und Nervenphysiologie. *Pflüg. Arch. Ges. Physiol.* **92**: 115-280, 346-386, 1902.
- OXENDER, D. AND QUAY, S.: Binding proteins and membrane transport. *Ann. N. Y. Acad. Sci.* **264**: 358-372, 1975.
- OXFORD J. S. AND GALBRAITH A.: Antiviral activity of amantadine: A review of laboratory and clinical data. *Pharmacol. Ther.* **11**: 181-262, 1980.
- PARKES, D.: Amantadine. *Adv. Drug Res.* **8**: 8-11, 1974.
- PATLAK, C. S.: Contributions to the theory of active transport. II. The gate-type non-carrier mechanism and generalization concerning tracer glow efficiency, and measurement of energy expenditure. *Bull. Math. Biophys.* **19**: 209-235, 1957.

- PETERS, L.: Renal tubular excretion of organic bases. *Pharmacol. Rev.* 12: 1-35, 1960.
- PILOTTI, A.: Biosynthesis and mammalian metabolism of nicotine. *Acta Physiol. Scand.* 479 (suppl.): 13-17, 1980.
- POWELL, J. R. AND DONN, K. H.: Histamine H₂-antagonist drug interactions in perspective: Mechanistic concepts and clinical implications. *Am. J. Med.* 77(suppl. 5b): 57-84, 1984.
- PODEVIN, R. A. AND BOUMENDIL-PODEVIN, E. F.: Monovalent cation and ouabain effects of PAH uptake by rabbit kidney slices. *Am. J. Physiol.* 232: F239-F247, 1977.
- PORTER, R. D., CATHCART-RAKE, W. F., WAN, S. H., WHITTIER, F. C. AND GRANTHAM, J. J.: Secretory activity and aryl acid content of serum, urine, and cerebrospinal fluid in normal and uremic man. *J. Lab. Clin. Med.* 85: 723-733, 1975.
- PREUSS, H. G., MASSRY, S. G., MAHER, J. F., GILLIECE, M. AND SCHREINER, G. E.: Effects of uremic sera on renal tubular *p*-aminohippurate transport. *Nephron* 3: 265-273, 1966.
- PRITCHARD, J. B.: Coupled transport of *p*-aminohippurate by rat kidney basolateral membrane vesicles. *Am. J. Physiol.* 255: F597-F604, 1988.
- RAMACHANDRAN, C. AND BRUNETTE, M. G.: The renal Na⁺/Ca²⁺ exchange system is located exclusively in the distal tubule. *Biochem. J.* 257: 259-264, 1989.

REINECK, H. J. AND STEIN, J. H.: Mechanisms of action and clinical uses of diuretics. *In* The kidney, 2nd edition, ed. by B. M. Brenner and F. C. Rector, pp. 1097-1131, W. B. Saunders Company, Philadelphia, PA, 1981.

RENNICK, B. R.: Renal tubule transport of organic cations. *Am. J. Physiol.* **240**: F83-F89, 1981.

RENNICK, B. R. AND FARAH, A.: Studies on the renal tubule transport of tetraethylammonium ion in the dog. *J. Pharmacol. Exp. Ther.* **116**: 287-295, 1956.

RENNICK, B. R., KANDEL, A. AND PETERS, L.: Inhibition of the renal tubular excretion of tetraethylammonium and N²-methylnicotinamide by basic cyanine dyes. *J. Pharmacol. Exp. Ther.* **118**: 204-219, 1956.

RENNICK, B. R., MOE, G. K., LYONS, R. H., HOUBLER, S. W. AND NELIGH, R.: Absorption and renal excretion of the tetraethylammonium ion. *J. Pharmacol. Exp. Ther.* **91**: 210-217, 1947.

REYNOLDS, R. A., WALD, H., McNAMARA, P. D. AND SEGAL, S.: An improved method for isolation of basolateral membranes from rat kidney. *Biochim. Biophys. Acta* **601**: 92-100, 1980.

ROBERTS, C. J. C.: Clinical pharmacokinetics of ranitidine. *Clin. Pharmacokinet.* **9**: 211-221, 1984.

RODNAN, G. P.: Treatment of the gout and other forms of crystal-induced arthritis. *Bull. Rheum. Dis.* **32**: 43-53, 1982.

- RODVOLD, K. A., PALOUCZEK, F. P., JUNG, D. AND GALLASTEGUI, J.: Interaction of steady-state procainamide with H₂-receptor antagonists cimetidine and ranitidine. *Ther. Drug Monit.* **9**: 378-383, 1987.
- ROSE, R. C., BIANCHI, J. AND SCHUETTE, S. A.: Effective use of renal cortical slices in transport and metabolic studies. *Biochim. Biophys. Acta* **821**: 431-436, 1985.
- ROSENBERG, T. H.: On accumulation and active transport in biological systems. I. Thermodynamic considerations. *Acta. Chem. Scand.* **2**: 14-33, 1948.
- ROSENBERG, T. H. AND WILBRANDT, W.: The kinetics of membrane transport involving chemical reactions. *Exp. Cell Res.* **9**: 49-67, 1955.
- ROSS, C. R. AND HOLOHAN, P. D.: Transport of organic anions and cations in isolated renal plasma vesicles. *Ann. Rev. Pharmacol. Toxicol.* **23**: 65-85, 1983.
- ROSS, C. R. AND WEINER, I. M.: Adenine nucleotides and PAH transport in slices of renal cortex: Effects of DNP and CN. *Am. J. Physiol.* **222**: 356-359, 1972.
- RUSSELL, M. A. H.: Cigarette smoking: A dependence on high-nicotine boli. *Drug Metab. Rev.* **8**: 29-57, 1978.
- SCATCHARD, G.: The attractions of proteins for small molecules and ions. *Ann. N. Y. Acad. Sci.* **51**: 660-672, 1949.
- SCHALI, C. AND ROCH-RAMEL, F.: Accumulation of ¹⁴C-urate and ³H-PAH in isolated proximal tubular segments of the rabbit kidney. *Am. J. Physiol.* **239**: F222-F227, 1980.
- SCHALI, C. AND ROCH-RAMEL, F.: Uptake of ³H-PAH and ¹⁴C-urate into isolated proximal tubular segments of the pig kidney. *Am. J. Physiol.* **241**: F591-F596, 1981.

- SCHALI, C., SCHILD, L., OVERNEY, J. AND ROCH-RAMEL, F.: Secretion of tetraethylammonium by proximal tubules of rabbit kidneys. *Am. J. Physiol.* **245**: F238-F246, 1983.
- SCHILD, L. AND ROCH-RAMEL, F.: Transport of salicylate in proximal tubule (S2 segment) isolated from rabbit kidney. *Am. J. Physiol.* **254**: F554-F561, 1988.
- SCHOLER, D. W. AND EDELMAN, I. S.: Isolation of rat kidney cortical tubules enriched in proximal and distal segments. *Am. J. Physiol.* **237**: F350-F359, 1979.
- SCHUNACK, W.: Pharmacology of H₂-receptor antagonists: An overview. *J. Int. Med. Res.* **17** (suppl. 1): 9A-16A, 1989.
- SCHWAB, R. S., ENGLAND, A. C., POSKANZER, D. C. AND YOUNG, R. R.: Amantadine in the treatment of Parkinson's disease. *J. Am. Med. Assoc.* **208**: 1168-1170, 1969.
- SHEIKH, M. I. AND MÖLLER, J. V.: The kinetic parameters of renal transport of *p*-aminohippurate *in vitro*. *Biochim. Biophys. Acta* **196**: 305-319, 1970.
- SHIMADA, H., MOEWES, B. AND BURCKHARDT, G.: Indirect coupling to sodium of *p*-aminohippurate by rat kidney basolateral vesicles. *Am. J. Physiol.* **253**: F795-F801, 1988.
- SHIMOMURA, A., CHONKO, A. M. AND GRANTHAM, J. J.: Basis for heterogeneity of *p*-aminohippurate secretion in rabbit proximal tubules. *Am. J. Physiol.* **240**: F430-F436, 1981.
- SINGER, S. J. AND NICHOLSON, G. L.: The fluid mosaic model of the structure of cell membranes. *Science* **175**: 720-731, 1972.

- SITAR, D. S., GAUDRY, S., SMYTH, D. D., MCKENZIE, J. K. AND AOKI, F. Y.: Sex but not age-associated interference with renal elimination of amantadine in humans. *The Gerontologist* **30**: 169 (187A), 1990.
- SMITH, P. M., PRITCHARD, J. B. AND MILLER, D. S.: Membrane potential drives organic cation transport into teleost renal proximal tubules. *Am. J. Physiol.* **255**: R492-R499, 1988.
- SOKOL, P. P.: Effect of DQ-2556, a new cephalosporin, on organic ion transport in renal plasma membrane vesicles from the dog, rabbit and rat. *J. Pharmacol. Exp. Ther.* **255**: 436-441, 1990.
- SOKOL, P. P. AND GATES, S. B.: Effects of endogenous and exogenous polyamines on organic cation transport in rabbit renal plasma membrane vesicles. *J. Pharmacol. Exp. Ther.* **255**: 52-58, 1990.
- SOKOL, P. P., HOLOHAN, P. D. AND ROSS, C. R.: Electroneutral transport of organic cations in canine renal brush-border membrane vesicles. *J. Pharmacol. Exp. Ther.* **233**: 694-699, 1985.
- SOKOL, P. P., HUIATT, K. R., HOLOHAN, P. D. AND ROSS, C. R.: Gentamycin and verapamil compete for a common transport mechanism in renal brush border membrane vesicles. *J. Pharmacol. Exp. Ther.* **251**: 937-942, 1989.
- SOKOL, P. P. AND MCKINNEY, T. D.: Mechanism of organic cation transport in rabbit renal basolateral membrane vesicles. *Am. J. Physiol.* **258**: F1599-F1607, 1990.
- SOMOGYI, A.: New insights into the renal secretion of drugs. *Trends Pharmacol. Sci.* **8**: 354-357, 1987.

SOMOGYI, A. AND BOCHNER, F.: Dose and concentration effect of ranitidine on procainamide disposition and renal clearance in man. *Br. J. Clin. Pharmacol.* **18**: 175-181, 1984.

SOMOGYI, A. A., HOVENS, C. M., MUIRHEAD, M. R. AND BOCHNER, F.: Renal tubular secretion of amiloride and its inhibition by cimetidine in humans and in an animal model. *Drug Metab. Dispos.* **17**: 190-196, 1988.

SOMOGYI, A., MCLEAN, A. AND HEINZOW, B.: Cimetidine-procainamide pharmacokinetic interaction in man: Evidence of competition for tubular secretion of basic drugs. *Eur. J. Clin. Pharmacol.* **25**: 339-345, 1983.

SPERBER, I.: A new method for the study of renal tubular excretion in birds. *Nature, Lond.* **158**: 131, 1946.

SPERBER, I.: The mechanism of renal excretion of some detoxification products in the chicken. *Proc. Int. Congr. Physiol.*, 17th, Oxford, pp. 217-218, 1947.

SPERBER, I.: The excretion of piperidine, guanidine, methylguanidine and N¹-methylnicotinamide in the chicken. *Lantbrukshoegsk. Ann.* **16**: 49-64, 1948.

SPERBER, I.: The excretion of some organic bases and some phenols and phenol derivatives. *Scand. J. Clin. Lab. Invest.* **1**: 345-, 1949.

SPERBER, I.: Competitive inhibition and specificity of renal tubular transport mechanisms. *Arch. Int. Pharmacodyn. Ther.* **97**: 221-, 1954.

SPERBER, I.: Secretion of organic anions in the formation of urine and bile. *Pharmacol. Rev.* **11**: 109-134, 1959.

- STADIE, W. C. AND RIGGS, B. C.: Microtome for the preparation of tissue slices for metabolic studies *in vitro*. *J. Biol. Chem.* **154**: 687-690, 1944.
- STONER, L. C. AND TRIMBLE, M. E.: Effects of MK-196 and furosemide on rat medullary thick ascending limbs of Henle *in vitro*. *J. Pharmacol. Exp. Ther.* **221**: 715-720, 1982.
- SUNDARESAN, P. R., FORTIN, T. L. AND KELVIE, S. L.: α - and β -adrenergic receptors in proximal tubules of the rat kidney. *Am. J. Physiol.* **253**: F848-F856, 1987.
- TAKANO, M., INUI, K., OKANO, T., SAITO, H. AND HORI, R.: Carrier mediated transport systems of tetraethylammonium in rat renal brush-border and basolateral membrane vesicles. *Biochim. Biophys. Acta.* **773**: 113-124, 1984.
- TAKANO, M., OKANO, T., INUI, K.-I. AND HORI, R.: Transport mechanisms of cationic drugs in rat renal brush-border and basolateral membranes. *J. Pharmacobiodyn.* **8**: s-115, 1985.
- TAMAI, I, TSUJI, A AND KIN, Y.: Carrier-mediated transport of cefixime, a new cephalosporin antibiotic, *via* an organic anion transport system in the rat renal brush-border membrane. *J. Pharmacol. Exp. Ther.* **246**: 338-344, 1988.
- TARLOFF, J. B. AND BRAND, P. H.: Active tetraethylammonium uptake across the basolateral membrane of rabbit proximal tubule. *Am. J. Physiol.* **251**: F141-F149, 1986.
- TISHER, C. C. AND MADSEN, K. M.: Anatomy of the kidney. *In* *The Kidney*, 4th edition, ed. by B. M. Brenner and F. C. Rector, pp. 3-75, W. B. Saunders Company, Philadelphia, PA, 1991.

- TRIFILLIS, A. L., REGEC, A. L. AND TRUMP, B. F.: Isolation, culture and characterization of human renal tubular cells. *J. Urol.* **133**: 324-329, 1985.
- TRIFILLIS, A. L. AND KAHNG, M. W.: Characterization of an in vitro system of human renal papillary collecting duct cells. *In Vitro Cell. Dev. Biol.* **26**: 441-446, 1990.
- TRUMP, B. F. AND HARRIS, C. C.: Human tissues in biomedical research. *Hum. Pathol.* **10**: 245-248, 1979.
- TUNE, B. M., BURG, M. B. AND PATLAK, C. S.: Characteristics of *p*-aminohippurate transport in proximal renal tubules. *Am. J. Physiol.* **217**: 1057-1063, 1969.
- TUNE, B. M. AND FERNHOLT, M.: Relationship between cephaloridine and *p*-aminohippurate transport in the kidney. *Am. J. Physiol.* **225**: 1114-1117, 1973.
- TURNER, R. J. AND SILVERMAN, M.: Sugar uptake into brush border vesicles from dog kidney. *Biochim. Biophys. Acta* **507**: 305-321, 1977.
- ULLRICH, K. J.: Epithelial transport: An introduction. *Methods Enzymol.* **191**: 1-4, 1990.
- VAN CRUGTEN, J., BOCHNER, F., KEAL, J. AND SOMOGYI, A.: Selectivity of the cimetidine-induced alterations in the renal handling of organic substrates in humans. Studies with anionic, cationic and zwitterionic drugs. *J. Pharmacol. Exp. Ther.* **236**: 481-487, 1986.
- VAN GINNEKEN, C. A. M. AND RUSSEL, F. G. M.: Saturable pharmacokinetics in the renal excretion of drugs. *Clin. Pharmacokinet.* **16**: 38-54, 1989.

- VANDER, A. J.: Functions and structures of the kidneys. *In renal physiology*, 4th edition, pp.1-18, McGraw-Hill, Inc., New York, 1991.
- VAUGHAN WILLIAMS, E. M.: Classification of antidysrhythmic drugs. *Pharmacol. Ther.* 1: 115-138, 1985.
- VINAY, P., GOUGOUX, A. AND LEMIEUX, G.: Isolation of a pure suspension of rat proximal tubules. *Am. J. Physiol.* 241: F403-F411, 1981.
- WEBSTER, L. T. Jr.: Drugs used in the chemotherapy of protozoal infections. *In The pharmacological basis of therapeutics*, 7th edition, ed. by A. G. Gilman, L. S. Goodman, T. W. Rall and F. Murad, pp. 1029-1048, Macmillan Publishing Company, New York, 1985.
- WEBSTER, L. T. Jr.: Drugs used in the chemotherapy of protozoal infections. *In The pharmacological basis of therapeutics*, 8th edition, ed. by A. G. Gilman, T. W. Rall, A. S. Nies and P. Taylor, pp. 978-998, Pergamon Press, Inc., New York, 1990.
- WEDEEN, R. P. AND JERNOW, H. I.: Autoradiographic study of cellular transport of Hippuran-¹²⁵I in the rat nephron. *Am. J. Physiol.* 214: 776-785, 1968.
- WEDEEN, R. P. AND WEINER, B.: The distribution of *p*-aminohippuric acid in rat kidney slices. I. Tubular localization. *Kidney Int.* 3: 205-213, 1973a.
- WEDEEN, R. P. AND WEINER, B.: The distribution of *p*-aminohippuric acid in rat kidney slices. II. Depth of uptake. *Kidney Int.* 3: 214-221, 1973b.
- WEDEEN, R. P. AND VYAS, B. T.: Phlorizin stimulation of *p*-aminohippurate uptake in rat kidney cortex slices. *Kidney Int.* 14: 158-168, 1978.

- WEINER, I. M. AND ROTH, L.: Renal excretion of cimetidine. *J. Pharmacol. Exp. Ther.* **216**: 516-520, 1981.
- WEST, I. C.: Energy coupling in secondary active transport. *Biochim. Biophys. Acta* **604**: 91-126, 1980.
- WHITE, A. G.: Uremic serum inhibition of renal para-aminohippurate transport. *Proc. Soc. Exp. Biol. Med.* **123**: 309-310, 1966.
- WHITE, N. J.: Clinical pharmacokinetics of antimalarial drugs. *Clin. Pharmacinet.* **10**: 187-215, 1985.
- WHITE, N. J., LOOAREESWAN, S. AND WARELL, D. A.: Quinine and quinidine: a comparison of EKG effects during the treatment of malaria. *J. Cardiovasc. Pharmacol.* **5**: 173-175, 1983.
- WILBRANDT, W. AND ROSENBERG, T.: The concept of carrier transport and its corollaries in pharmacology. *Pharmacol. Rev.* **13**: 109-183, 1961.
- WILSON, D. B.: Cellular transport mechanisms. *Ann. Rev. Biochem.* **47**: 933-965, 1978.
- WONG, L. T. Y., SMYTH, D. D. AND SITAR, D. S.: Stereoselective inhibition of amantadine accumulation by quinine and quinidine in rat renal cortical slices and proximal tubules. *J. Pharmacol. Exp. Ther.* **255**: 271-275, 1990.
- WONG, L. T. Y., SMYTH, D. D. AND SITAR, D. S.: Differential effects of histamine H₂ receptor antagonists on amantadine uptake in rat renal cortical slice, isolated proximal tubule and distal tubule. *J. Pharmacol. Exp. Ther.* **258**: 320-324, 1991.

WONG, L. T. Y., SMYTH, D. D. AND SITAR, D. S.: Interference of renal organic cation transport by (-) & (+) nicotine at concentrations documented in plasma of habitual tobacco smokers. *J. Pharmacol. Exp. Ther.* In press, 1992.

WOODHALL, P. B., TISHER, C. C., SIMONTON, C. A. AND ROBINSON, R. R.: Relationship between paraminohippurate secretion and cellular morphology in rabbit proximal tubules. *J. Clin. Invest.* **61**: 1320-1329, 1978.

WRIGHT, S. H. AND WUNZ, T. M.: Transport of tetraethylammonium by rabbit renal brush-border and basolateral membrane vesicles. *Am. J. Physiol.* **253**: F1040-F1050, 1987.

ZIMMERMAN, W. B., BYUN, E., MCKINNEY, T. D. AND SOKOL, P. P.: Sulfhydryl groups are essential for organic cation exchange in rabbit renal basolateral membrane vesicles. *J. Biol. Chem.* **266**: 5459-5463, 1991.